Université de Toulouse

THÈSE

En vue de l'obtention du

DOCTORAT DE L'UNIVERSITÉ DE TOULOUSE

Délivré par :

Université Toulouse 3 Paul Sabatier (UT3 Paul Sabatier)

Présentée et soutenue par :
Thibaut BILLARD

Le vendredi 3 octobre 2014

Titre :

Off-line and On-line Partial Discharges Detection in Low Voltage Motors of Electric Vehicle fed by a PWM Inverter using Non-Intrusive Sensor

---

ED GEET : Génie Electrique

Unité de recherche :

Laboratoire LAPLACE, UMR 5213 CNRS/UPS/INP, MDCE

Directeur(s) de Thèse :

M. Thierry LEBEY, Directeur de Recherche CNRS
M. Pierre BIDAN, Professeur à l'université Toulouse 3 Paul Sabatier

Rapporteurs :

M. Gian Carlo MONTANARI, Professeur à l'université de Bologne, Italie
M. Juan Manuel MARTINEZ-TARIFA, Professeur à l'université Carlos III de Madrid, Espagne

Autre(s) membre(s) du jury :

M. Greg STONE, Docteur Ingénieur à Iris Power - Qualitrol, Canada, Président du jury
M. François FRESNET, Docteur Ingénieur à Renault, France, Examinateur

Author:	Thibaut BILLARD
Title:	Off-line and On-line Partial Discharges Detection in Low Voltage Motors of Electric Vehicle fed by a PWM Inverter using Non-Intrusive Sensor
Advisors:	Thierry LEBEY, head of research at CNRS Pierre BIDAN, Professor at the university of Toulouse III
Ph.D Defense:	Ph.D defended on the 3rd October 2014 at University of Toulouse III
Area of research:	Electrical Engineering
Laboratory:	Laplace Laboratory, CNRS/UPS/INP UMR 5213
Address:	118, route de Narbonne 31062 Toulouse cedex 9, France
Keywords:	Partial Discharges, Off-line, On-line, PWM inverter drive, Non-intrusive sensor, Electric Vehicle, Electric Motor

Abstract:

To control the speed of the motor in an electric vehicle, one solution is to use in the powertrain an inverter drive with pulse width modulation (PWM). This device is recreating a sinusoidal current on each phase with a high number of short pulses of the same amplitude but with a dynamic duty cycle. Recent advances in power electronics allowed switching time to be quicker and quicker thus creating voltage pulses with shorter and shorter rise time. The use of PWM inverter to fed low voltage is now widespread but not without posing well-known problems regarding the reliability of the machine.

When an electric motor is fed with a very number of pulses per second, each pulse is not propagating immediately along the winding and thus the voltage distribution is not uniform as in the sinusoidal case. As a result, most of the voltage is located within the first turns of the coil during the first moment of the switching. When the motor is random wound, first and last turns of the same coil could be adjacent thus putting high demand on the turn-to-turn insulation.
Impedance mismatch between power cables and motors terminals could lead to overvoltage which are increasing the electrical stress on the insulation system.
In the worst-case scenario, partial discharges could occur and contribute to the gradual deterioration of the insulation materials thus leading to premature failure

If partial discharges are easily detected with sinusoidal voltage with standard testing procedure, it becomes much harder to so when the sample under test is fed by a PWM inverter drive. Indeed, it is very difficult to spot very low amplitude partial discharges signals among very large amplitude voltage and current. Moreover, the PWM inverter is generating electro-magnetical noise, which is highly disturbing in partial discharge detection using RF non-intrusive sensor. Worse still, some electric motors having passed successfully AC or repetitive impulses acceptance tests may still fail prematurely when fed by a PWM inverter drive

The aim of this Ph.D thesis is thus to develop a non-intrusive partial discharges detection method, using a non-intrusive sensor, off-line and on-line in an electric motor fed by a PWM inverter drive. To achieve this, a series of experiments, gradually growing in complexity, will test the detection method with harsher and harsher conditions, thus closer and closer to realistic electric vehicle operating conditions. From a single-phase test on an electric stator to a full-scale test on an industrial engine test bench, off-line and on-line detection proves to be possible. In addition, visual observations and experiments have been carried out to better understand the physics of the observed light emitting discharges.

Auteur:	Thibaut BILLARD
Titre:	Détection off-line et on-line de décharges partielles dans un moteur basse tension de véhicule électrique à l'aide de capteur non-intrusif
Directeurs:	Thierry LEBEY, directeur de recherche CNRS Pierre BIDAN, Professeur à l'université Toulouse III
Soutenance:	Le 3 octobre 2014 à l'université Toulouse III
Domaine:	Génie Electrique
Laboratoire:	Laboratoire Laplace, CNRS/UPS/INP UMR 5213
Adresse:	118, route de Narbonne 31062 Toulouse cedex 9, France
Mots clés:	Décharges partielles, Off-line, On-line, Onduleur de tension MLI, Capteur non-intrusif, Véhicule électrique, Moteur électrique

Résumé:

Pour faire varier la vitesse d'un moteur d'une voiture électrique, un onduleur de tension avec une modulation de largeur d'impulsion (MLI) est utilisé. Les temps de commutation de plus en plus courts créent un grand nombre de fronts de tension. L'utilisation d'un onduleur sur une machine basse tension est de plus en plus répandue et peut provoquer une réduction de la durée de vie des machines.

Tout d'abord, la répartition de la tension au sein de la bobine est fortement inhomogène à cause de la nature impulsionnelle de la tension. Dans des machines basse tension avec un bobinage en vrac, il y a donc une probabilité non négligeable que les quelques premières spires de la bobine supportant la tension lors de la commutation soient adjacentes avec les dernières, faisant ainsi supporter à l'isolation interspire une forte différence de potentiel. La désadaptation d'impédance entre les câbles de puissance et les bornes de la machine peuvent également générer des surtensions, augmentant encore la sollicitation sur l'isolation électrique.

Dans ces conditions défavorables, des décharges partielles peuvent apparaitre et contribuer à la dégradation de l'isolation électrique, réduisant ainsi la durée de vie des machines. Pire encore, des moteurs ayant passé avec succès des essais de qualification en impulsionnel pour être alimentés par un onduleur de tension ont malgré tout des durées de vie réduites. Si de tels phénomènes sont facilement détectables en 50Hz, il devient difficile de les détecter de manière électrique avec un onduleur de tension avec l'amplitude et la variation du courant. De plus, l'onduleur de tension génère un bruit électromagnétique important perturbant les mesures avec les capteurs non-intrusifs.

L'objectif de cette thèse est donc de développer une méthode de détection de décharges partielles, à l'aide d'un capteur non-intrusif, dans un moteur de voiture électrique alimenté par un onduleur de tension en on-line, ainsi qu'en off-line, afin de fournir des données pertinentes lors de la conception d'un moteur électrique, de test fin de chaine ou d'essai en fatigue. Pour atteindre cet objectif, une suite d'expériences montant en complexité ont permis de confronter le dispositif de détection à des conditions de plus en plus proches de celles d'une voiture électrique.

Acknowledgments

This work has been carried out at Laplace Laboratory of Toulouse France, in the MDCE team and in Renault company.

First and foremost I wish to thank my advisor, **Thierry Lebey,** head of research at CNRS and future director of the Laplace Laboratory. It has been an honour to be one of his Ph.D students, he is one of the smartest people I know, yet at the same time one the funniest as well! He has been supportive since the first days I began working on this Ph.D thesis in a research field I did not know. He helped me understand the key points in the thesis topic and guided me over almost three of development. He taught me how good experimental physics is done and I fully appreciate the time spent with me to make this Ph.D thesis productive, stimulating and full of enthusiasm. I remember he used to say something like "In the first year you are learning, in the second year we are tackling your subject and in the last year you are teaching me things" to encourage me to focus hard on this new topic. I am not sure I'd be able to teach him anything, but I am sure I have learned personally and professionally quite a lot. We used to run together more (or less for me) regularly to discuss science or personal life matters which add a more friendship color to this professional relationship.

I wish to thank my thesis committee that guided me through all these years.
Pierre Bidan, professor at the university of Toulouse. Always available, always taking time to explain thing in a very comprehensive way, always looking to help, always friendly, it's my regret not to have attend his courses over the past three year. He helped when regarding high-pass filtering and bring his technical expertise in numerous experiences.
Philippe Castelan, professor at the university of Toulouse**.** He is one of the nicest, friendly, good-natured and helpful person I have met. He is the kind of person you can trust blindly and rely on. He helped me greatly when I was trying to develop a signal processing method and found time in his busy schedule. I personally enjoyed the numerous formula one discussion we had over the years as well, commenting on technological evolution and historical facts.
Sorin Dinculescu, research engineer at the Laplace Laboratory. I hope that one I could be as skilled as he is when it comes to understand power electronics, electronics and electrical engineering. His technical expertise has been invaluable during all this work. He built two different and lab-made high-voltage PWM inverter that prove to be key in the long term goal of detecting partial discharge. Without him, this Ph.D thesis could not have been completed and I am very grateful to him.
I am grateful to **François Fresnet,** research engineer at Renault for his good advices, pertinent questions and willingness to follow my work closely from the start to the end either by visiting or by long phone calls. He trusted me and gave me the freedom to carry out my research and pursue various objectives without objection. Thanks to him, I've got amazing electric motors samples, availability to an engine test bench and the opportunity to present my work at the company.
Maxime Makarov, research engineer and head of my working group at Renault. I hope I'd be able to explain ideas, strategic goals and long terms plan like he did numerous time and manage a team like him. I'd especially like to thank him for trusting me while I was still an engineering student and point me towards this Ph.D thesis that was not in my technical area. He convinced me to candidate and trusted my abilities to start and finish this work.

For this dissertation I would like to thank my reading committee members: **Gian Carlo Montanari, Juan Manuel Martinez Tarifa, and Greg Stone** for their time, interest, and helpful comments.

Dozens of people have helped and taught me immensely at the Laplace Laboratory or at Renault during this work, bringing technical support, specific advice, practical or theoretical learning or interesting. I can not be exhaustive, but at the lab, I can especially stress the contribution of **Nicolas Gherardi, Nicolas Naudé** and **Antoine Bellinger** for their invaluable help and discussions when investigating the physics of discharge**. Yannick Deville** regarding signal processing has been very helpful and available as well. I'd like to thank all **MDCE** team members as well but, more generally, I am very grateful to all the persons who contributed to this Ph.D thesis in scientific, technical or administrative way.
At Renault, I'd like to thank **José Fernandez** for allowing us to perform partial discharge measurements on industrial engine test bench, which proves to be the main contribution of this work. **Frédéric Auzas** has always been interest in my work, asking questions, pointing me towards books or articles and providing good advices. Finally, **Nathalie Bouque** has been of a great help regarding all administrative matters and saves me a lot of time and energy. More generally, I am grateful to all the persons that supported, or were interested in, my work during my time at Renault.

I gratefully acknowledge the funding sources that made my Ph.D. work possible. I was funded by Renault and national association of research technology (ANRT) in a CIFRE contract.

The **group of Ph.D and Post.Doc students** at Laplace laboratory have been very important for the friendly, laid-back yet serious working atmosphere. I am especially very grateful to **Laurent Roske**, he has been so much supportive, available and always to help in any way he could that he is a key part of this work. I really wish him all the bests professionally and personally, he is a very good person. Among all the group of Ph.D and Post.Doc student I am grateful to, I'd like to thank especially **Chafé, Cédric, Guillaume, Simon and Rick** for the numerous personal and funny discussions we had, best of lucks guys.

I'd like to thank all of my family and especially my **father-in-law**, he showed confidence, interest and faith in myself and in my success. I deeply thank my **mom, dad and my close family**. My hard-working parents have sacrificed their lives and gave everything they had for myself and my sister and brother, they provided unconditional love and care and I would not have made it this far without them.

Finally, I'd like to deeply thank my **wife**, there are no words to convey how much I love her. She has been non-judgmental of me and gave me confidence. She always had faith in me even when I didn't have faith in myself. During, these past three years we got married and we both learned quite a lot about life and strengthened our commitment to each other and to our future family.

Thibaut Billard

Laplace Laboratory, Toulouse, France

July 2014

Table of contents

List of figures

List of tables

1. Introduction

This chapter gives the background, goals and motivations of this Ph.D. dissertation. The major contributions made by the author are also listed. Finally, the thesis outline is also given in details to give the reader an overview of the work presented, chapter-by-chapter.

1.1. Historical overview of electric vehicle evolution

Today's electric cars are representative of an innovative history of more than a hundred of years. In itself, the idea of using electrical energy stored in a battery to propel a vehicle with an electric motor is not new and was quite popular at the beginning of the last century. Indeed, electric cars were quiet, clean and, mostly, easy to use while offering good overall performances. For example, the first car to ever reach 100 km/h was an electric one. On a broader scale, a cab company in New-York used electric cars and battery swapping. But, despite its inherent advantages, this evolution slowed down when facing several technical issues, such as battery capacity, distance range or refuel time. In the meantime, technological progress in internal combustion engine, combined with the raise of cheap oil, definitely started the decline of electric cars.

The two oil crisis in the 1970s shortly brought back some interest in electric cars. But it's only with global economic recession, large increase in oil prices and greenhouse gas emission concerns in the beginning of the 2000s that the revival truly began. In Europe, European emission standards are also meant to support development of electric car technology. As a result cars manufacturers, making the most of governments' tax credits, subsidies and incentives in the process, build on recent breakthroughs in battery technology and power electronics to develop their own electric or hybrid car.

But, for car manufacturers used to design and built internal combustion engines, the shift from thermal to electric energy is clearly a new design paradigm. Although body, vehicle internal framework or suspension could easily be adapted to an electric vehicle, the whole powertrain almost needs to be designed from scratch, using battery, power electronics and electric motor. Subcontracting the whole powertrain design, production and assembly while gaining experience can only be a short-term option since this is exactly where the competitive advantage lies in the electric vehicle. For that reason, and even if electric vehicle adoption is not widespread due to high prices, lack of recharging infrastructure and a range deemed insufficient, significant investments in research and development have already been made to encourage innovation in an emerging, although highly competitive, market.

Being labelled as an innovative company could be enough to win early market shares, especially in an burgeoning market, but proposing reliable electric vehicles is paramount to strengthen and develop. Once competition has caught up, a poor starting reputation caused by unreliable, unsatisfactory or overpriced products would mean no return on investments and a crisis situation difficult to overcome.

1.2. Technical problem and inherent constraint of electric vehicle

Among several causes of unreliability or technological under-achievements in the electric vehicle powertrain, the electric motor insulation system is, in real use, subjected to a lot of different and specific stresses, mainly electrical but also mechanical, thermal, chemical, load variations and climatic conditions.
Worse still, electric motors having successfully passed current tests and conventional procedures to assess insulation performance may still fail prematurely when in service. Which means that these conventional testing procedures, used with sinusoidal or surge voltage, are not suited to test electric motors fed by an inverter drive.
Indeed, powertrain design, voltage level and power electronics used to feed the motor are especially nocive and are causing overvoltages and non-uniform voltage distribution within motor's coils. The electric vehicle environment is thus putting high demands on the electric motor insulation system.

Moreover, electric motors, like other components, are designed in a cost-efficient way and often result in the choice of random-wound motors. In other words, the manufacturer is aiming to find the best trade-off between insulation performance and cost, but if the latter is a known economical figure, the former is more difficult to estimate and rely on partial discharges measurements. Indeed, as there is no direct physics relating insulation materials properties and their performance under electrical stresses, most of design rules are based on experience, trial and errors and partial discharges measurements.

Partial discharges are localized and small electrical discharges occurring under strong electrical stresses in voids, bubbles or even on the surface of the insulating material. These discharges are called partial because they are not short-circuiting the whole insulation system; they are either limited by the insufficient local electrical field or blocked by the insulating material. Partial discharges are an early warning sign of the future failure of the insulation system, nothing more. In other words, there is a big difference between predicting a failure and predicting when the failure will occur. About failure mechanisms identification, partial discharges are causing physical erosion due to charged particle impact, chemical deterioration and thermal stress on the insulation system. Likewise, one should be very careful when identifying such partial discharges patterns or magnitude to a specific failure mechanism. Indeed, partial discharge measurements are highly dependent on the object under test and could thus only be used on similar type of machines.

Still, it's critical to be able to determine the inception threshold of partial discharges in the electric motor to assess insulation system performance. This partial discharge diagnosis should ideally be carried out when the electric motor is in operating conditions to reflect real stresses, thus providing insulation system real performances.
But at the moment, such on-line measurements prove to be very difficult because of the inverter drive feeding the electric motor creating electro-magnetical and electric noise interfering with small PD signals detection, thus leading to false positive. From a practical point of view, reliability concern on the whole electric vehicle powertrain prevent the connexion of the most widely used sensor, capacitive couplers, on motor terminals.

1.3. Technological lock and objective of the Ph.D thesis

The technological lock here is the ability to safely and accurately detect partial discharge inception voltage in the electric motor fed by its inverter drive under operating conditions. Therefore, the objective of this Ph.D. thesis is to overcome this difficulty by developing an on-line PD measurement method using at the same time non-intrusive sensors and filtering techniques in order to assess insulation system performance to provide relevant information and feedback on electric motor design.

This Ph.D. thesis is the result of a three-years work within the "Dielectrics Material in Energy Conversion" team of Laplace Laboratory in Toulouse, France, whose one of its recognised activity is in the field of partial discharge detection. This work has also been carried out in close collaboration with electric car manufacturer Renault.

1.4. Main contributions

- Use of a non-intrusive, cost-effective sensor associated with a high-pass filtering in order to safely and accurately detect partial discharges and reject noise generated by the inverter drive. This sensor-filtering combination proves to be very efficient for detecting partial discharge inception voltage in electric vehicle machines in different off-line experimentations. Above all, the main achievement is the ability to detect partial discharge on-line in a running electric motor under operating conditions fed by an inverter drive in the very harsh industrial engine test bench environment.

- Use of a fully configurable bipolar inverter drive associated with a high voltage power supply in order to feed an electric vehicle stator off-line with inverter-like signals. Technology used in this equipment has been chosen to create rise time comparable to real inverter drive use in electric vehicle. This equipment allows the ability to supply an electric vehicle stator, either one phase at a time or three-phases at the same time, and to reach partial discharge inception threshold. Moreover, voltage waveforms are entirely adaptable so that this equipment is able to create a large range of inverter-like waveforms, from simplest to more complex ones, in order to test assumptions regarding the nature of the discharges.

- In an electric stator or motor fed by an inverter drive, observation of partial discharge signals which are only detected during rise time and not during the following voltage plateau. Moreover, once a partial discharge has occurred in a rise time, none will occur in following rise time until polarity has changed with our testi conditions

- Visual observation of light-emitting surface discharges in stator end windings and slots when fed off-line by the high power inverter drive in our experimental conditions. From that observation, study of the physics of discharges on a twisted pair when fed by the high voltage inverter, using an intensified CCD camera, has been carried out in order to try to explain the physics of the observed surface discharges compared to sensor signals.

1.5. Contents

This thesis is organized into the following chapters

Chapter 2: Technological background.

This chapter contains technological information about the constitution of an electric vehicle and the electric motor. The PWM inverter drive main concepts are presented and illustrated. Key points regarding the electrical stress generated by the PWM inverter on the motor are presented.

Chapter 3: Electrical insulation system and partial discharges in electric motor fed by PWM inverter drive.

This chapter contains information on constitution and main characteristic of insulation system. The basic mechanism of creation of partial discharge and its negative effects on the insulation system are presented. Finally, keys points regarding off-line and on-line testing, including standard EIC procedure and its limitation are explained.

Chapter 4: Experimental set-up, test procedures and results.

This chapter contains the logic sequence of four experiments, growing in complexity, starting from detection of partial discharge on twisted pair to on-line detection on an electric machine. All experimental results and observations are discussed

Chapter 5: Complementary experiment: surface discharge and numerical processing

This chapter is two fold and contains one experiment on the physics of light emitting partial discharge using a intensified CCD Camera. In a second time, a starting step of numerical analysis based on Energy Spectral Density in different frequency band is discussed.

Chapter 6: Conclusions.

This final chapter contains the summary and conclusions of the research work. The future developments are also discussed.

2. Technological background

The recent changes in economical and ecological contexts, emissions standards or political green subsidies have resulted in a more attractive and innovative environment for the development of the electric vehicle, bringing it back in several car manufacturers showcase. As highlighted in the previous chapter, this regain in interest has encouraged classical, internal combustion engine car makers to design an electric vehicle, but not without facing new challenges, especially regarding electrical insulation system and, as the consequence, the on-line partial discharge detection, which is at the core of this Ph.D thesis problematic.
Before going into details, experiments and results, a technical background is needed in order to clearly grab how this study and its problematic are fitting within the whole technological scheme of things.

2.1. Electric Vehicle

2.1.1. Electric Vehicle environment

Obviously, an electric vehicle (EV) uses one or more electric motors for their propulsion with electrical energy either stored on-board or fed externally. The former case (energy stored on-board) is the one which is considered here even if other type of EVs using external power sources could face similar electrical insulation problems.

EVs category includes different sorts of cars like hybrid electric cars, in which an electric motor is paired with an internal combustion engine, or full EV car where all the energy is stored in a battery pack, or in a hydrogen fuel cell, and feeds one or more electric motors. Recently, plug-in hybrid cars have emerged and have a rechargeable battery pack and share both characteristics of an internal combustion engine car and full EV. This study focuses on full EVs where no internal combustion engine is paired with the electric motor.

An important point in studying electrical insulation performance in an EV is to keep in mind that there is no constant mission profile, contrary to externally fed EVs like subways or trains whose acceleration and braking phases are known. Even in an airplane, a typical mission profile could be planned and anticipated, more so with the constant monitoring of flight parameters. So, on-line testing is even more important to realistically assess the performance of the electrical insulation system in EV and put results in regard of off-line motor qualifications, endurance testing and motor design choices. Without any means of really assessing electrical insulation performance on-line, the feedback loop necessary to gaining the mandatory experience in insulation design choices could be weakened, the learning curve could be longer and the performance not necessarily reaching the target even though off-line and qualification tests prove the contrary.

Another important point is the general environment in which the EV powertrain will be running and its unpredictability. Obviously, mechanical vibrations and mechanical stresses are coming into play to a degree and are influencing electrical insulation system behaviour, fatigue and could lead to degradation or delamination. Thermal stresses are important and can range from largely below 0°C to more than a hundred °C when the motor is running. Humidity plays also a role in the apparition of undesired partial discharge phenomena by local inhomogeneities of the electrical field due to condensation and other reasons and could be paired with temperature (icing) or even long-term diffusion within the insulation system. Likewise pressure or chemical interaction with moisture on the electrical insulation system could influence performance by

creating unwanted species altering the insulation materials. Worst-case scenario could still be defined for each or several parameters at a time doing an exhaustive testing off-line on brand new or aged motors or insulation materials samples. Some of these effects will be precised later in this work when it comes to influence on partial discharge.

Even if some actors on the EV market are brand new car companies, significant investments have been made by numerous historical car companies to take the lead in this emerging market. The shift from, and the coexistence between, internal combustion engines to electric motors is not a simple step. A whole new design logic has to be learnt, assimilated, applied and checked by gathering experience or interacting with widely chosen suppliers or subcontractors. From the car manufacturer point of view, it is important to know how its motor design choices and production are really doing in EV in service or on-line especially since its off-line qualified motors failed prematurely only after a few dozen of hours of service.

Last but not least, from an economical point of view, producing electric motors or actuators for EVs is not the same paradigm as producing electric motors for train or airplane applications. It's a totally different logic where the EVs are aimed to be mass produced with the best trade-off between overall performance, reliability and selling cost. Mass production (thousands or even hundreds of thousand of units) means that every little part of the EV counts even if it seems negligible at first, but the design process and choices should be as cost efficient as possible. Indeed, in this burgeoning market, competition is high and harsh to establish a company as an early leader and then to keep that level. In the context of this study, it means that the ability to really match performance to demand regarding the insulation system could prove to be be key to have adequate costs and a reliable and innovative brand image. In the case of a massive on-board use of a detection device it also means, on the other hand that the device used to assess insulation performance should be as reliable, cheap and safe as possible.

All in all, between the especially harsh environment, the economical context, the design paradigm and the uncertainty of mission profile while in service, monitoring insulation system performance while doing fatigue or qualification tests on-line and thus collecting data and experience could prove to be key in increasing reliability of EV's insulation system.

2.1.2. Typical EV Architecture

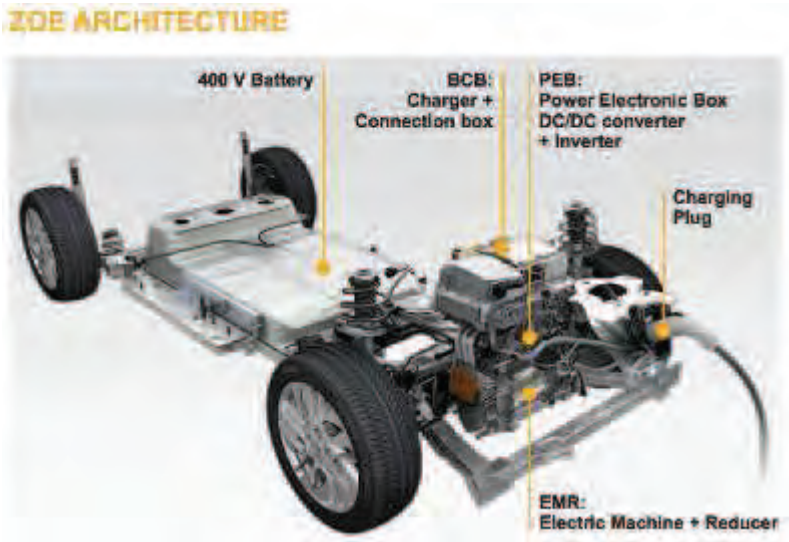

Figure 1 Typical traction EV architecture (public document Continental – Renault) [ARC1]*

Figure 1 shows the typical powertrain of an electric vehicle, which is usually made up of three key elements. An energy storage device, like a battery pack or a hydrogen fuel cell, an electric machine and its reducer and a group made up of a charger, a connection box and a converter.

To date, the battery pack is one of the heaviest parts of the EV, embarking 22 kWh or energy for 300kg and supplying up to 400V. The charger and connection box is made up the Cameleon charger embedded in the car and using elements of the powertrain (motor windings and inverter) to recharge the battery which enable a large range of charging rate, up to 43kW. The connection box (or junction box) is linking the motor to the battery. In the Power Electronics Box, the inverter drive and other power electronics components are located right on top of the electric machine and its reducer. [REN1][REN2]

The key point to note here is how congested is the electric machine reducer zone to perform future partial discharge detection on-line on an electric vehicle. While performing off-line tests on electric stator or motor with similar inverter drive, the positioning of the sensor should always take into account the final geometry of the EV design

**Important Note: Electric stators and electrics motors used in this Ph.D thesis are prototypes only and are not used in the Renault Zoe for commercial use at this point. The use of the above picture is for demonstration purpose only.*

2.2. Electric Motor

There are four principal types of AC electric motors used in industrial applications: squirrel cage induction, wound rotor induction and synchronous induction motors. All motor types are based on the same physics principle in which a stator generated rotating magnetical field is driving a rotor, thus converting electrical power to rotating mechanical power. The main components of electric motors are the following as in Figure 2.

The **rotor** is the moving part of the electric motor which turns to deliver the mechanical power. The rotor has a magnetic field, created either with a permanent magnet or induced or created by electric power, which interacts with the rotating field of the stator to generate the rotating torque.

The **stator** is the stationary part of the motor and is usually made of windings. The frame of the stator in which windings are located is made of thin metal sheets that are insulated to each other and laminated to reduce energy losses.

The **air gap** is the thin space between the rotor and the stator and should be as small as possible.

The **windings** are usually made up of conductive cooper wires laid out in a specific and symmetrical pattern to form electromagnetic coils and are wrapped around and within the stator core. The magnetic flux is travelling from coil to coil, thus to creating a rotating magnetic field. All three phases axes could be seen in Figure 2 (red arrows).

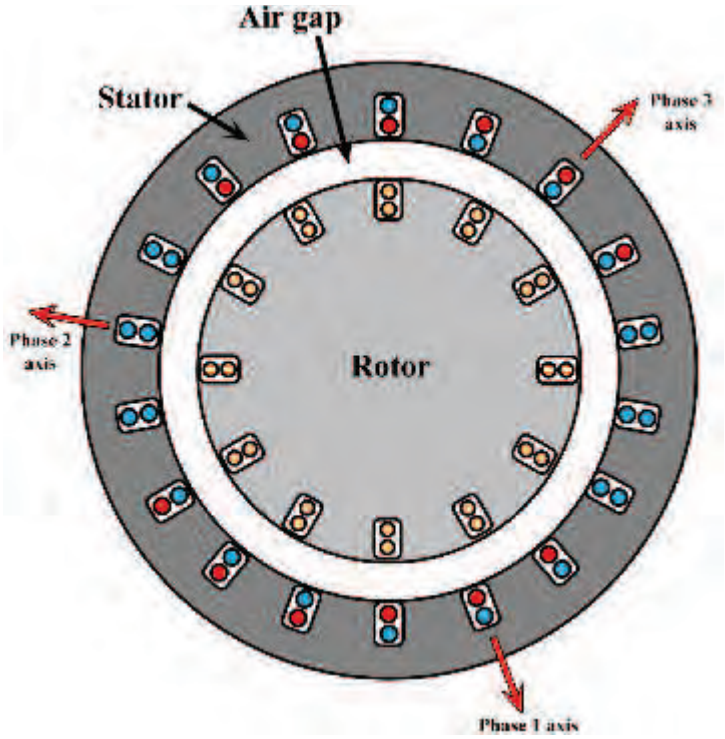

Figure 2: Simplified AC Electric motor – sectional drawing

2.2.1. Squirrel cage induction motor

The most commonly used motor is the squirrel cage induction motor because of its low cost and proven reliability. This motor uses a symmetrical squirrel cage winding made up usually of cooper bars placed within rotor slots. All these rotor conductors are not insulated between each other but are connected together by the means of shorting ring so that a circuit is made. As the rotating magnetic field generated by the stator passes through rotor conductors, a current is induced and is forming the corresponding number of poles in the rotor. The rotor poles accelerate and try to rotate in synchronism with stator poles until a state of equilibrium is reached in which the rotor speed is slightly less than the speed of the rotating field in the stator. Torque provided is function of this difference between stator and rotor rotational speed. For that very reason, these motors are called asynchronous motors

2.2.2. Wound rotor motor

The wound rotor is used when special requirements are needed in the starting phase where limiting starting current, controlling torque, position or speed is important like in EV applications. This motor is made of a three-phase rotor, insulated rotor windings. An external power source, three phases as well, is connected to the windings by the mean of carbon brushes and rings. The characteristics of the external power can be adjusted to modify the torque of the rotor, for example to reduce the current in the starting phase while having a higher starting torque.

2.2.3. Synchronous motor

Finally, the synchronous motor is used in a large range of applications and, like in EV case, where an accurate control of speed and power factor is needed. The rotational speed of the magnetical field within the stator is, at steady state, equal to the rotational speed of the rotor. The rotor could be energized either by permanent magnets or by DC current excitation. The latter usually feeds the rotor of the synchronous motor during during the starting phase, as an induction motor, is finished so that the rotor then puts itself in synchronism with the rotating stator field. [REN4]

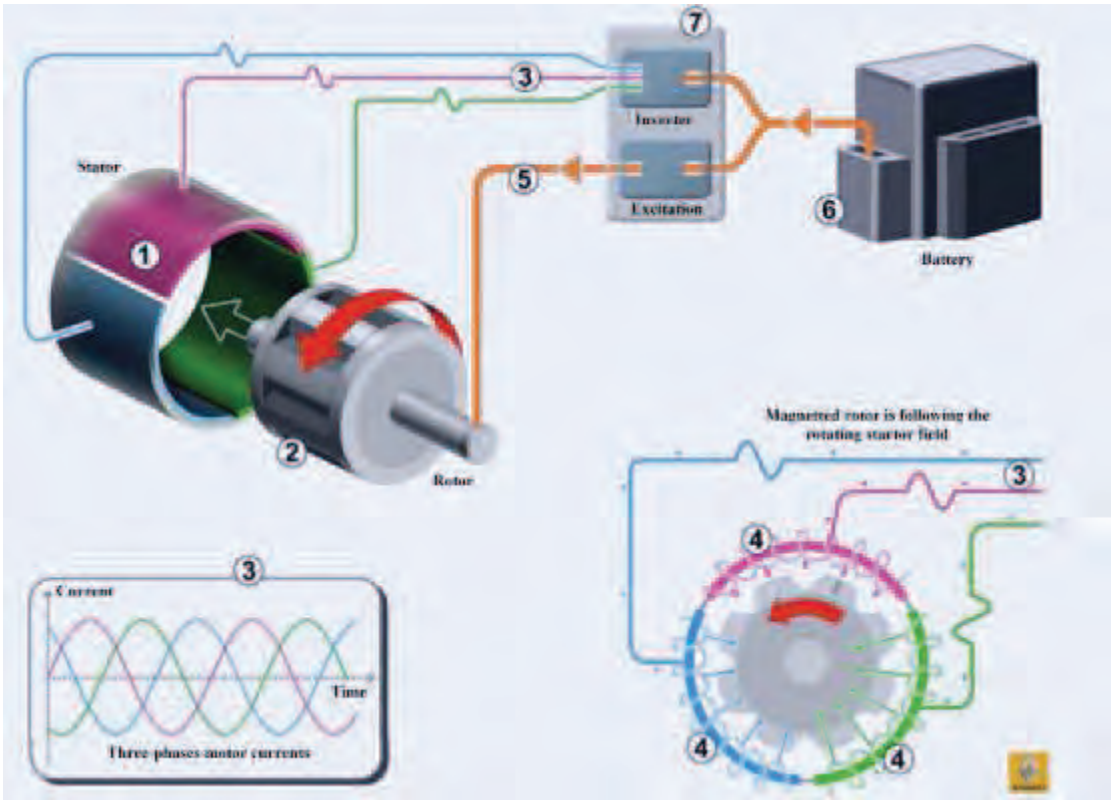

Figure 3 : Synchronous rotor wound motor, translated from [REN4]

The above figure is a simplified diagram of the functioning of a three-phases synchronous – rotor wound motor. The stator (1) is fed by the inverter drive (7) to create a three-phase alternating current (3) inducing a rotating magnetical field (4). The wound rotor (2) is fed with a direct current (7) and is creating a constant magnetic field which will tend to rotate in synchronism with the stator rotating field, thus moving the rotor (4). Modifying the inverter drive and excitation allows to drive the motor at different speed and torque. This technique allows for a better control of the power factor. [REN4]

2.2.4. Electric Motor in EVs

In typical EV application, the electric motor is synchronous wound-rotor induction motor of power ranging from 50kW to 70kW with a maximum voltage of 430V. This is an externally - excited synchronous motor – so that no permanent magnet rotor requiring rare earth metals are needed, thus lowering the cost. The electric motor, transmission, differential and parking lock are all accommodated in a single frame as shown in Figure 4. [ARC1] [REN3] [CONT1]

As for the majority of low voltage machines, windings are random wound and so are the prototypes tested in this work. The fact that the inverter drive is right on top of the electric motor allows a reduction of cable length, which is an important parameter as it will be recalled later. The three phases going to the electric motor could be seen in white and yellow in the figure below. From a practical point of view, the electric motor is protected on each side by shields and is totally enclosed in order to protect it from the climatic environment. Thus, it's impossible to place a sensor in the direct vicinity of the windings or end-windings. Placing the sensor right at motor terminals, or within the power electronics box or in the junction box, are the only possibilities to allow on-line detection.

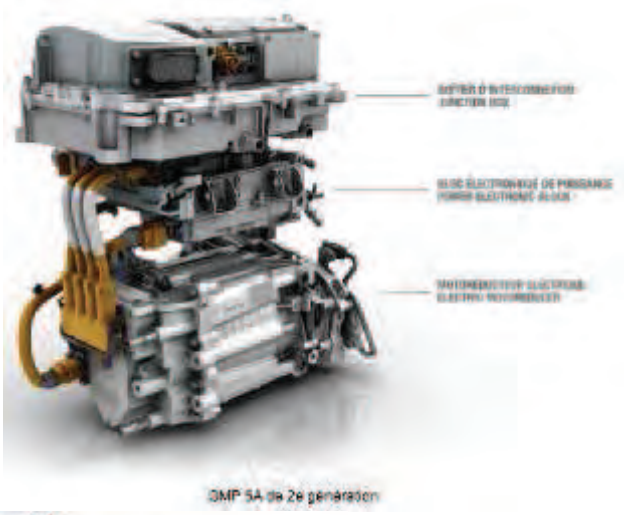

Figure 4 Motor architecture [REN1][ARC1]. On the right Kango ZE GMP (120kg)

2.3. Adjustable Speed Drive and the impact on electrical stress

The Adjustable Speed Drive (ASD) is a device used to control the speed at which an electric motor is running. This equipment usually controls AC motor speed and torque by varying input frequency and voltage. Different techniques could be used to design this speed control function from a purely mechanical set-up, hydraulic device and, of course, electrical components leading to numerous developments in power electronics.

2.3.1. Introduction to ASD

Focusing on low voltage type of motor as those used in EV, the Direct Current (DC) drive was during a long time the leading device due to its simple control in constant speed application (fan, compressor, pumps) or in crane, elevator, mills where the torque could be controlled.

Alternative Current (AC) induction motors which are less costly, need less maintenance (no brushes), more reliable (no collector) and are more compact than DC motors lead to a new paradigm when energy should be saved or conserved. The motivating force behind the evolution of ASD for AC motors has always been energy flux conservation (efficiency), higher performance, higher productivity and at a lower cost. Indeed, many applications of motors do not always require the full power output, electric energy can thus be saved by slowing down the motor when high output is not required.

These reasons encourage the design of better ASD to use AC motor with all their advantages in more applications. But, early AC PWM ASD had several drawbacks like switching losses in inverters, voltage reflection in motor cables, motors reliability problems and an increased complexity. From Silicon Controlled Rectifiers (SCR), to Gate Turn-Off transistors (GTO), Metal Oxide Semiconductor Field-Effect Transistor (MOSFET) and more recently Insulated Gate Bipolar Transistor (IGBT), several components helped towards the larger use of AC PWM ASD. [EPRI93]

2.3.2. Insulated Gate Bipolar Transistor

The core component of the inverter drive to date, the IGBT, is a high-efficient and fast semiconductor power device used to switch power. It combines the best of the power MOSFET and the bipolar transistor in a single component. It was firstly introduced in the early 1980's. Thanks to developments in power electronics, IGBT began to be commonly used in the early 1990's. Now affordable, efficient and reliable, IGBT are widespread in EV application as well as in other areas. As these innovations happen, maximum switching frequency increases up to 20kHz range or more, thermal efficiency increases allowing even higher switching frequency, power losses decrease significantly, size of power module decreases and rise times are shorter and shorter. [OLI95]

2.3.3. Inverter Drive

The pairing of low voltage, low cost and reliable inductive AC motors with inverter drives using IGBTs is forming a very common ASD. As an example, in EVs application where the energy is stored on-board chemically and with the use of an AC driven motor, this function is carried out by a PWM inverter drive.

The inverter drive is transforming DC from the battery in order to AC to supply the motor with the adequate voltage waveform to control its speed and torque. Energy efficiency is, once again, the key since the energy is available in a limited amount, even with regenerative braking. Cost efficiency is very important as well since the EV is supposed to be mass-produced.

Before showing how the use of PWM inverter drive featuring IGBTs lead to a negative impact regarding the insulation system in low-voltage motor applications, a quick overview of the design and principle of a two-level inverter drive is needed, the most widespread in industrial application.

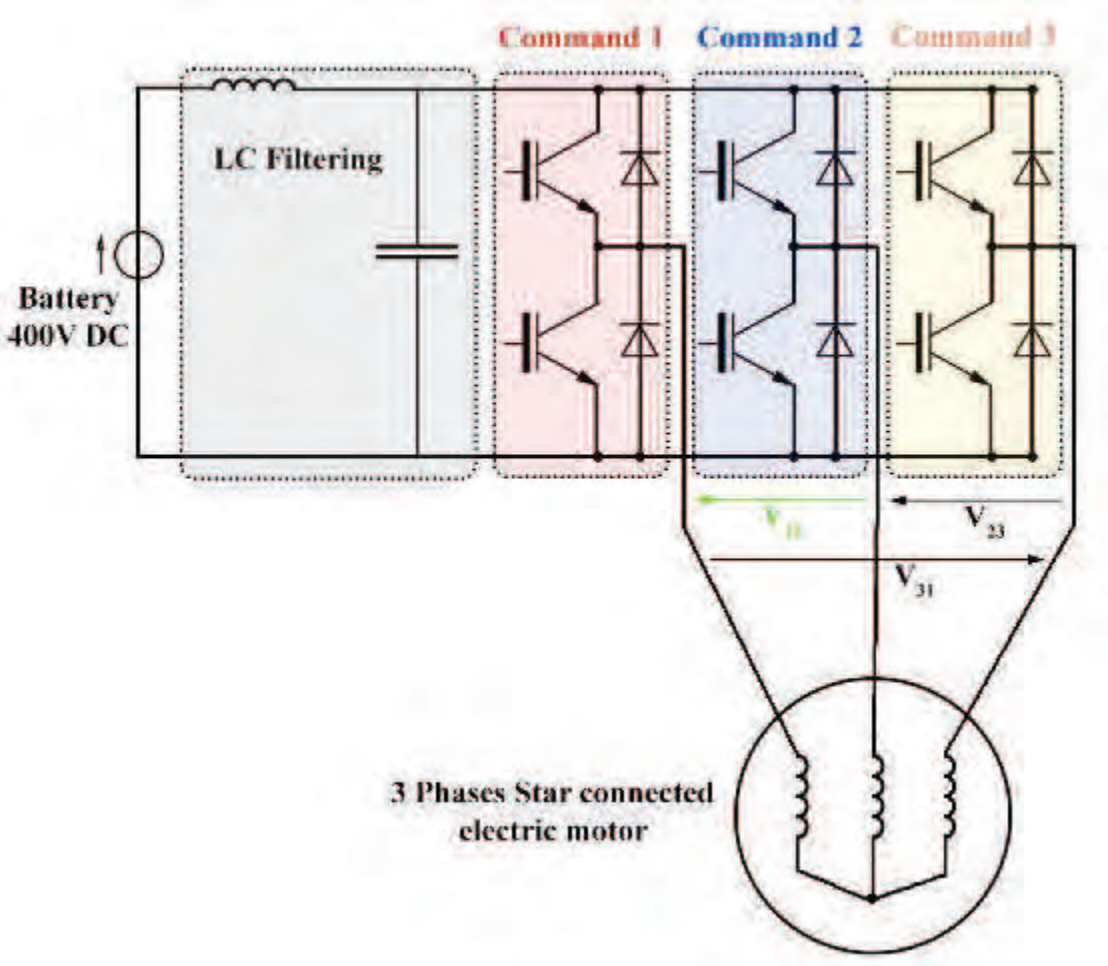

Figure 5 : Inverter drive

The aim of using a power inverter drive is to transform DC current into AC current to feed an electric motor. In itself, the inverter drive is not producing any power and it should consume by its operation as less power (power loss) as possible to be efficient. The electric power transformed by the inverter is supplied by the DC source. In most EV applications, the input voltage is set to +400V DC, in order to allow the power source to supply enough current for the

range of application in term of torque or speed for the electric motor. The DC source is also able to collect energy form the motor in regenerative braking phase as in most EVs.

In figure 5 above, the circuit of a basic three-phases inverter is presented. The battery pack is supplying +400V DC electric power. In grey, a passive filtering (usually low-pass) circuit could be noticed. Although this filtering function is not in itself about power converter, such components are definitely needed due to the very nature of the electrical conversion. Here only an input filter is represented and its duty is to filter to avoid harmonics disturbance coming from the converter on the battery supply. LC output filters could be placed at he output the converter unit to have a purer voltage waveform without switching low frequency harmonics.

The switching components are in red, blue and orange. In a three-phases inverter, each phase has its own switching components and is known as “leg” or “switching cells”. So each switching component is directly “in line” with a single electric motor phase. All inverter’s legs are similar, so the output voltage of each leg is only function of the DC supply voltage and the switches status.

Each switching component is made up of 2 three-terminal transistors, IGBT here. Each IGBT is associated with its freewheeling diodes to allow bidirectional current flow. In each switching cell, if the upper IGBT is closed, the phase is connected to the DC source 400V. On the contrary, if the lower IGBT is closed the phase is connected to zero voltage. The two IGBT should not be closed at the same time to prevent a short-circuit on the battery.

From a practical point of view, each IGBT has a switching time that should be taken into account and the main task of improving efficiency in inverter drive is to reduce this switching loss switch . This non-ideal behaviour is also leading to other potential issues, that are not the purpose of this work, when the two IGBT are open at the same time.

2.3.4. Pulse Width Modulation

The most commonly used way to operate an inverter drive is the Pulse Width Modulation (PWM) switching. This method stands out for its performance speed and torque control (vector control theory). The widespread adoption of PWM switching method has been possible thanks to breakthrough in power electronics device, lowering cost and power loss and increasing efficiency.

After the circuit description of a three-phases inverter drive, it's important to focus on the PWM in itself, which should not be confused with the inverter drive. Below is a typical sinusoidal – triangular intersective PWM command, which is the simplest and easiest way to represent for our purpose.

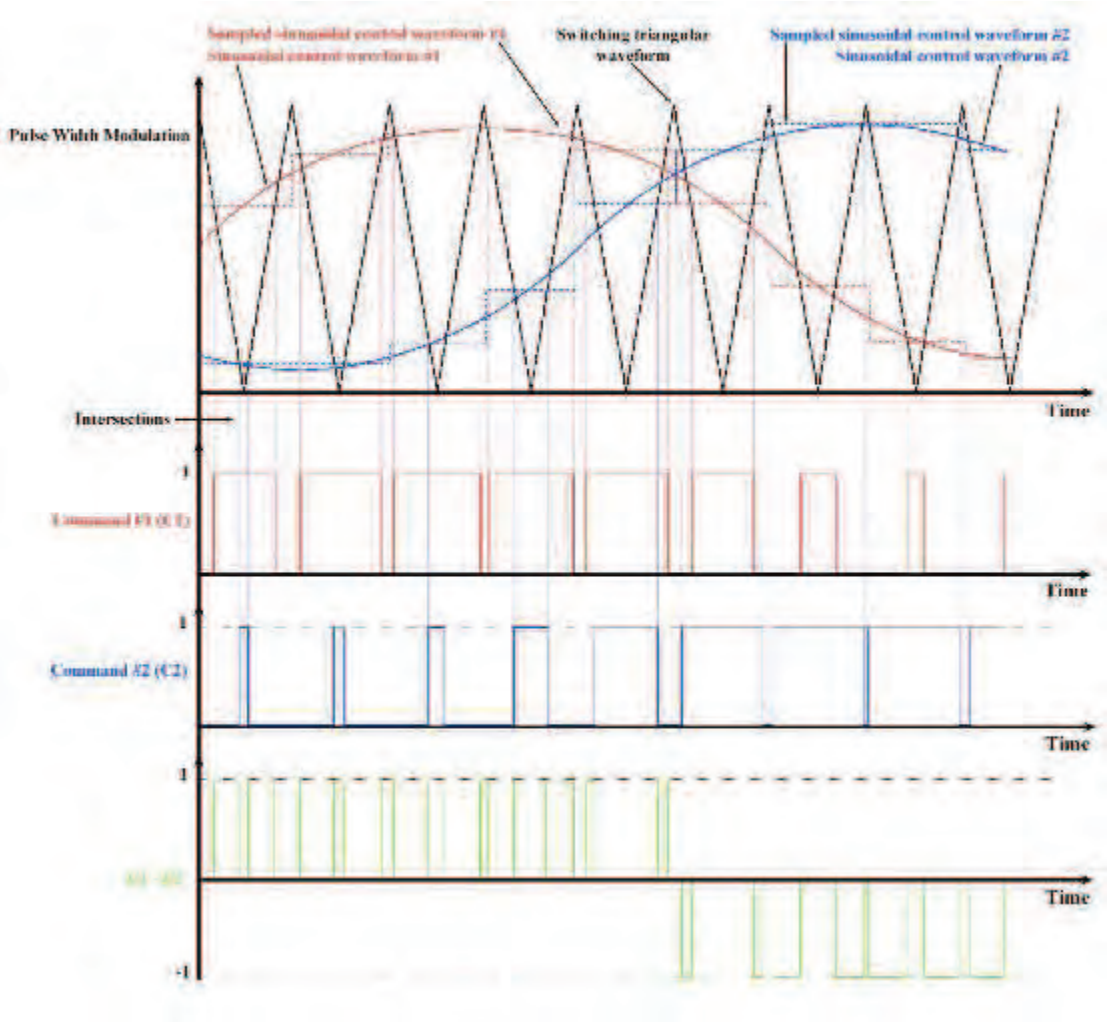

Figure 6 : PWM theory

The intersective PWM relies on the comparison of a triangular waveform (in black) with a reference signal [SCHO64] and has often been done using an analog comparator providing that the frequency of the triangular waveform is larger than the frequency of the reference signal. This reference signal could also be sampled to allow a simpler, efficient memory, use in micro-controller application [BOW85]
In both case, the logic of the comparator is the following:

- If the reference signal > triangular waveform, then output = 1.
- If the reference signal < triangular waveform, then output =0.

In the above diagram, 2 commands have been represented in blue and red with a phase shift of 120°. These two references signals have been sampled at the same frequency than the triangular waveform, which is actually the switching frequency.

By applying the aforementioned comparison on intersection points, the two commands for each phase could be defined over time. As a result, each switching cell will be driven accordingly and produce a very high number of voltage pulses of different length on each phase. The higher the switching frequency, the higher the number of voltage pulses per unit of time. The green signal is representing an image of the voltage between phases 1 and 2.

From a practical point of view, numerous different PWM methods could be used and this example is only presented to show why and how voltage pulses are generated by PWM inverter drive.

In our application with a DC voltage of 400V, the output voltage between each phases in a bipolar three-phases inverter drive is thus equal to plus or minus the voltage of the DC source or zero (+400 V, 0V, -400V bus). The rotation frequency of the motor could be controlled by the sinusoidal control waveform, the number of pulses and the width of pulses. This will result in a period that is either longer or shorter. In addition, even if the amplitude of each pulse is constant through time and determined by the level of the DC voltage, the width of the pulse is related to the average output voltage and the larger the pulse, the larger the average output voltage.

2.3.5. PWM Inverter drive and phase-to-phase voltage: overvoltages and reflections

One of the main problems when connecting an inverter drive to an electric machine is the presence of overvoltage at the motor terminals as seen in figure 7 below. To better understand this mechanism, one should focus on one voltage pulse coming from the inverter drive at a time. A reflection phenomenon is occurring on an incident wave travelling at a fraction of the speed of light in a cable (depending on the physical construction of the cable) when there is an impedance mismatch between the cable, acting as a transmission line, and the impedance at the end of the cable. At the cable's end (or at motor terminal), the reflected wave is added to the incident wave and the total voltage is thus increased. In other words, when pulses like voltage signals are transmitted along a line, which is not terminated by its characteristics impedance, reflections could occur. This phenomenon has been known and studied for a long time [WEED22] [RUD40] [BEW51]

From a practical point of view, the impedance of an electric motor is always larger than the cable impedance. The inverter drive is usually of low impedance, so when the reflected wave could then reach the inverter, a new reflection (negative) occurs this time and so on. In fact, the maximum voltage at motor terminal (including reflection amplitude), deriving from the transmission line theory, could approximately double in case of large impedance mismatches. The total amplitude is also function of the rise time relative to the travelling speed and of the cable length. [PERSS92][JOUAN96][SAUND96][KER96]

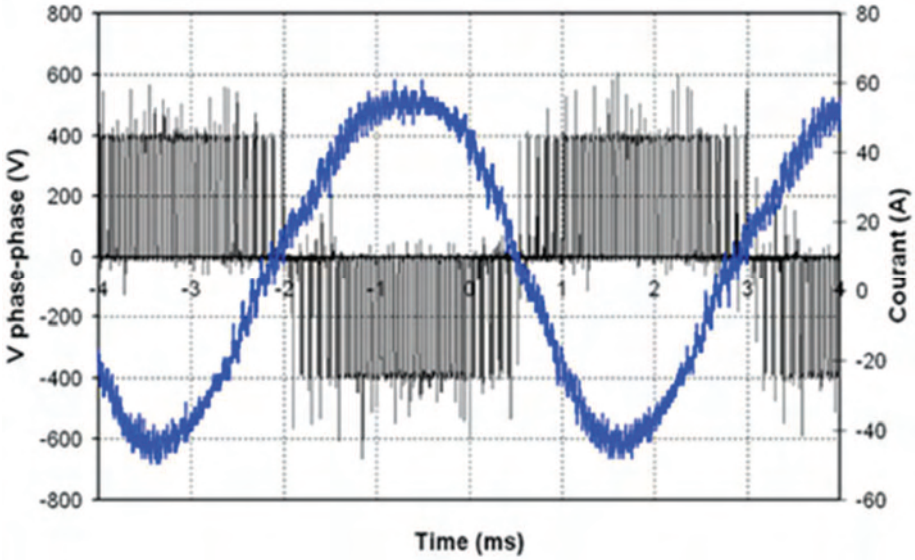

Figure 7 : PWM voltage between phases (black) and current on a phase (blue)

As explained previously in the PWM section, the voltage between phases is not sinusoidal but composed of a series of pulses of the same amplitude but of different width. This recording, in Figure 7, of voltage between phases on an engine test bench with a long cable length, clearly demonstrates positive or negative overvoltages at motor terminals caused by impedance mismatch. The PWM inverter drive does not generate a perfect AC sinusoidal current on an observed phase as well.

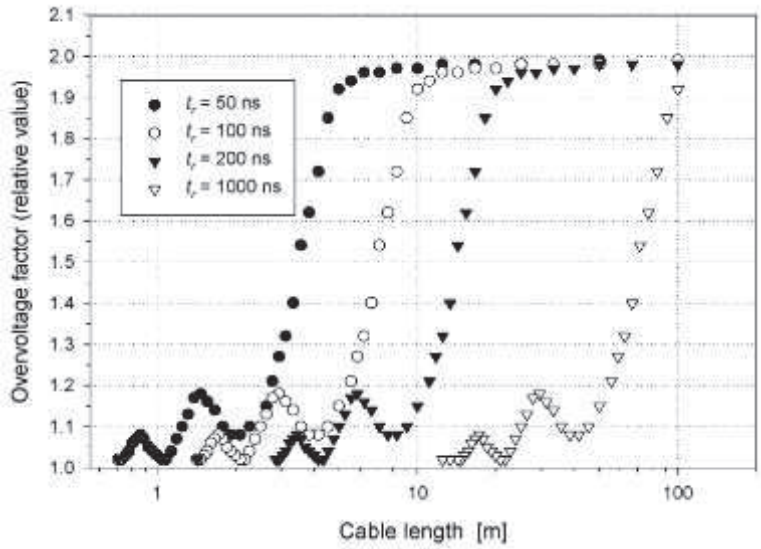

Figure 8 Influence of cable length and rise time as in [FABIANI]

As shown by D. Fabiani in his Ph.D Thesis, mathematical models and circuits could be used to define the amplitude of overvoltage function of cable length and rise time when a pulse shape is applied on a machine winding. The overvoltage factor is defined as the ratio between the peak voltage at motor terminal and the inverter drive output voltage. His figure, summarizing the results obtained, shows that the shorter the rise time (4 different rise times), the larger the amplitude of the overvoltage at motors terminals for a given cable length. Another conclusion is that the longer the cable (100m here), the larger the overvoltage will be whatever the rise time. The maximum overvoltage approaches two times the inverter drive output voltage.

It explains why, with the advance in power electronics in regard to rise time, the failure rate is more important in PWM-fed machine. Indeed, the IGBT inverter drive could produce rise time ranging from 50 to 200ns thus increasing the overvoltage. Even more shorter rise time could be expected with the most recent technology advances towards increased efficiency in inverter drives where a key point is reducing dead time as much as much as possible to reduce power loss. Indeed, designing switching devices with rise times as short as possible is reducing power loss while both “transistors” are off. It also means that an electrical motor performing without any problems with one generation of power converter could be affected by the use of a more recent power converter technology.

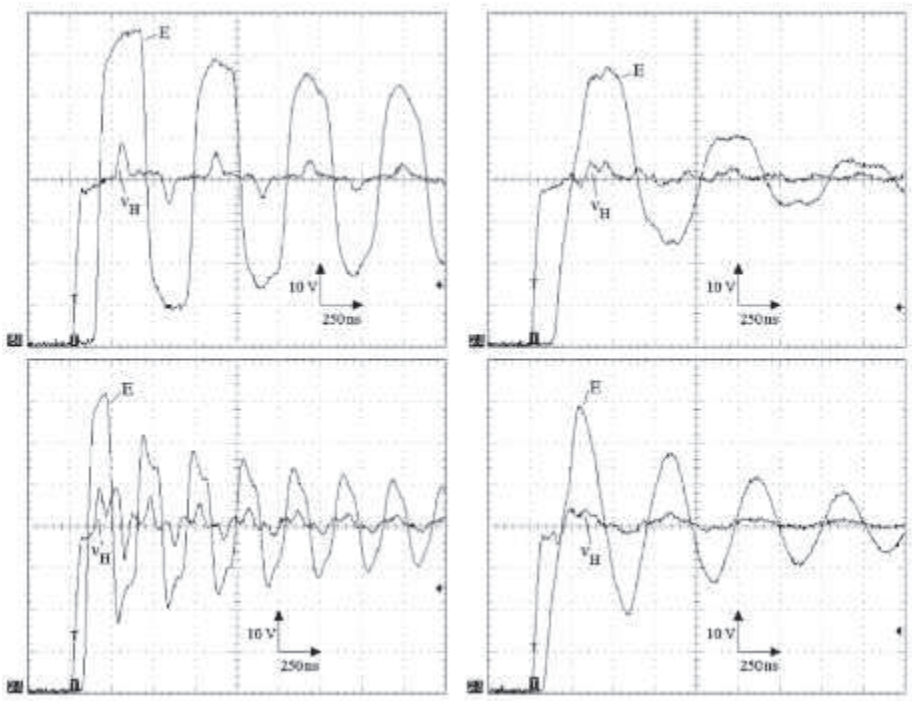

Figure 9 Wave reflection as in [NEASCU]. Bottom (13m long cable), Top, (26m long cable), Left (open circuit), Right (Regular phase connected)

As shown in [NEACSU] Ph.D thesis, the period of wave reflection generated by an inverter drive is function of the length of the cable. The shorter the cable, the shorter the period and the quicker oscillation loose amplitude as shown in figure 9.

In addition, the high number of pulses per second created by a PWM inverter is even more accelerating the degradation of the insulation system compared to a partial discharge (PD) free electrical motor fed by a 50Hz sinusoidal voltage.

Thus, the combination of the aforementioned factors (rise time, impedance mismatch, switching frequency) is amplifying the electrical stress on the winding insulation system, contributing to its ageing, moreso when reaching the partial discharge inception voltage (PDIV).

2.3.6. Phase to ground voltage

Phase to ground voltage waveform is composed of high frequency bipolar voltage pulses. The phase-to-ground voltage presents similar pulse modulations than the phase-to-phase voltage but the amplitude of the latter is half the DC bus whereas the amplitude of the former is the DC bus voltage. In other words, if the phase-to-phase voltage amplitude is usually + or -510V then the phase to ground voltage amplitude is + or – 255 V. The ground insulation is usually made up of thick tapes to withstand high voltage and avoid phase-to-ground short circuit between the windings and the stator frame (usually connected to ground). As shown in the figures below, even the phase-to-ground voltage is affected with overvoltages caused by impedance mismatches between cable and motor. Moreover, voltage spikes could be observed on figure B when a switching is occurring on another phase. [MBA96] [LEB98]

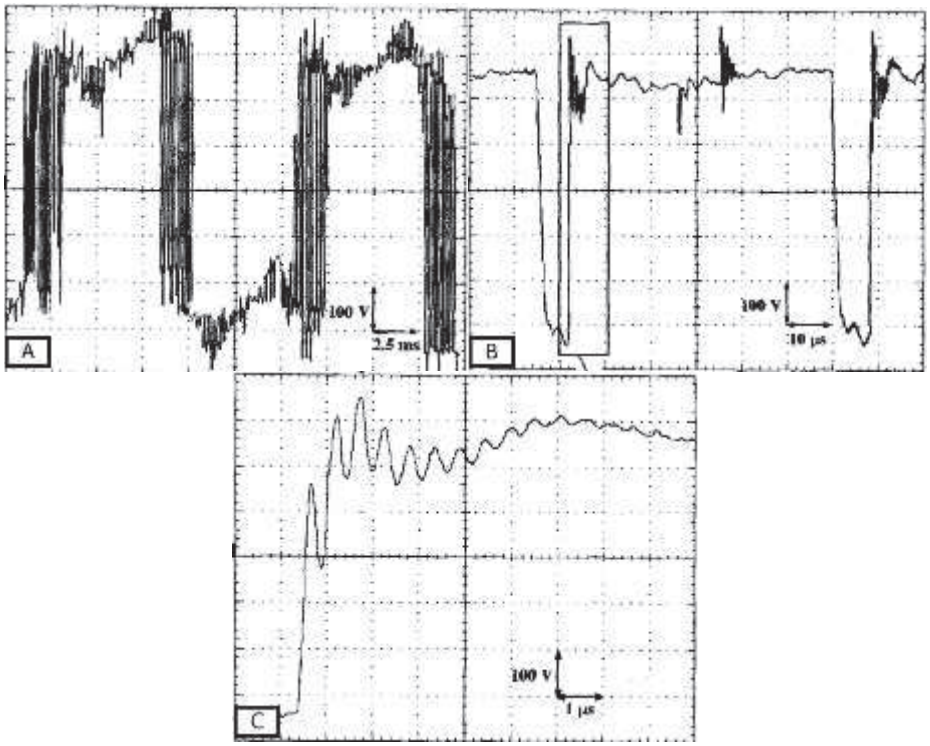

Figure 10 Phase-to-ground voltage at different time scale as in [MBA96] and [LEB98]

2.3.7. Turn-to-turn stress

At the beginning of studying the reason behind the higher failure rate of machine fed by inverter drive, most of studies focused on the voltage at motor terminals caused by impedance mismatch and rise time. But, what is equally, if not most, important in the way the electrical insulation is affected by a PWM inverter drive, is the shape of the turn-to-turn stress. Indeed, some failures are caused by the voltage distribution in the windings. While voltage distribution along a winding is usually uniform at all time under 50Hz voltage supply, (the winding is seen as a simple inductance), the distribution is very non-uniform under PWM voltage because of the propagation time of the pulse in the winding.

Indeed, the voltage is not propagating immediately along the winding causing a delay and dielectrics losses in the stator frame are decreasing rise time and smoothing the eventual overvoltage. It means the high frequency contents, which are "blocked" by the motor inductance are evacuated to ground by parasite capacitance. As highlighted by R.J Beeckman, 80% of the voltage of the most short rise time (over 5kV/µs) is concentrated on the first turns of the first coils. [BEE99] [BON96][STONE00]

An accurate and precise description and simulation of such behaviour would require a large amount of time, finite element analysis and equations. An approach using transmission line theory is simpler yet should take into account loss in the windings. [COR 82] [WRI83] [MBA97] [LEB98-1][LUF 99] [BID01]

In his Ph.D thesis, Claudiu Neacsu [NEACSU] did a lot of simulation and measurements on instrumented electric motors to highlight this propagation phenomenon. Below are figures extracted from his work.

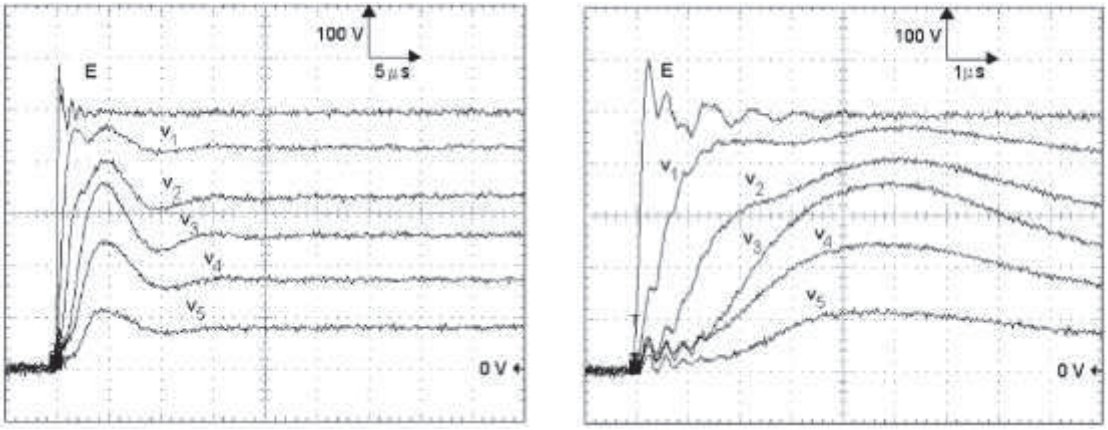

Figure 11 : Voltage difference between successive coils (last turn) with two time scale as in pp. 34 [NEACSU]

In the above figure, the delay of propagation of the voltage shape (E) in the successive coils is highlighted. The last turn of the coil is seeing less and less voltage because of the "dividing bridge" behavior.

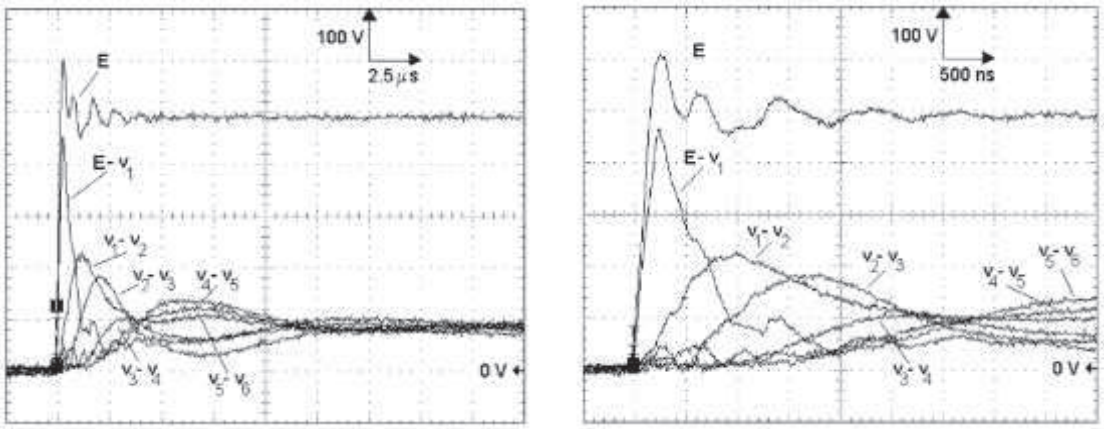

Figure 12: Voltage between coils (last turn) with two time scale as in pp35 [NEACSU]

As shown in figure 12, the turn-to-turn insulation could be severely stressed during the first µs of the pulse where large voltage differences could be observed between turns of coils of belonging to same phase.

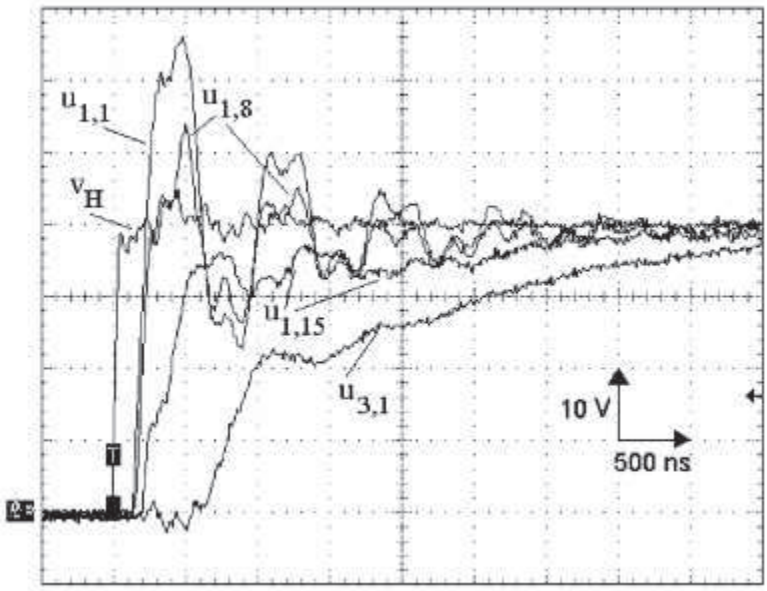

Figure 13: Voltage at turn 1,8 and 15 of the same coil as in pp.37 [NEACSU]

This time the voltage measured at turns of the same coils is observed compared to the inverter drive voltage shape. First reflexions are happening due to an impedance mismatch in the cable and overvoltage on the first turn is a bit more than 50% of the applied voltage. Then, the delay of propagation between turns 1 and 15 of the same coil and the attenuation effect of the overvoltage could be observed in the above figure. For reference, the voltage measured at the first turn of the third coil is plotted to illustrate the propagation delay a long the whole phase (6 coils).

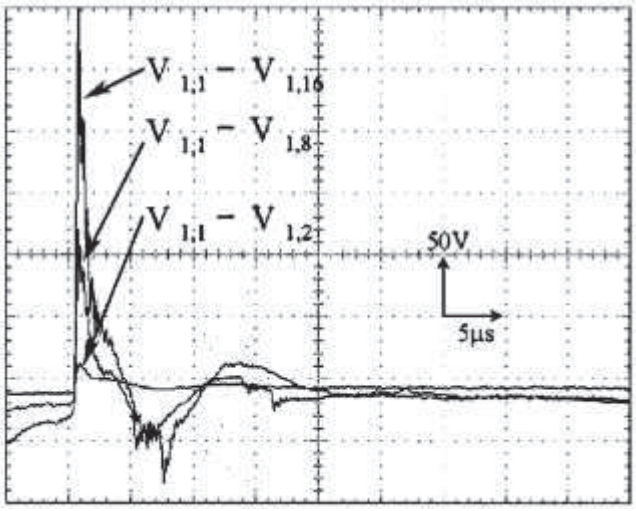

Figure 14: Voltage between turns of the same coil as in [BID01]

In figure 14, the voltage difference between turns of the same coils is plotted, this figure is from [BID01]. As it could be hinted in the previous figure, the voltage difference between the turns is larger with further away turns, for example between turn 1 and 16.

It means that, at the first instants of the pulse voltage, the combination of very short rise time, reflexions phenomena (impedance mismatches) and propagation delays are putting high demands on turn-to-turn insulation system whereas he may not be designed to withstand such electrical stresses.

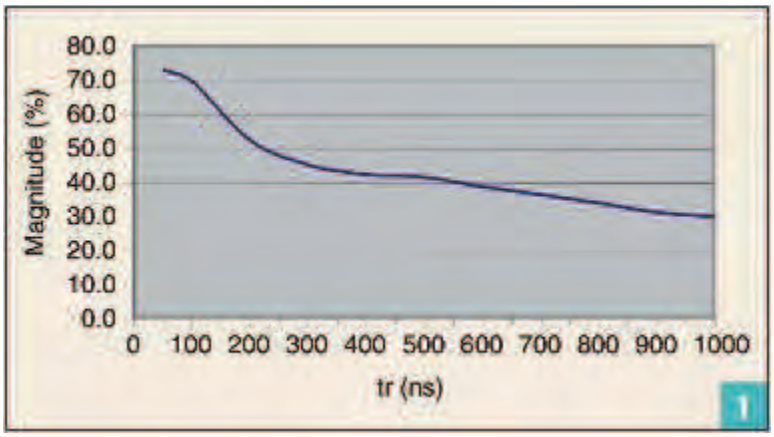

Figure 15: Voltage drop across first coil versus rise time (ns) as in [FENG03]

The more important point is the following. While at the first instants of the pulse, only the very first turns of a whole phase are seeing voltage and reflexions whereas almost all remaining turn are not seeing any, random wound motors are likely to have several zero potential turns in the vicinity of the few very first turns thus increasing the electrical stress on turn-to-turn insulation system. This may result in the apparition of partial discharge in the first turns of a windings and lead to failure close to motor terminals. Indeed, most of the time failure seems to be located either at very first or very last turns of one phase. [BON92][FENG03]

3. Electrical insulation system and partial discharges in electric motor fed by PWM inverter drive

3.1. Dielectric materials

3.1.1. Dielectric properties of insulating materials: definitions

Electrics motors insulation system has been subjected to greater demand in term of performance, cost, and environmental exposure. Adding to the equation the advent of ASD and PWM and the resultant waveforms and electrical stress on low voltage machine has increased. What are the physical key concepts to understand quickly how behaves an insulating material? Here are key definitions [BON97]

- Insulating materials are non-conductor material able to withstand an electrical stress. But not all electrical insulators (resistance to current high) are good dielectrics since the ability to withstand an electrical stress before breaking down is important as well.
- Thus, the dielectric strength is a measure of the breakdown electrical field intensity (V/mm).
- The leakage current is a conduction measure (by surface or volume) through the insulating material.
- The permittivity reflects how an electrical field is affected by, and affect, the material.
- Finally, the dielectric loss or constant is how much of the electro-magnetical energy is dissipated as heat within the material, often mentioned as tan delta. Because of the high number of pulses, heating dissipation could be inefficient thus causing over-heating. This can accelerate the aging process of the insulation materials through thermal degradation. □□Y□□□□□

3.1.2. Dielectric properties of insulating materials: stresses and aging

Dielectrics materials are subject to higher and higher demand in terms of operating temperature, starting currents, operating conditions and cycles, transients voltage, humidity and environmental conditions. The use of PWM waveform has added another layer of constraints while the requirement is the same: long life and reliable performance. Major stresses are: [BON97]

- Electrical stress caused by voltage gradient in the material is a contributor to the aging of insulation system, even under the breakdown voltage.
- Thermal stress is caused by a combination of power losses and the environment in which the motor is operating. Under high temperature, physical and chemical processes could occur thus weakening the insulating material. It has been shown that the influence of temperature could decrease lifetime of a sample for a given voltage by accelerating thermal aging and thus making the insulating materials more vulnerable to electrical stress. [BON92] In the case of EV, thermal shock between 0° C and 100°C could be used in fatigue tests
- Mechanical stress is caused by vibrations of the motor, shocks during operation or during the construction. A difference of thermal coefficient expansion could contribute to mechanical stress. Delamination and cavities that develop as a result of machine misoperation, thermal aging, or vibration. Vibrations and centrifugal force could also cause wires friction in bad-impregnated rotor leading to default (Table 1)

- Environmental stress such as ozone, oxidation, radiation, chemicals, dust causing abrasion or moisture could alter the performance of the insulation system. In electric vehicle environment, salt spray corrosion test is one of the harsher for the electric motor. Icing and water diffusion within the insulation system could cause problems as well.

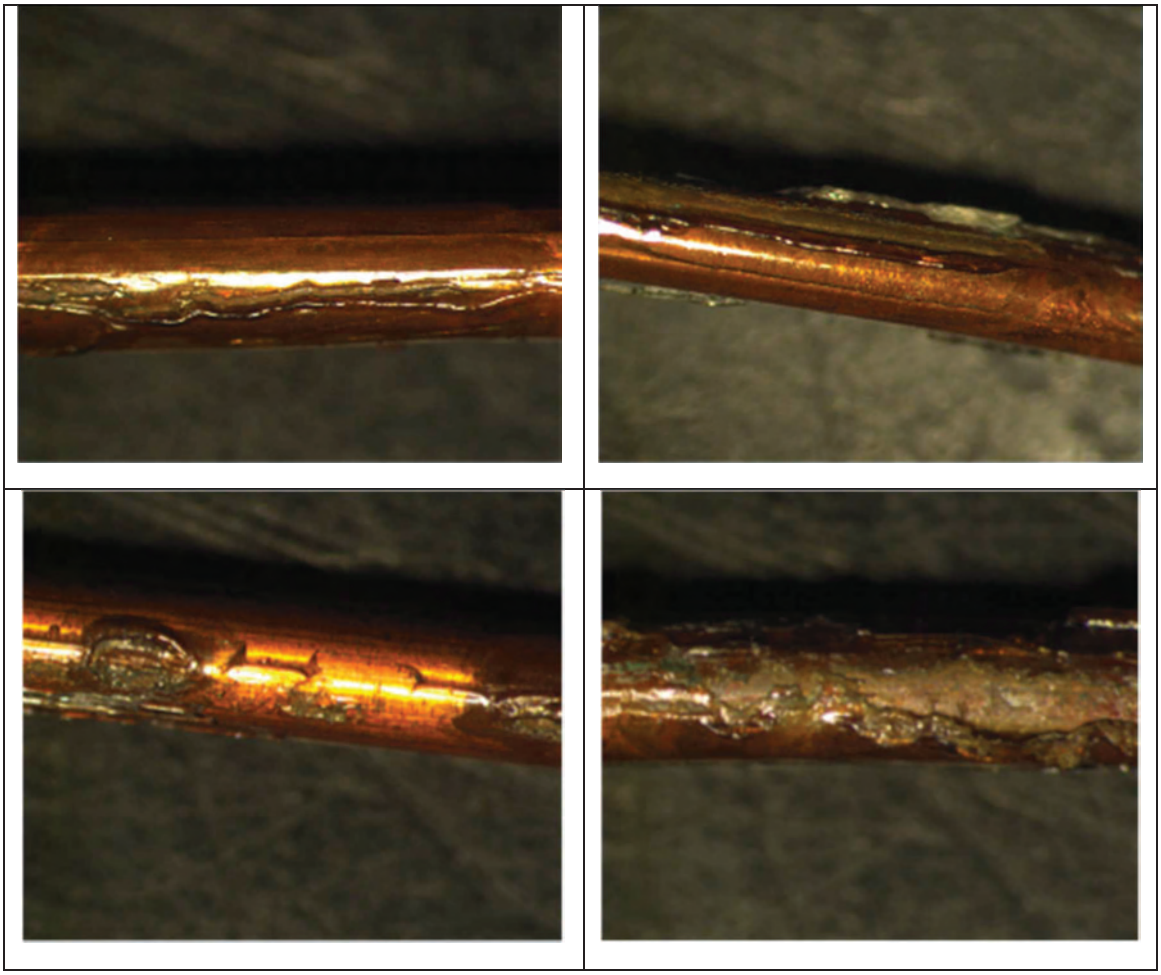

Table 1 : Enamel wires friction in rotor (F.Fresnet)

3.2. Electrical insulation system in random wound motor

Insulating system is usually the weakest link regarding the reliability of electric machine. The current trend is to use insulating materials close to their limits or to give them specific properties. It's a permanent trade-off between performance and cost.
An usual AC electric motor insulation system is made up of three different types of insulating materials: Phase to stator (ground), phase to phase and turn-to-turn.

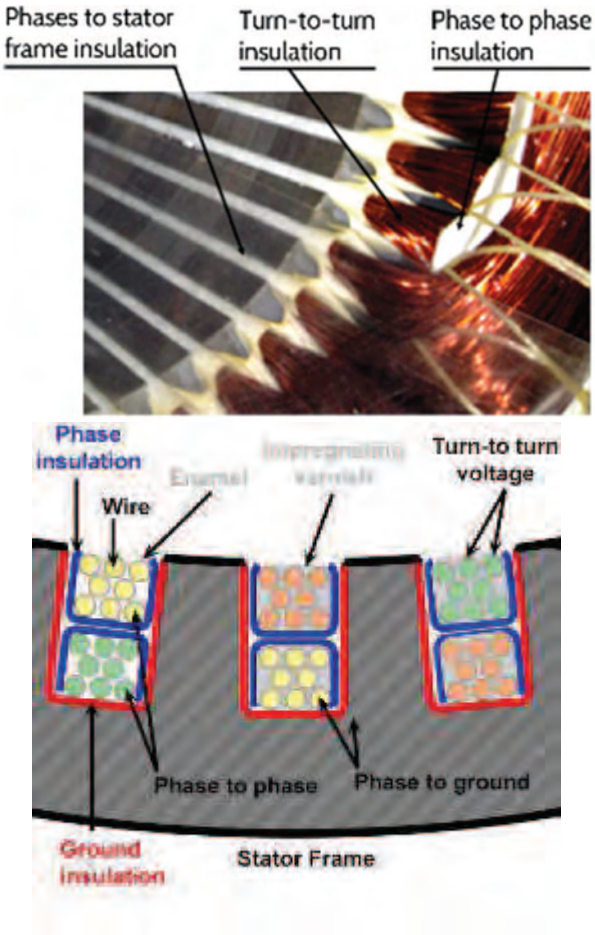

Figure 16 : Insulation system – sectional drawing

The figure above shows a typical low voltage, 3 phases, random wound stator with its different insulating systems:

- Wire insulation (grey – enamel): The aim of this insulation is to prevent short-circuit between adjacent wires. Usually, in low voltage machine, conductors wires are just varnished with an insulating enamel of a thickness ranging from 20 to 100µm
- Ground insulation (red): The aim of this insulation is to prevent any direct contacts between conductors wires and the stator frame which is connected to ground. The enamel layer of the conductors is reinforced with insulating paper (200-300µm thick) which, not only strengthening insulating system, is also used to facilitate the insertion of phase within the stator frame.
- Phase insulation (blue): The aim of this insulation is to prevent contact between wires of different voltage belonging to different phases. In addition to the basis enamel layer, insulating paper could be used as well.

- Stator frame (black): Once the motor has been wounded entirely, it is completely immerged into an insulating varnish, filling in the gap or leak and reinforcing the whole insulation system. This varnish has also mechanical properties to prevent windings to untie and thermal properties to dissipate heat. It is also protecting the conductors from dust or moisture.

Voltage differences are indicated with double arrows for phase-to-phase, phase to ground and turn-to-turn voltage to better understand the relation between the inverter drive electrical stress and the insulation system.

For the sake or clarity, end windings have not been represented in the drawing but could be observed on the picture at the forefront. All phases are brought together at the outside of the stator to connect with the connection box, linking to the inverter drive. In end-windings, phases are only separated by phase-to-phase insulation system. In 50/60 Hz applications, properly made random wound, low voltage (up to 690V) machines are not likely to experiment any aging or deterioration of the insulation itself caused by electrical stresses. Indeed, voltage waveform and magnitude are not large enough.

But, as shown by Persson [PERSS92], PWM inverter drives are causing significant voltage ageing and deterioration leading to a premature failure of the machines. As seen previously, the use of a PWM inverter drive is leading to a very high number of voltage pulses causing non-uniformity in voltage distribution in coils and overvoltage in case of impedance mismatch. As a result of the random wounding process, and as warned in the previous chapter, some turns of the same phase could be adjacent while exhibiting a voltage difference thus creating electrical stress

3.2.1. Voids and imperfection in insulation system

Moreover, by the very nature of the random wound motor process, the insulation system is not perfect and a lot small air gaps between turns, between phase or between turn and ground, could often been observed as well as imperfections within the insulating (cracks) material even with vacuum pressure injection and heating/cooling controlled process. Even if the whole windings are impregnated by varnish to fill in the gap between wires, the voids may still remain and the problem is encapsulated. Gas-filled cavities in solid dielectrics could result from many cause, air-leaking in the mold (more spherical cavities), insufficient pressure during injection and curing allowing vapor pressure to develop thus creating cavities. [BOGGS90] [BRA89]
The phase-to-phase insulation system in the end winding is not always perfectly positioned and may be not covering the whole phase, thus relying on turn insulation to withstand phase to phase voltage.

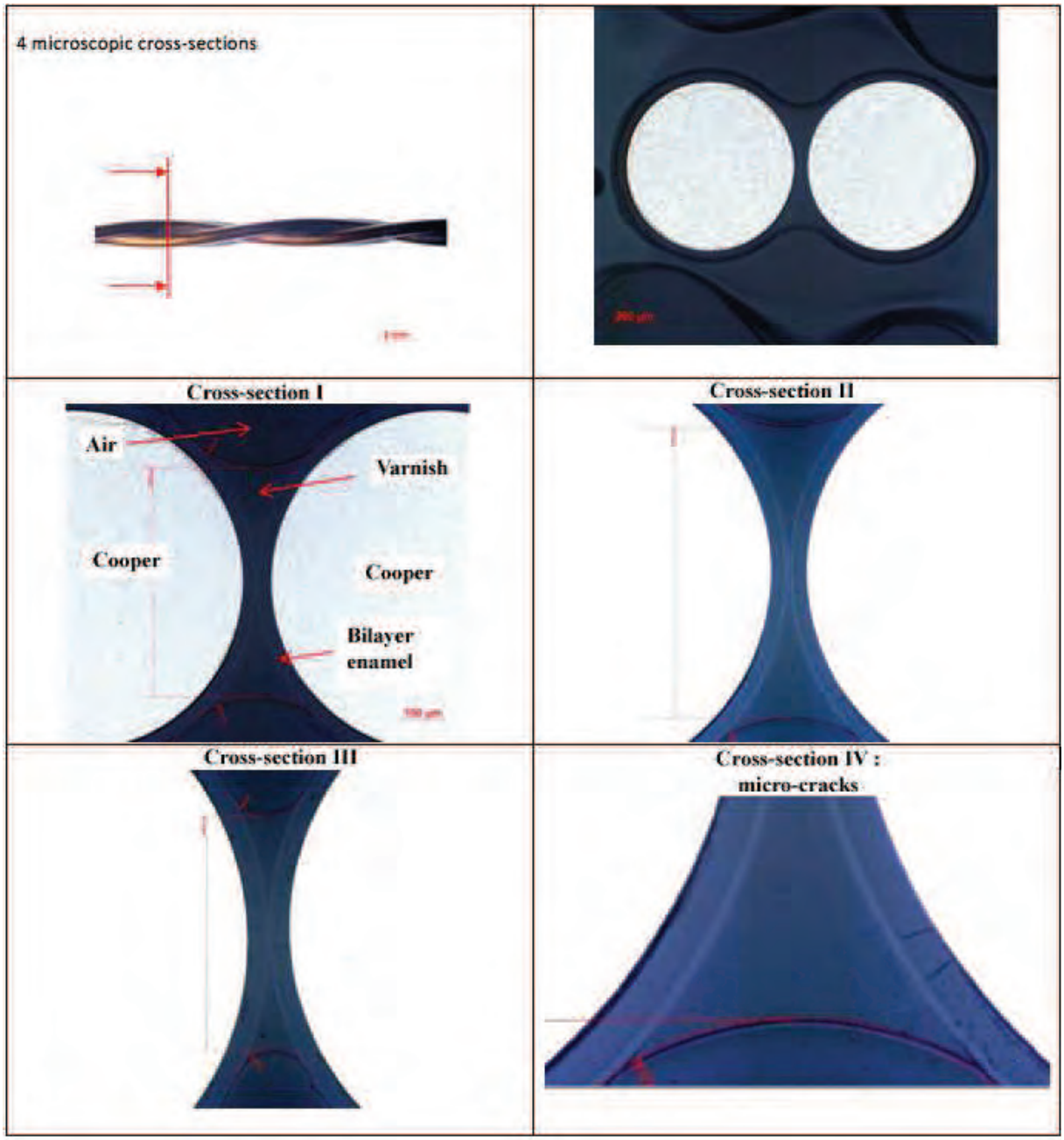

Table 2: Microscopic cross-section of a twisted pair (F. Fresnet)

Above (Table 2) are microscopic cross-sections of a twisted pair. Impregnation varnish and bilayer enamel could easily been observed in cross-sections 1 to 4

3.3. Partial discharge fundamentals

3.3.1. Partial discharge inception in voids

Since these small air gap within the whole insulation system do not have the same dielectrics properties as the insulating material, sharp variation of electrical field could be generated. The figure below is showing the typical electrical field between 2 close wires separated by an air gap, one at voltage while the other is connected to ground as in a twisted pair of enamel wire or in turn-to-turn insulation. On a small scale, the electric field could be calculated like in capacitor with a central symmetry located in the air gap with $\varepsilon_1 > \varepsilon_0$. Details of the calculation are not exposed here for brevity sake.

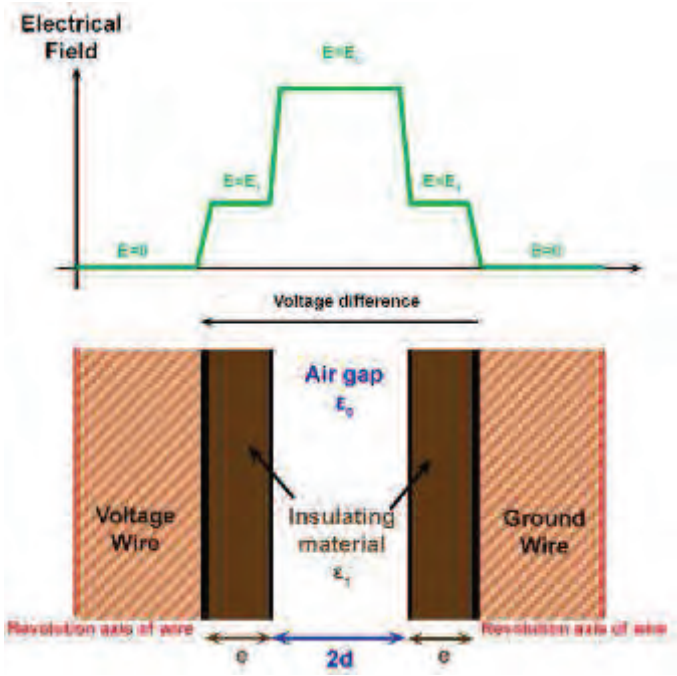

Figure 17 : Electrical field

Obviously, space charges accumulated on the surface of the insulating material could modify the electric field in the air as shown in [FAB04] and in figure 18. The modified electrical field in the air between the two wires depends on the charge accumulated at the interface. If both positive charges are accumulated within the insulated material or on its surface, the electrical field in the air is increased. The opposite process occurs with negative charges. These space charges could be accumulated by different process like traps but this is not the topic of this work.

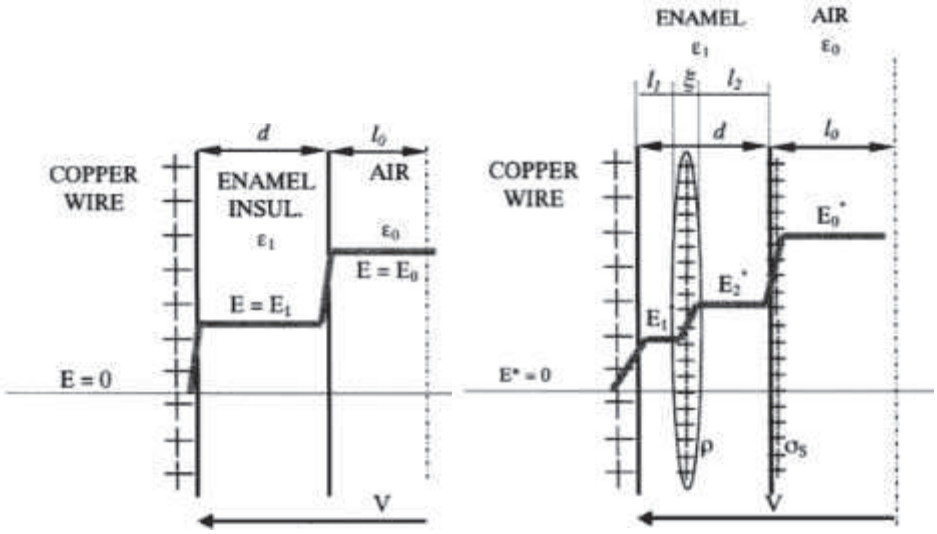

Figure 18: Electrical field without (left) and with (right) accumulated space charge on enamel-aur surface or within the insulation material (half part only due to symmetry) [FAB04]

It should be noted that the presence of condensation of water on the surface of the wire and short voids filled in with air or other gas within the insulation material are enhancing the electrical field by creating electric permittivity contrasts. Sharp geometric shape are enhancing electrical field as well.

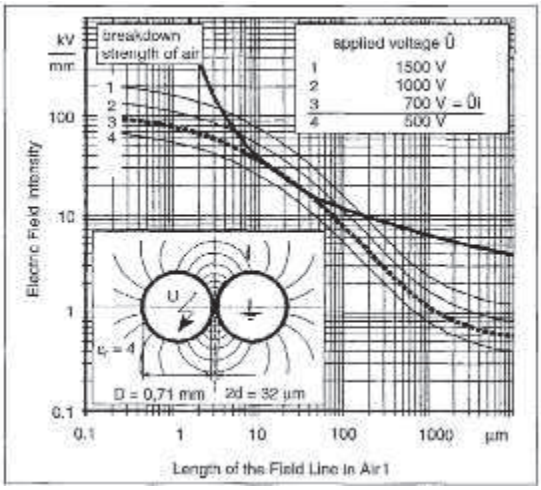

Figure 19: Comparison of electrical stress and breakdown strength of air gap between two enamel wires as in [KAU96]

The electrical stress in these small air gaps can exceed the electrical breakdown strength of the air (3kV/mm in uniform field) and cause a small spark, called partial discharge But only if a minimum distance is also met as defined by Paschen's law informing on the breakdown voltage. In other word, even if the electrical breakdown strength of the air under conditions of pressure, temperature and humidity is reached, it should be on a distance allowing an electron to be sufficiently accelerated to create the electronic avalanche and sustain it. [BARTNIKAS][KAU96]

3.3.2. Back to Paschen's curve

The figure above provides a typical set of Paschen curves obtained for air, nitrogen, oxygen, and hydrogen between parallel-plane metallic electrodes [SCHON69]

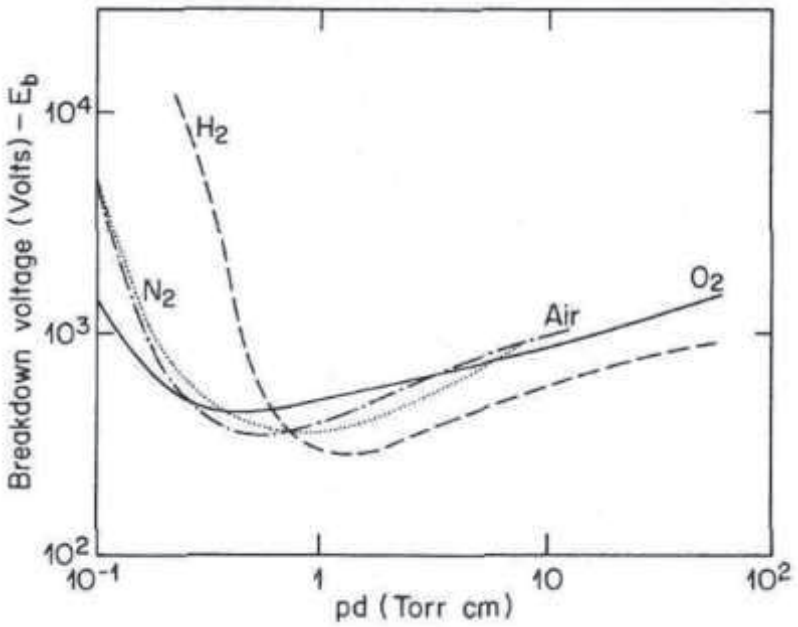

Figure 20: Paschen's curves for air, nytrogen, oxygen and hydrogen as in [SCHON69]

As with cavities having metallic boundaries or metallic electrodes, it has been demonstrated that the initial breakdown voltage, E_b (in volt and not volt/m), is function of the pressure-distance product (pd) and follows closely Paschen's Law. This still holds true with non-metallic electrodes or material like rubber, polyethylene or other dielectrics materials. The Paschen curve has a minimum breakdown voltage of around 320V in air for a given pd product called pd_{min}.

This pd_{min} value is the equivalent of a gap of 8µm at atmospheric pressure. At that point, a kinetic energy (effect of the electrical field) is acquired by the free electron at maximum efficiency to create collisions and yield an electronic avalanche. To the left of pd_{min} the number of collisions is too small (long mean free path) to result in a breakdown at the same voltage, to trigger breakdown the voltage has to be increased. To the right of pd_{min} the number of collisions is too important and kinetic energy is dissipated too quickly because of a smaller mean free path. [BARTNIKAS]

3.3.3. Townsend mechanism

Townsend has called the breakdown mechanism that occurs in uniform field between parallel planes metallic electrodes an electron avalanche. [VHIPP66]

Before going into more details, ionization should be recalled as the process by which an electron is lost from a neutral molecule to form positively or negatively charged particle. Townsend showed that when a free electron is moving in the direction of an electric field, accelerated by the same electric field and collide with a neutral molecule in the gas, the probability over the distance x of ejecting an electron is given by the first ionization coefficient α as αdx. The first ionization coefficient is equal to the number of ionizations that occur over a unit of distance. The first Townsend coefficient α depends on the gas (electronic structure of the gas atoms or molecules) and on the nature of collision and the kinetic energy of the electrons, the gas atoms or molecules are excited.

If one considers N_0 the starting number of free electrons coming from the cathode and N the final number of free electrons reaching the anode and D the distance between anode and cathode, we have the following relation

$$N=N_0 \exp(\alpha D)$$

In other words, it means that each ionizing electrons subjected to a large enough electrical field is accompanied by an exponential number of free electrons, thus increasing the number of collisions and creating an avalanche that may initiate a breakdown between the anode and the cathode. The breakdown results in a spark lasting less than a dozen of ns.

While collisions are occurring and electrons are moving quickly towards the anode and disappear, slower moving ions are left behind. As they reach the cathode, they may liberate on impact (ionic bombardment) other electrons with a probability γ, called second ionization coefficient. The second Townsend coefficient represents the electron regeneration probability at the cathode.

When the number of ion is large enough to regenerate free electrons, the discharge is self-sustaining. Additional free electrons could be created by photoelectric emission at the cathode, by ionization of gas by photon radiated from metastable and excited gas atoms or molecule. [BARTNIKAS]

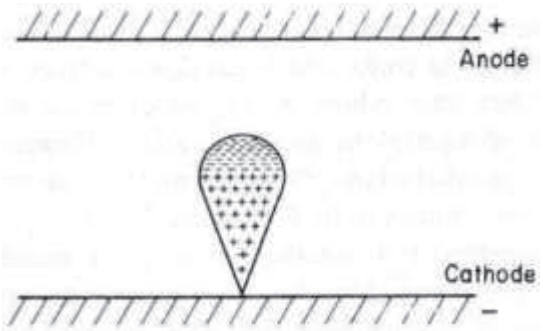

Figure 21: Electron avalanche formation as in [MC53]

3.3.4. Streamer mechanism

Another breakdown process is called streamer discharge mechanism. It starts like Townsend mechanism with a free electron accelerated enough to create an electron avalanche. If the free electrons reach a high enough velocity to move a hundred times quicker than ion, a space charge field is created as depicted in the figure above, case (a). When all the electrons have disappeared in the anode, a positive cone of ion is left behind and bridging the gap (b). The ionized volume is emitting photons causing additional electron avalanches towards the main one (c). The positive space charge field is thus reinforced and a self-propagating streamer begins to form at the anode (d). Finally, the streamer bridges the gap (e) and create a highly conductive plasma channel and a spark.

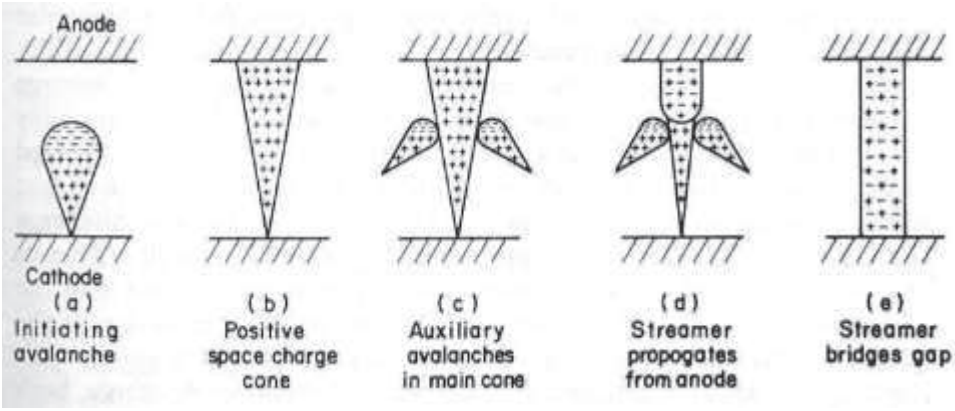

Figure 22: Streamer formation as in [MC53]

The discharge mechanism occurring in gap can be different if the electrodes are dielectrics. First regarding the second ionization coefficient γ. It has been demonstrated that the breakdown voltage is lower with dielectrics electrodes than with metallic ones in plane parallel and voids case. Then, in case of void, insulating materials seems to favour streamer process with the field distortion coming from deposited charge and increased surface resistivity.

These physics considerations are just reminders of basic mechanisms at work when talking more generally about partial discharge, more complex mechanism like corona, treeing, pulseless or pseudo-glow are not expanded here yet. [BARTNIKAS]

3.3.5. Types of partial discharge location

Here are the main types of partial discharge location that are either internal, surface or corona or even treeing. [KREUGER]

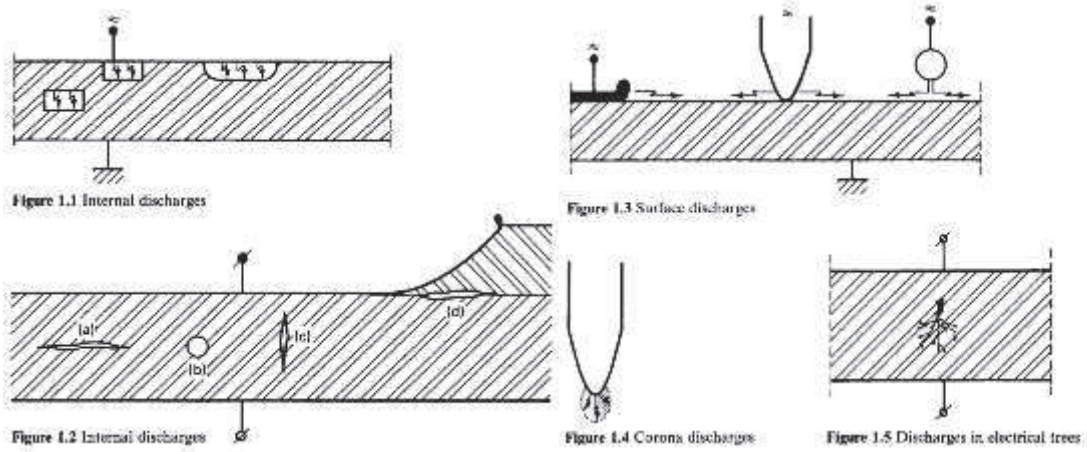

Figure 23 Partial discharge type as in [KREUGER]

Following the part on the discharge and breakdown mechanism, it's time to actually have a definition of partial discharge:

> **Partial discharge (PD):** A localized and quick electric discharge that only partially bridges the insulation material between the conductor's materials or electrodes. The propagation of the discharge is partial because of either a non large enough electrical stress or a resistant enough insulating material. A transient gaseous ionization is occurring in an electrical insulation system when the electrical stress is higher than the inception/critical value. Even if the magnitude of partial discharge is usually small, progressive deterioration is started and may lead to ultimate failure. Indeed, partial discharges transform a part of the capacitive stored energy in the insulation into destructive energy (radiation, mechanical, thermal or chemical) which can degrade insulation materials.
>
> **Partial discharge inception voltage (PDIV):** The lowest voltage at which partial discharges (PDs) occur as the applied voltage is increased. Many factors may influence the value of PDIV, including the rate at which the voltage is increased as well as the previous history of the voltage applied to the sample or environmental conditions.
>
> **Partial discharge extinction voltage (PDEV):** The highest voltage at which partial discharges (PDs) no longer occur as the applied voltage is decreased from above the inception voltage. PDEV is less, or at most equal, than PDIV. [IEE00]

3.3.6. Discharge equivalent circuit in voids

In the case of voids inclusion, an equivalent electrical circuit could be realized to better understand discharge parameters such as repetition rate and charge transfer.

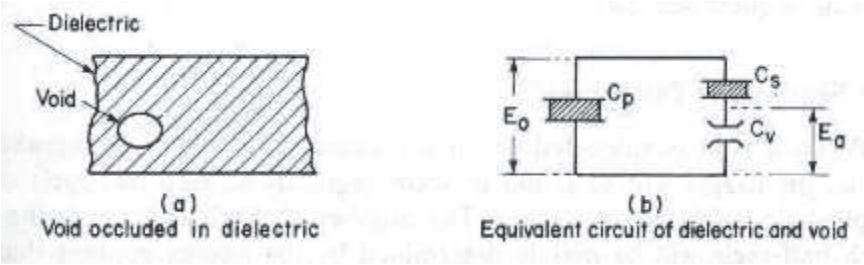

Figure 24: Void inclusion electrical equivalent circuit [BARTNIKAS]

In the void drawing and in the equivalent circuit above, C_V is the capacitance of the void filled in with air or another gas. C_s is the sound capacitance of the insulating materials series with the void. Finally C_P is the remaining capacitance, in parallel.

When a discharge occurs in the void while the dielectric is fed by a sinusoidal voltage, the voltage inside the void drops from its breakdown value E_B to its residual value E_R. This drop is equivalent to a step (or pulse function) applied to the cavity and the charge transfer ΔQ caused by the discharge is equal to $C_P . (E_B - E_R)$, approximately since leakage and loss are not taken into account in the model. This charge transfer is thus an image of the magnitude of the discharge. The discharge energy is also function of the voltage drop and the capacitance value. [WHITE53][AUS44][BARTNIKAS]

3.3.7. Repetition rate of discharge and detection under AC voltage

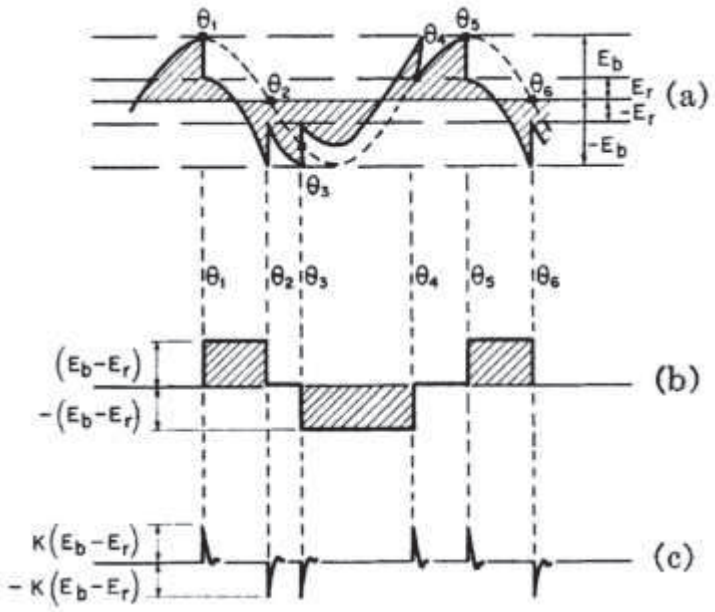

Figure 25: (a) Voltage waveform across cavity, (b) corresponding excitation pulse train, (c) conventional discharge detector output [BART71]

When a cavity is submitted to AC voltage, the voltage increase until breakdown (E_B) then drop to the residual voltage in the cavity (E_R). In the figure above, the first partial discharge event is located at θ1 and the partial discharge sensor detects the charge transfer caused by the voltage drop and the resulting image of the current flow. The polarity of the voltage drop should be reflected on the sensor value and polarity.

The K factor just means the amplitude of the sensor signal is a proportional image of the intensity of the discharge. The voltage in the cavity, after the first discharge, is decreasing, following the AC supply, until another breakdown occurs ($-E_B$) in the opposite polarity. Then, the voltage drops ($-E_R$) to its opposed residual voltage. It should be noted that breakdown and residual voltage are not necessarily the same in the two opposite polarity. The sensor detects another pulse like signal. In these conditions, there are two discharges per half-period.

3.3.8. Apparent charge, sensitivity, propagation and calibration of detection device

From a practical point of view, neither the voltage drop magnitude nor the void capacitance value are known. But, this charge transfer process is nonetheless the basis of discharge detection in electrical system because it creates different sort of physical phenomena. In the electrical circuit, the apparent charge of a partial discharge is, if injected instantaneously between the terminals of the test object, the charge that would momentarily change the voltage between its terminals by the same amount as the partial discharge did when the drop in voltage occurs. The apparent charge is expressed in coulombs.

Injecting a known quantity of charge in the circuit and linking it with the discharge sensor output is an apparent charge calibration before performing actual detection. In this process, all cables connecting to the charge injector should be as short as possible to prevent any distortion. In true, this process is more a normalization than a true calibration and another main goal of this calibration is more to assess measurement sensitivity than giving accurate quantitative value to compare between systems. The sensitivity is aimed to quantify the level at which pulses may not be background noise. So, one should be aware that all results are inherently function of the sample under test, especially with complex windings, the measurement system and the entire test arrangement (cables length, impedance, capacitive couplers, etc…)

Indeed, when a partial discharge is created, each electrical machine has its own response function of the geometry of the windings, the dimension of the stator, the end-winding geometry, the insulation materials and other parameters. Similarly, electromagnetic waves could propagate through the winding, acting as a transmission line (having its own inductance and capacitance) or through the medium and its transfer function. Moreover, reflection of partial discharge travelling wave could be observed with a reduced magnitude and could be interpreted as another partial discharge impact

Going back to the discharge intensity is next to impossible because all discharge locations and electrical systems are different. So the comparison of the image of discharge magnitude is meaningless between two separate systems. Still comparison of discharge intensity on the same system and in the same testing conditions should be carefully considered. [BARTNIKAS][IEEE00]

3.3.9. Quick survey of detection devices

Partial discharge are accompanied with several different physical manifestations such as electrical pulse, radio frequency (RF) pulses, acoustic pulses, light emission, chemical reaction producing ozone. How could these phenomena be measured to detect partial discharge? [IEEE00][BARTNIKAS]

- **Electrical pulse sensor:** Based on the fact that a current flow of electrons is created at each partial discharge event, a current could be measured, the total current being function of the number of charge transported by the partial discharge. The current flow is creating a voltage pulse across the impedance of the insulation system. The aim of the sensor is to measure the resulting pulse. This is called conventional partial discharge sensor
- **Radio Frequency sensor:** the partial discharges also create some RF electromagnetics waves that propagate away from the discharge location site in the gaseous medium or within the windings. The discharge spectrum range from a hundred of kHz to several hundred of MHz or more. Suitable bandwidth antenna could thus detect the fact the partial discharge activity is occurring. **This sensor will be used in this work.**
- **Energy-based methods:** Since the partial discharge is creating light, RF and pulse emission, energy is absorbed from the system and increase dielectric losses. Thus power factor tip-up method and other integration algorithm could be used.
- **Ozone detection:** One of the by-product of partial discharge activity in air is the creation of ozone, which is a gas with a characteristic odour. As the concentration increase, partial discharge activity at the surface of the insulation material is increasing. From inexpensive chemical measure to electronic sensor, the concentration of ozone could be measured even if it is affected by temperature, humidity and airflow rate.
- **Acoustic and ultrasonic detection:** Partial discharges are creating shockwave that could be detected by a microphone. If intense partial discharge activity is occurring, one could hear a sound similar to a frying.
- **Light:** Partial discharges are emitting light that could be observed in a dark room with a photomultiplier or even with the naked eye when discharges are occurring at the surface of the insulating material.

3.3.10. Effect of temperature, pressure and humidity on PDIV

Regarding the effect of pressure in surface discharge, one should follow the Paschen's law for a qualitative answer. Simply put, a decrease in pressure results in a drop of PDIV, but up to a certain point only. As explained previously, it depends of the number of collisions. Even in voids inclusion in the insulating materials, diffusion on the long term will make the pressure homogeneous to the surrounding medium, for example atmospheric pressure.

Temperature effect one PDIV could be compared to the pressure effect to some extent since it is related to a lower air density, thus decreasing the breakdown strength. In a void, an increase in temperature is also equivalent to an increase of pressure, thus tending to lower the PDIV as well. Moreover, permittivity of insulating material, such as polyimide, increase with temperature, leading to higher electrical field intensity in the air filled gap on the short term. [GUAS10][KAU96]

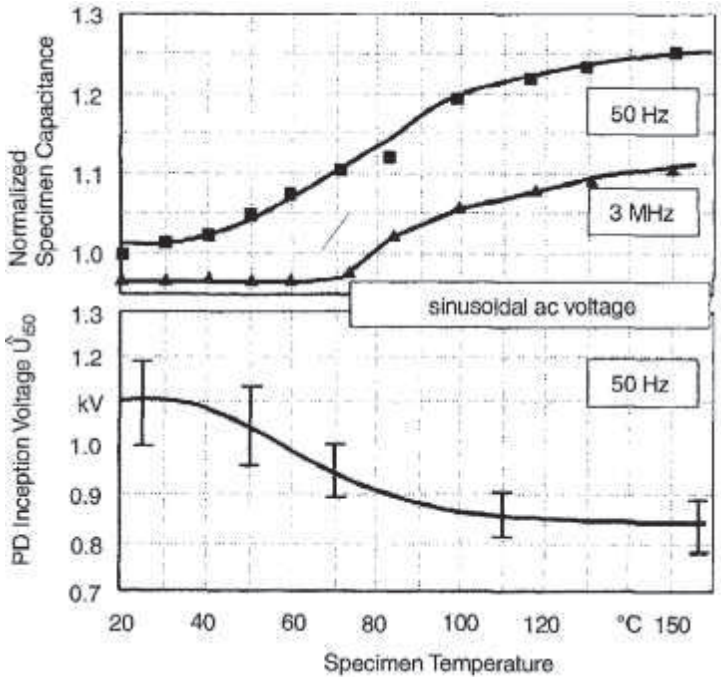

Figure 26: Effect of temperature on capacitance (permittivity) and PDIV as in [KAU96]

Humidity effects is one of the most tricky because it seems that two mechanisms are at work, outweighing each other function of absolute humidity and relative humidity when considering its effect on PDIV. Absolute humidity being preferably used at lower humidity value while at higher humidity value, relative humidity seems to fit better with results.

The first mechanism, mainly at lower value of absolute humidity, is the increase of electrical breakdown strength of air due to the increase of absolute humidity, thus the PDIV is increased as well. Another mechanism is occurring at higher value of absolute humidity, this time condensation on the surface, creating droplets, is altering the electrical field and thus decreasing the PDIV. [FEN03][FEN05]

3.3.11. Deterioration mechanism of partial discharge

Partial discharges are known to cause deterioration of insulating material by several means. [KREUGER][BARTNIKAS][MAS51][MCMA68][CAV11]

- Localized heating of the insulating material and power loss in the power supply. This effect could be compared to the one of a hot needle, triggering chemical and physical modifications in the materials or even evaporation of some components.
- Mechanical erosion due to ions bombardment. This effect could be compared to a localized sandblasting
- Formation of chemical species such as nitric acid (in the presence of moisture) and ozone. Other exotics species could appear as well depending on the nature of the insulating materials such as oxalic acid with polyethylene. Chemicals reactions in polymer are usually oxidative
- Attack by ultraviolet rays

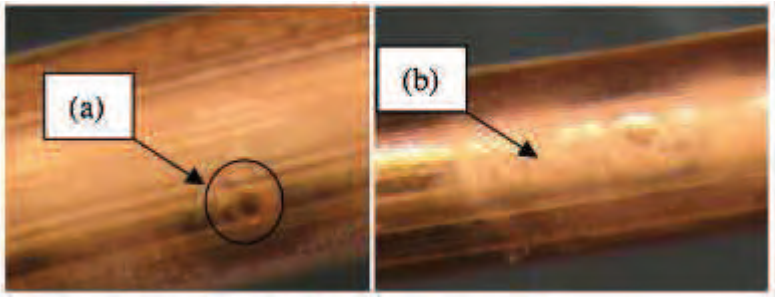

Figure 27: Effect of ion bombardment on wire (a) and effect of chemical attack on enamel wire with the loss of transparency (b) [CAV11]

With such harmful effects, it is obvious why partial discharges are not desirable in an insulating system. As such, partial discharges don't immediately lead to the failure of the insulation system, but with its destructive effects, partial discharges may lead, in an unknown period of time, to failure. Below (Table 3) are erosion zone after partial discharge activity on a twisted pair of enamel wires

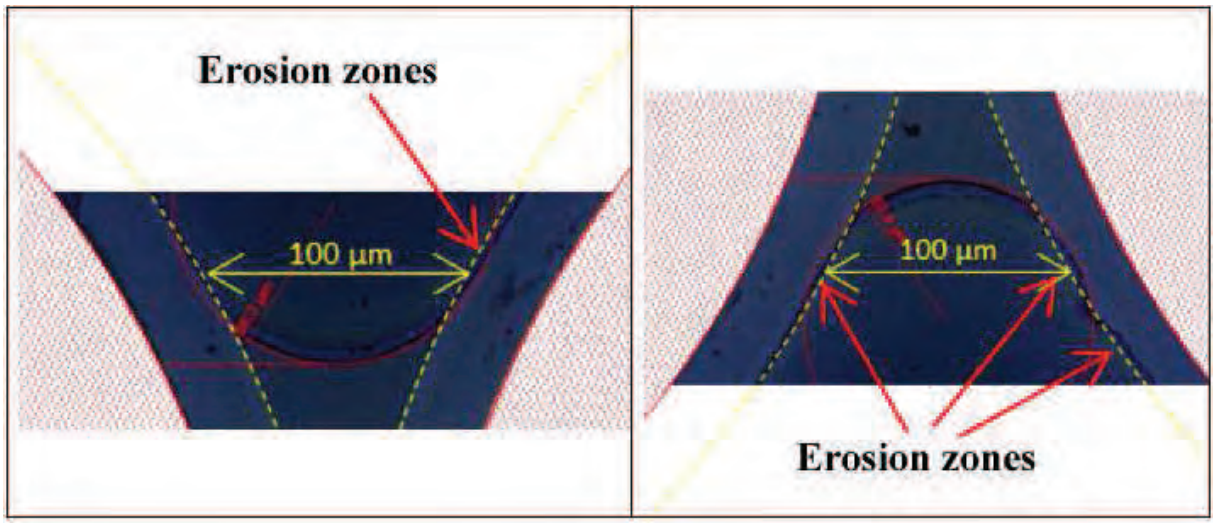

Table 3 : Erosion zone after partial discharge activity (F. Fresnet)

3.4. Partial discharge detection as a diagnosis tool on machine fed by PWM inverter drive

3.4.1. Interest

The symptomatic nature of partial discharge and the criticality of the use of PWM inverter drive make its detection key to assess and control the quality of insulation system of an electric machine and validate or re-examine the design and material choice. Another use of using partial discharge, as a diagnosis tool, is not to check an expected quality but rather determine if the insulation system is deteriorating and at which degree. The measure of trend regarding PD activity from periodic tests could tell if any insulation degradation is occurring and how machine are behaving under fatigue test

3.4.2. Partial discharge tests requirements

When performing partial discharge diagnosis, a few things should be expected:

- The test must not harm the reliability of the whole electrical system if carried out on-line. In EV on-line case, connecting any device to the powertrain is not even considered since it would affect the reliability of the whole car.
- The cost of performing should be lower than the cost of mandatory and unexpected maintenance operation. In EV case, an on-line and on-board detection system should largely be cheaper than the cost of changing the whole electrical engine and the immobilization time. In case of off-line testing, the test should be able to design and choose the most reliable insulating system within the determined cost
- The test should be reliable not to give false indication of partial discharge activity prompting an unneeded maintenance operation. In the case of EV on-line application, any false positive would ring an alarm bell or turn-off an alarm light indicating to the driver that something is wrong with its engine. Regarding off-line test, it could be sometimes difficult to obtain electric motor sample and results need to be reliable to make the most out of the limited samples available.
- The test should be effective to detect as soon as possible all kind of partial discharge activity. In EV case, since there is no expected remaining lifetime when partial discharge activity is first detected, the sensitivity of the method should be good enough to give time for carrying out maintenance or follow fatigue in off-line tests.

3.4.3. Off-line and on-line partial discharge testing characteristics

Off-line testing: Tests that are made with the rotating machine alone with the necessary test voltage applied to the winding from a separate and independent power supply. The machine is thus out of service.

Off-line testing of partial discharge advantages are the fact tests can be performed under defined and controlled conditions. Disconnection from the corresponding power supply and the absence of electromagnetic noise generated during operation allows measurements to be carried out more easily to increase or decrease voltage at will to determine PDIV and PDEV. Testing could be focused on one phase at a time before energizing the three phases simultaneously to identify phase-to-phase or phase to ground default. The ability to remove or place the stator inside the machine allows a better observation of slot default.

The main drawback of off-line testing is the fact that the voltage applied is not representative of the one usually feeding the machine nor its temperature, so an oven may be needed if necessary. Additionally, the absence of electro-mechanical force may prevent the detection of some type of PD. Environmental condition may be different in regard to humidity of pressure and, of course, another power source is needed.

On-line testing: Tests that are continuously, or periodically or for a short time only, made with the rotating machine running as in operation with its power supply. The machine is in service

On-line testing of partial discharges main advantage is the fact that the electric machine under test is fed by its own power supply, electrical stress is thus representative of the usual operating conditions with mechanical force.

The main drawbacks of on-line testing are the fact that numerous signal are interfering with the detection and which are of greater magnitude than searched PD signal. Noise suppression has to be effective. Moreover, accessibility is not often convenient with either protecting frame or plate and could lead to PD signal distortions and attenuation when travelling through windings.

3.4.4. IEC TS 60034-18-41 procedure, tackling the problem?

Following the widely recognized problem of failure rate of low voltage machine fed by inverter drive, the International Electrotechnical Commission (IEC) created documents on the subject, with one of most important being the IEC TS 60034-18-41, focusing on type I motor in low voltage applications such as EV. Type I motor are initially wire-wound, or random wound, motor operating at low voltage (below 1000V) where partial discharge activity should not occur during the life time in AC voltage. As we have seen, when these motors are fed by a PWM inverter drive, the failure rate is much more important and the main cause of failure is partial discharge.

The important point of understanding the IEC TS 60034-41 is that both qualification and acceptance tests are designed to ensure that no PD activity is likely to occur during the lifetime of the electrical machine in operation once manufactured for inverter use. The kind of insulation usually used in type I motor is mainly organic is not able to withstand for a long time PD activity. For example, the relatively weak polyimide-imide enamels wire insulation could not withstand the electrical stress between turns that is generated by the high number of voltage pulses at high rise time and overvoltage. Thus, failure could be much more quicker than in AC voltage due to the higher frequency of the power supply. Indeed, the number of potential discharge per unit of time has to be taken into account.

To carry out such qualification or acceptance tests, a criterion as to be established: RPDIV. [CAV10] [CAV10-1][CAV-11] [IEC-41][STONE07]

3.4.5. Stress categories and motor type

Many different type of combination between electric motors and PWM inverter are possible, listing all combination is next to impossible and would lead to a complex database. The voltage waveform is supposed to be fully characterised by three parameters: impulse repetition frequency, peak impulse voltage (overvoltage at first coil) and impulse rise time (distribution of voltage in the coil). Overshoot factor is defined as the ratio of voltage at motor terminal on the DC bus voltage of the inverter drive. The impulse rise time is self-explanatory.

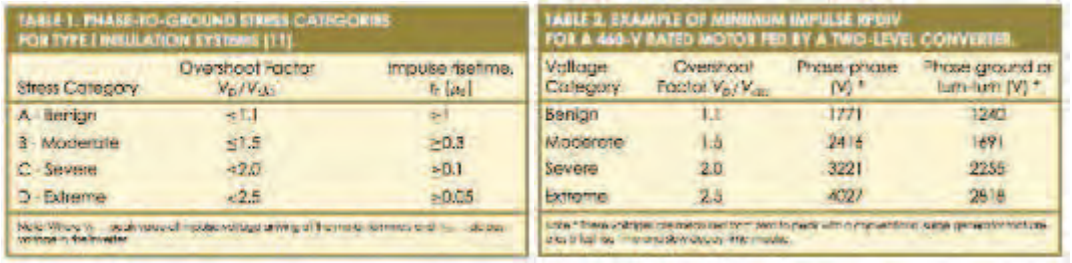

Stress Category	Overshoot Factor V_p/V_{dc}	Impulse risetime, t_r [μs]
A - Benign	≤1.1	≥1
B - Moderate	≤1.5	≥0.3
C - Severe	≤2.0	≥0.1
D - Extreme	≤2.5	≥0.05

Voltage Category	Overshoot Factor V_p/V_{dc}	Phase-phase [V] *	Phase-ground or turn-turn [V] *
Benign	1.1	1771	1240
Moderate	1.5	2416	1691
Severe	2.0	3221	2255
Extreme	2.5	4027	2818

Figure 28 Stress category [STONE07]

Therefore, motors could be more or less stressed depending on the combination of the 2 last aforementioned factors, the impulse repetition rate is not considered for the stress category. So, the IEC defined 4 stress categories: A-Benign, B-Moderate, C-Severe and D-Extreme. (Table 1) Function of in which category a motor is falling, the TS 60034-41 proposed qualification levels for RPDIV levels. Problems could be encountered when a severe overshoot factor is accompanied with only a benign impulse rise time, or the opposite benign overshoot factor but severe impulse rise time. Thus, both parameters are considered separately and to an overshot factor corresponds a phase-phase and phase to ground/turn RPDIV minimum level. (Table 2)[STONE07]

3.4.6. Concept of RPDIV and IEC TS 60034-41 test procedure

The idea of PDIV was explained previously as the minimum voltage at which partial discharges are first occurring when voltage is increased. At PDIV, only a few events could be observed. As shown previously, as partial discharges are occurring space charge distributions made up of positive ions are created in the defect. Given enough time, these space charge distributions tend to recombine towards an electric state similar to the one before the discharge.

But, as frequency of voltage supply is increased, recombination process may well be not be long enough so that when the voltage is switched off, another discharge could actually occur since the remaining electrical field is opposed to the initial igniting electrical field. Thus the number of PD per cycle is function of the frequency of the voltage supply and maybe as well of the duty cycle. For that reason, the RPDIV concept was designed. [FAB04]

The concept of Repetitive Partial Discharge Inception Voltage, PDIV is defined as the minimum peak-to-peak voltage at which partial discharges occur with a repetition rate of 1 or more PD pulses per every 2 voltage impulses when voltage is raised gradually from zero. In the standard, an impulse refers to a voltage transient generated by an inverter drive with no more precisions of the width of the pulse.

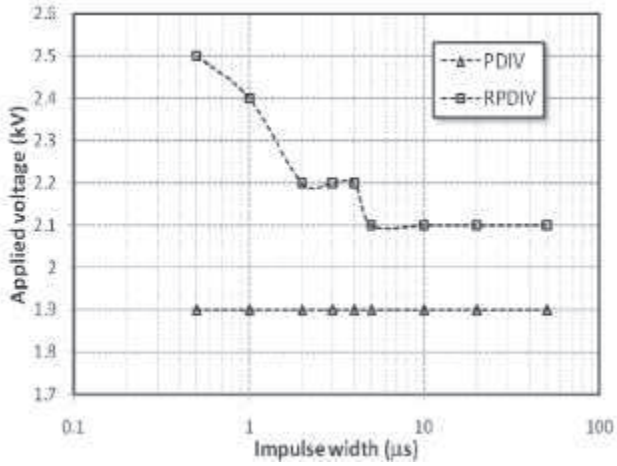

Figure 29: PDIV and RPDIV in a twisted pair fed by square voltage impulse with variable width [CAV10-1]

On the figure above, trying to plot the difference between PDIV and RPDIV, one can observed that with decreasing the impulse width (from 50 to 0.5 µs), a larger voltage is required to incept repetitive PD phenomena in twisted pair of a square voltage at 50Hz frequency. On the contrary, PDIV for impulse voltage is almost independent of impulse width providing the voltage increase is slow enough. In other words, RPDIV is mostly a statistical quantity with a much more strict requirement than PDIV as hinted by the definition of one PD per every 2 impulse. In all cases, if the RPDIV falls above a certain level, qualification and acceptance test, the system under test failed.[CAV10-1]

The tests are performed off-line which means the stresses experienced by the machine are not necessarily representative of those likely to be faced during service both for an electro-mechanical or an environmental point of view.

Qualification tests are used to test, before manufacturing, a combination of insulating material and building techniques.

Qualification tests could be performed with either sinusoidal voltage, thus measuring PDIV, or impulse voltage waveform with sufficiently short rise time using RPDIV. Impulse voltage waveform is mandatory to stress turn-to-turn insulation. In the case of RPDIV, the rise time should be in the same range that the one expected to be faced by the electrical machine. Aging under thermal, vibration and humidity in fatigue cycle could be carried out as well on dedicated sample like motorette and RPDIV qualification is performed after each cycle. Thermal class safety factor could be taken into account for RPDIV minimum level.

Acceptance tests are performed on complete machine or coils to check, in hindsight, the ability of the design.
Acceptance tests are carried out on a randomly selected small sample of manufactured stator extracted from a bigger lot to check if the manufacturing is conform to the design. To pass the acceptance test, samples must have a RPDIV higher than the minimum required level for the stress category.

So, acceptance is controlling the final product whereas qualification helps in the design choice of material or manufacturing process. Still, qualification and acceptance have limitations (weakness and imprecisions in procedure) and motors having passed successfully qualifications and acceptance test may still fail. As a result, on-line partial discharge test still appears to be mandatory to really qualify and accept motor design, insulating material choice and manufacturing process. Indeed, the only real way to know how an electric machine will behave under operation is to test it. Still, on-line monitoring has shown to be difficult in motor fed by PWM inverter as discussed previously. [TOZ09][TOZ10][TOZ11]

3.4.7. Towards on-line and off-line detection of partial discharges in low-voltage electric motor fed by PWM inverter drive

In the more recent work of detecting partial discharge only in electric machines fed by a PWM inverter, the more promising track has been the pioneering work done by Davide Fabiani, Andrea Cavallini and Giancarlo Montanari in “A UHF technique for advanced PD measurements on inverter fed motors” [FAB08] when conventional technique for measuring technique could not be used due to noise generated by the inverter

Still, the use of a high pass filter with an electromagnetic sensor has proven to be successful to detect PDs created by a bipolar voltage shape feeding with commercial power supply a small 400 V three-phase induction motors having a power of 0.3 kW in off-line and on-line conditions.

Building on this work, an experimental set-up has been set up to go one step further in the field of EV electric motor and detect partial discharges on-line in electric motor. It consists in 5 key parts: non-intrusive electromagnetic sensor, high-pass filtering, controllable high voltage PWM power supply, high speed acquisition and low voltage (400V) and high power random wound electric motor sample (around 60 kW). [BIL14]

4. Experimental set-up, test procedures and results

4.1. Introduction

As it has been highlighted in previous chapters, partial discharge activity is one of the main cause of winding insulation gradual deterioration leading to premature failure of electric motors when fed by a PWM inverter drive. Moreover, electric vehicle specific environment adds further constraints such as climatic conditions and cost-efficient design policy, making it critical to assess winding insulation performance with partial discharge measurements. But now, partial discharge inception voltage measurements on electric motors, under sinusoidal voltage, do not represent accurately surge voltages stresses created by a PWM inverter and are, thus, mostly meaningless for our purpose. Worse, electric motors having successfully passed, for example, IEC Technical Specification 60034-18-41 or in-house qualification tests off-line may still ultimately fail prematurely in service or in fatigue tests.

Hence, several experimental tests were developed and carried out during this work with one purpose always in mind, providing car manufacturers with a non-intrusive electrically, reliable and easy-to use tool to evaluate partial discharge inception voltage in electric motors fed by PWM inverter. To overcome this technological lock, four tests set-up, increasingly growing in complexity and in representativeness, were thoroughly thought, designed and performed and consist of:

1. Partial discharge detection in a twisted pair sample in a PWM environment.
2. Off-line partial discharge detection in an electric stator fed by a PWM inverter: one phase at the same time.
3. Off-line partial discharge detection in an electric stator fed by a PWM inverter: three-phases at the same time.
4. On-line partial discharge detection in an electric motor fed by a PWM inverter: industrial engine test bench.

The first experiment can test the detection efficiency of non-intrusive sensors to detect partial discharge in a controlled environment and on a known sample, a twisted pair of enamel wires, but with the main characteristics of PWM noise in behind. The sample is thus connected in parallel to a PWM inverter normally feeding an electric motor. In addition, this test can provide information about typical PWM waveforms as seen by non-intrusive sensors as well as their partial discharge detection abilities. Finally, some filtering methods are tested and different kinds of sensors are compared one to another.

The second experiment is the first on an electric stator fed with a controllable PWM inverter. These tests are targeted on one phase at a time by feeding through the neutral point of the stator. With a high voltage power supply backing up the PWM inverter, the aim is to reach and detect partial discharge inception voltage off-line with a non-intrusive sensor. A crucial breakthrough is made regarding filtering in a PWM environment as well as about the nature of discharge occurring in the electric stator.

The third experiment's aim is to reach and detect partial discharge inception voltage with more complex and representative voltage signals on all phases at the same time. Thus, bringing these off-line testing conditions as close as possible to real on-line service conditions to assess potential on-board performance of this detection method. Further information are gathered about partial discharge inception pattern.

Finally, an on-line partial discharge detection test will prove to be the main challenge and achievement of this work. Bringing together all the experience and knowledge from previous experiment, detection in an industrial engine test bench on a running electric motor fed by its PWM inverter has been performed. Thus, drawing conclusions on the efficiency of this detection method in an on-line use.

Providing a convenient, reliable and simple tool to assess electric motor insulation fed by PWM inverter can be very useful for cars and motors manufacturers to choose among different enamel wires, impregnating resin and winding process and create end of line tests, fatigue testing or even monitoring partial discharge in an on-board use.

4.2. Samples under test

During all the experiments, partial discharge tests were performed on four different kinds of samples. All samples are representative of materials and insulation system technologies used in electric vehicle applications. These samples are representative as well of all type of insulation: phase to phase, phase to ground and turn-to-turn. For confidential reasons, accurate composition and properties of enamel wires and all insulation system design can not be revealed in this work. But, as a matter of fact, insulating materials under tests here are fairly standard and representative of what is really used in such low voltage electric motor application.

4.2.1. Twisted pair of enameled wires

The first kind of sample is a twisted pair, which is made of two enameled wires used in electric motors. This sample is quick, easy and cheap to build and in thus perfectly suitable for destructive tests such as fatigue experiment. Following a standard process, two enamelled wires of (diameter around 1mm) are twisted around each other a given number of time (ten times for example) while applying a tensile strain and with a given number of turns function of the diameter of the wire. During tests, one wire is connected to one phase while the other one is connected to one of the two remaining phases in order to submit the turn-to-turn insulation to the most severe electrical stress. Actually, the twisted pair sample is representative of the PWM inverter worst-case scenario when the first turns of a coil are in close contact as it may be the case in the end-winding of a random wound machine. As noted in previous chapters, when an electric motor is fed by a PWM inverter drive, large voltage difference could be found within turns of the same coil, thus favouring partial discharge inception. In this work, this kind of sample has mainly been used to model the turn-to-turn insulation. Below in Figure 30 is an example of a typical twisted pair made of two wires (red and blue).

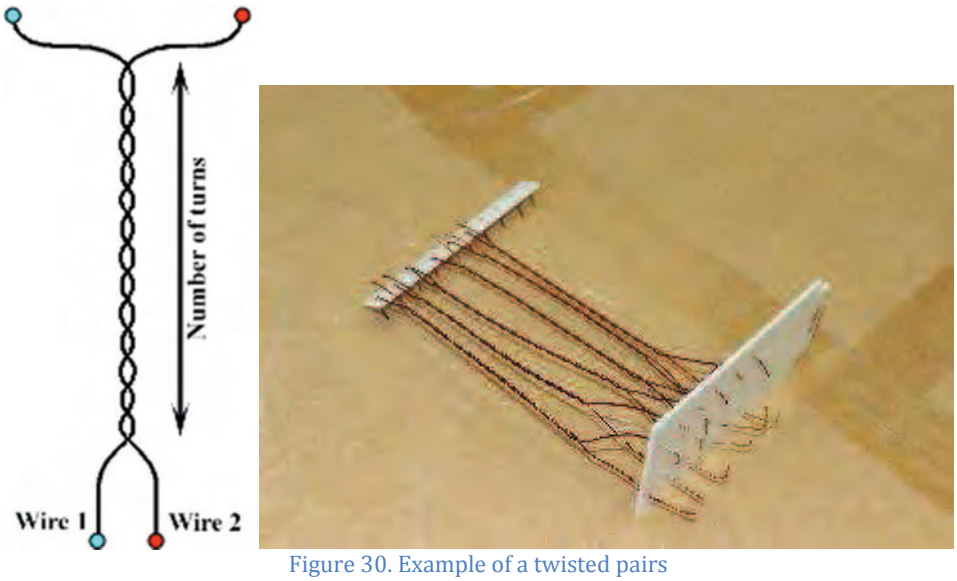

Figure 30. Example of a twisted pairs

4.2.2. Statorette

The second kind of sample is a bit more complex that the twisted pair and is usually a more versatile object. The statorette is supposed to be a scaled-model of the whole insulation system of the electric stator. The statorette is made up of two different coils placed one on top of the other and separated with an impregnated insulating paper as used between phases of real electric motors. Each coil is usually impregnated and is made of two, electrically independent, wires wound at the same time within a metallic frame as in a phase winding. These two wires are not twisted around each other but rather wound together in the same movement. Between the frame and phases, slot insulation paper is incorporated as well. So, one could test the insulation system between two wires of the same coil (turn-to-turn), test the insulation system between the ground (metallic frame) and one phase (phase to ground) and, of course, test the insulation system between the two coils (phase to phase). A statorette is made of wires, insulating paper and resin typically used in electric motor. Statorettes have not been widely used in the following experiments since this work mainly focus on turn-to-turn insulation system. Figure 31 presents a typical statorette with the upper coil made of blue and yellow wires, while the base coil is made of purple and green wires. Insulation paper could be noticed in light brown for both phase-to-phase insulation and phase-to ground insulation.

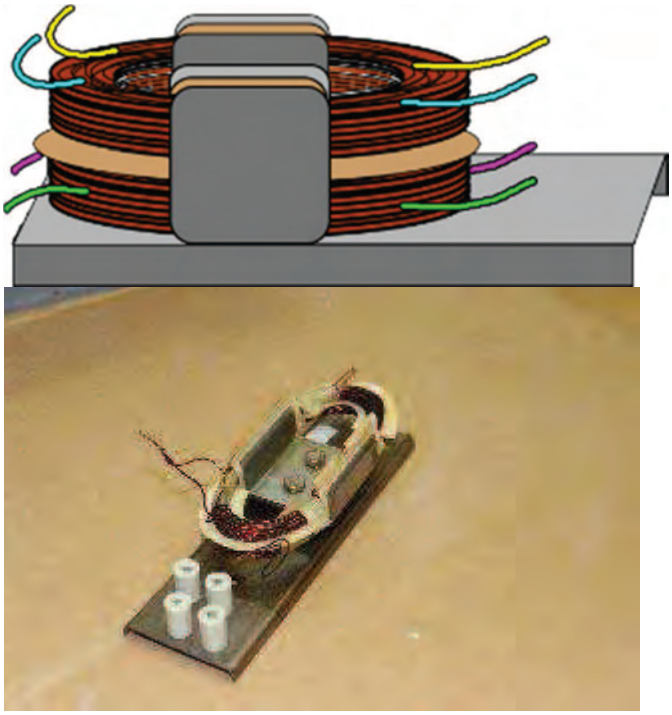

Figure 31 : Statorette (or motorette)

4.2.3. Electric stator

With electric stators available, the third type of sample is highly representative of a real electric motor. To perform and enhance off-line partial discharge detection before going on-line, having two electric stators available is a really thrilling opportunity. These stators are brand new prototype machines that could even have been used as electric motor to propel an electric vehicle. In other words, these stators are real electric motors, which could be tested off-line, and are exactly representative of those used in service regarding insulating materials, design and winding process. During tests, several combinations are possible because all phases and the neutral point are made available. So, for example, by connecting one phase and the neutral point to the PWM inverter, only one phase is stressed by surge voltage, thus testing turn-to-turn insulation each phase at a time. By connecting three-phases at the same time to a PWM inverter will be representative of electric stresses on phase-to-phase and turn-to-turn insulation. Connecting the stator frame to the ground will stress phase-to-ground insulation system. Or even put the rotor within the stator while testing is a perfectly valid option as long as all security measures are respected (no contact between rotor and stator). Figure 32 below presents the typical geometry of an electric stator with all three phases and the neutral point available. Stators tested here are not impregnated.

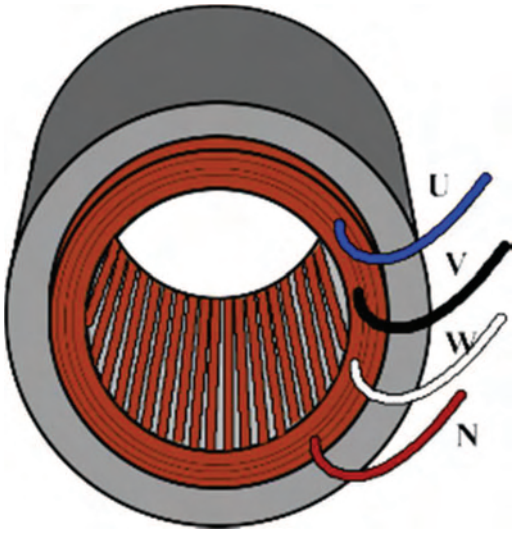

Figure 32 : electric stator

4.2.4. Electric motor

Finally, a full electric motor is used as a fourth sample in this work and is connected to its own PWM inverter so that a real on-line test can be carried out. This electric motor is, of course, the ideal sample because it could be stressed with voltage waveforms at different service point (steady state, braking, high speed or low speed). As the electric stator, electric motor under test is a prototype supposed to be fed with a three-phases voltage and a DC bus up to 400V to model an electric vehicle. This electric motor is a low voltage, random wound machine of around 60kW power and is only available in car manufacturer's engine test bench usually used to perform mechanical, thermal, fatigue tests or performance measurements. The typical architecture of an electric motor is presented below in Figure 33. The machine is not always impregnated.

The machine is protected with shielding plates so that the inside of the motor is not as available as it is for the electric stator and partial discharge electro-magnetic waves are confined within the machine. So sensors should be put outside, close to either motors or rotor terminals to be able to perform partial discharge detection. Moreover, no direct partial discharge electro-magnetic waves could possibly exit the inside of the engine with direct radiation. So, these discharges radiations will have to be circuit transmitted first to go out of the motor by motor terminals. In addition, to that it should be noted, that the inside of the electric motor does not have huge amount of space for the electro-magnetic wave to propagate in the air and these waves are likely to be attenuated in the process. Whereas, for circuit conducted electro-magnetic waves, the transfer function is dependant of the circuit, which should be similar to the electric stator previously presented. The detection strategy is thus to place the sensors at the vicinity of sample terminals, anticipating future space and access restrictions.

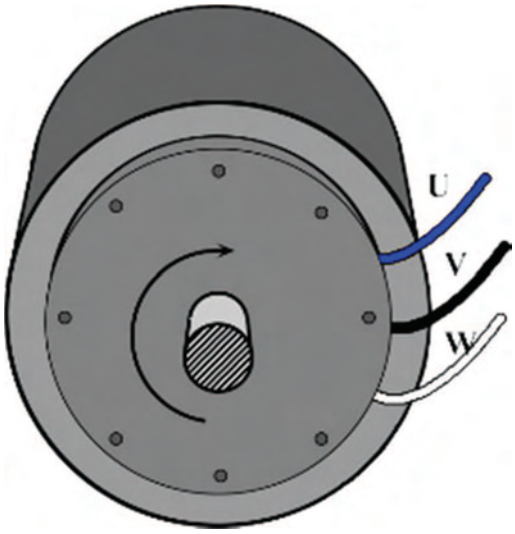

Figure 33 : electric motor

4.3. Non-intrusive sensors

As stated in previous chapters, not being connected electrically is the main advantage of non-intrusive sensors from a reliability point of view. The mandatory performance of a PD sensor in a PWM environment is to be able to detect the small signals of the high frequency part of the partial discharge spectrum in large signals and low-medium frequencies noise generated by voltage pulses produced by the inverter drive.

Ideally, the sensor has a kind of natural high-pass filtering behaviour to improve the signal to noise ratio. As stated in previous chapters, electrically connected sensors based on high frequency current detection (standard RLC partial discharge detection) are very hard to use in an electrical power train due to the high level of current.

4.3.1. D-Dot sensor

The starting sensor, or electro-magnetical coupling device, is an ACD-3A D-DOT from EG&G. This company is known as an United States national defence contractor and this sensor has likely been design for military or aircraft applications. This kind of sensor has also been used in aeronautics applications to try to detect partial discharges. A picture of the ACD-3A D-DOT sensor is shown in Figure 34, one of the main characteristics is the hemispherical sensing surface.

Figure 34 : D-Dot sensor

The sensor's response is a function of the electric field displacement changes as given by the following equation and the summary table.

$$V_0 = A_{eq} \cdot R \cdot \frac{dD}{dt} \cdot \cos\theta$$

Where V_0 is the output voltage (V), A_{eq} is the equivalent area (m^2), R its impedance (Ω), D the electric field displacement and θ the incident angle (measured from the symmetry axis)

Main Characteristics	ACD-3A D-DOT
A_{eq} (m^2) or Equivalent Area	$1x10^{-2}$ m^2
Bandwidth (Hz)	1MHz to 1GHz
Impedance (Ω)	50Ω
Risetime (ns)	<0.33ns

Table 4 : D-Dot characteristics

4.3.2. Coaxial cable sensor

In order to establish some performance comparisons with the previous sensor and to provide a cheaper alternative, a self-made sensor has been realized. This sensor has been made using a 3m coaxial cable cut in a half, then stripped on its cut extremity to expose its metallic inner core on 1cm length. The coaxial cable is further stripped but only to expose the inner insulator on 1cm without any ground shield. To prevent any unwelcomed contact between the metallic inner core and the shortened ground shield, an adhesive tape has been added on potential contact areas.

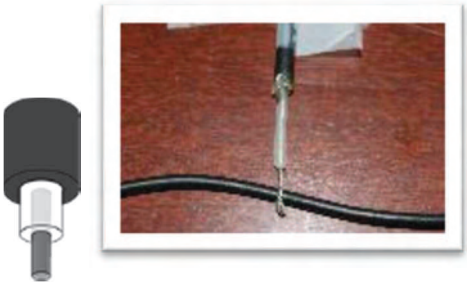

Figure 35 : coaxial cable sensor

4.3.3. Jack-SMA sensor

When it is needed to use two sensors at the same time to compare results from different location, the self-made sensors could not, obviously, be exactly the same and could evolve over time with manipulation. So, to solve these reproducibility and comparison problems, it appears necessary to have a strengthen version of the cheap sensor. This has been achieved by using a Jack-SMA connector, plugged at the end of a coaxial cable. This sensor is robust, cheap and standardized and has about the same kind of geometry and size than the self-made, coaxial cable sensor.

Figure 36 : Jack-SMA sensor

4.3.4. Non-intrusive current transformer sensors

As for non-intrusive current transformer sensors, they will be tested as well in a PWM environment. [NEACSU] These sensors basically have transformer architecture. The primary winding is actually the circuit in which partial discharge have to be detected whose one cable is going through a tore ferrite loop representing the magnetic circuit. The output secondary winding is thus providing an image of the current going through the primary winding. In this work, their use is fairly limited.

4.4. Data and signals acquisition

All data and waveforms displayed in the following four experiments are acquired and recorded using a Tektronix DPO4034 Digital Oscilloscope with a numerical bandwidth of 350 MHz, 4 analogic channels and a 2.5 GS/s sampling rate. Unless stated otherwise, only this oscilloscope has been used.

4.5. Partial discharge detection in twisted pair in parallel to an electric motor fed by a PWM inverter

4.5.1. Purpose of the experiment

This experiment is the very first step of a series of experiments of increasing complexity towards an on-line test. First and foremost, non-intrusive sensors partial discharge detection abilities have to be validated on a twisted pair sample (the electric motor is not the sample here) in a PWM noisy environment. By connecting, changing or removing the sample from the experimental set-up, the aim is simply to try to identify partial discharge small signals and extract them from the surrounding noise. If this proves to be possible, then a comparison between different sensors will be made in order to pick the most efficient and simplest one for future tests. Finally, different filtering techniques are proposed and tested using a high-pass filter and two identical sensors at the same time in order to anticipate future signal-to-noise ratio problem.

4.5.2. Experimental set-up

As shown in Figure 37, the experimental set-up is a motor test bench and consists in a three-phases star connected asynchronous low-voltage electric motor fed by its PWM inverter drive with DC bus output voltage of around 540V. The three-phase electric power network is 230V50Hz where the phase-to-phase voltage is thus around 540V. To create a 540V DC bus for the PWM inverter, the AC voltage is first rectified, then a smoothing circuit is filtering unwanted harmonics distortion. The switching frequency of the PWM inverter is 10 kHz, a fairly standard rate for low voltage machine. It should be noted that the cable length between the motor and the inverter is around 5 meters so that overvoltage could be created at motor terminals and could impact the twisted pair sample. The nominal stator frequency is set steady at 50 Hz and the nominal rotational speed of the rotor is 1500 round per minute. No braking torque or loads are applied to slow down the machine or put demands on it. The electric motor and the PWM inverter are producing a typical background electro-magnetic noise to test the different sensors detection abilities in a harsh, yet representative, environment.

A twisted pair is connected in parallel between phases U and V and is, indirectly, fed by the inverter drive. The expected partial discharge inception voltage of the sample is 700V RMS, measured in a classical sinusoidal partial discharge test with a transformer, a coupling capacitor, a RLC filter and an oscilloscope. The idea is to rely on overvoltage created by cable length to, hopefully, trigger partial discharge in the twisted pair sample indirectly fed by the inverter driven thus creating partial discharge signals to look for. To our knowledge, the electric motor has be running fine for many years and should be free of any known partial discharge activity. The key here is to have a sample, which will present partial discharge activity long enough to detect and extract it from the PWM noise thus confirming the potential of non-intrusive sensors in such an environment. Trying to detect partial discharge in a controlled and known twisted pair sample outside of the electric motor should be easier than directly testing electric stators.

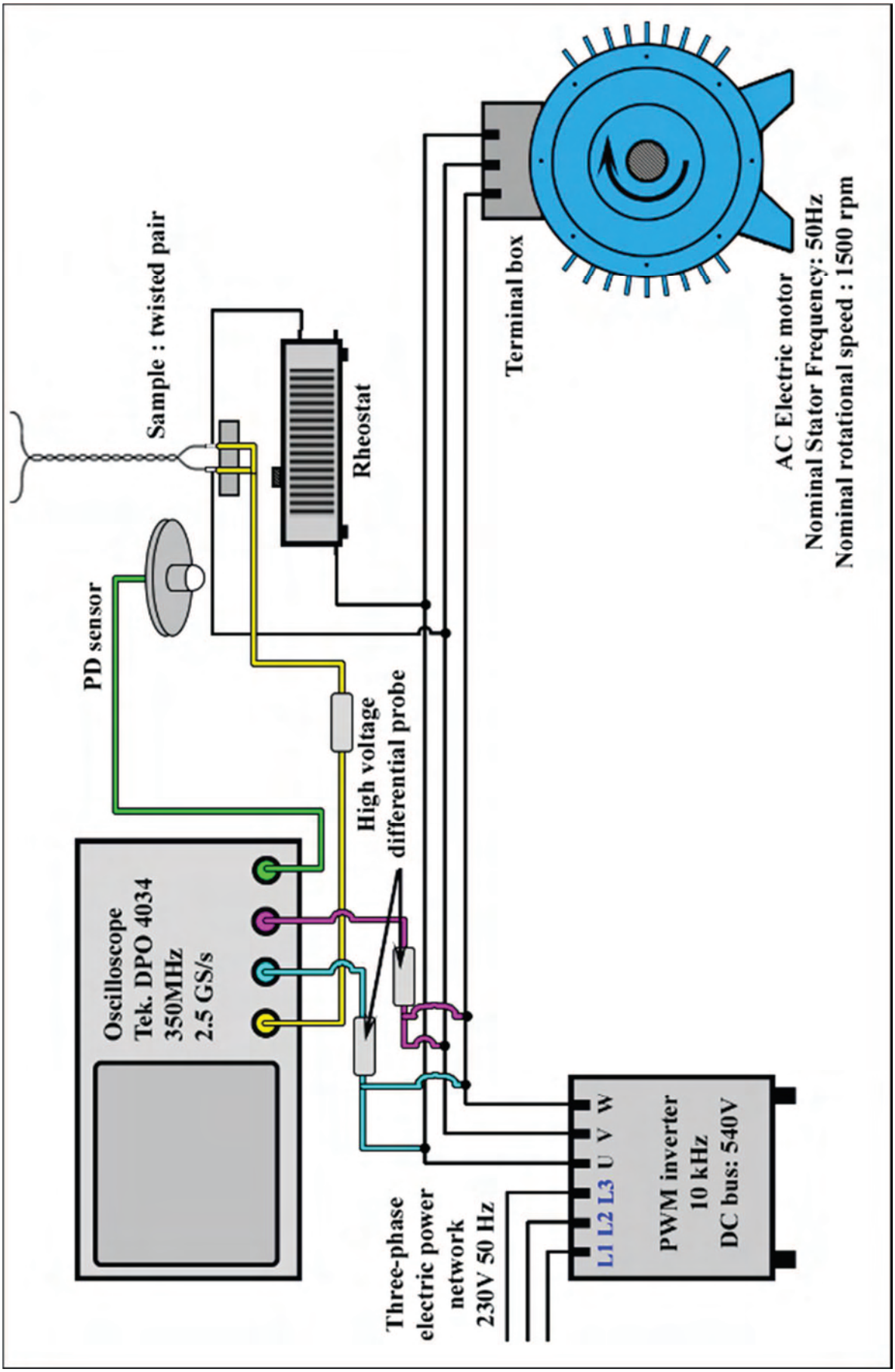

Figure 37: Experimental set-up n°1

Series with the twisted pair is the 1kΩ rheostat, first envisaged as an extra protection for the PWM inverter and the power supply, would the twisted pair broke down. But actually, its resistive and inductive behaviour, because of its wounded wire design, produce overvoltage at the terminal of the twisted pair, thus increasing the chance of causing partial discharge in the sample. Moreover, the rheostat is actually lowering the slew rate of the surge voltage generated by the inverter drive, which will prove to come handy when trying to detect partial discharges in the sample around switching area.

In the vicinity of the power cable connected to the twisted pair are the different non-intrusive sensors. Note that sensors are not aiming towards the sample but aiming towards cable connected to the sensor. Indeed, considering future test on electric motors, almost no space will be available neither in the direct vicinity of the motor nor inside it. More likely, sensors will have to be put at motors terminals or in the machine connection box. Sensors outputs are directly connected to the oscilloscope.

Finally, voltage across the sample is monitored through a high voltage differential probe directly connected at twisted pair terminals. Others phase-to-phase voltages could be displayed as well on the oscilloscope.

4.5.3. Test procedure

It should be noted that sensors detect some perturbations in the starting phase of the machine. Thus all measurements are only carried out when the electric motor is at steady state to avoid early false positive signals. Since phase's output voltage can not be controlled (DC bus 400V) partial discharge detection method only relies on trying to find them, hoping partial discharge inception voltage has been reached in the sample. Hopefully, some samples will feature partial discharge at that fixed output voltage considering overvoltage caused by cables and rheostat.

4.5.4. Discussion of results

4.5.4.1. Voltage waveforms

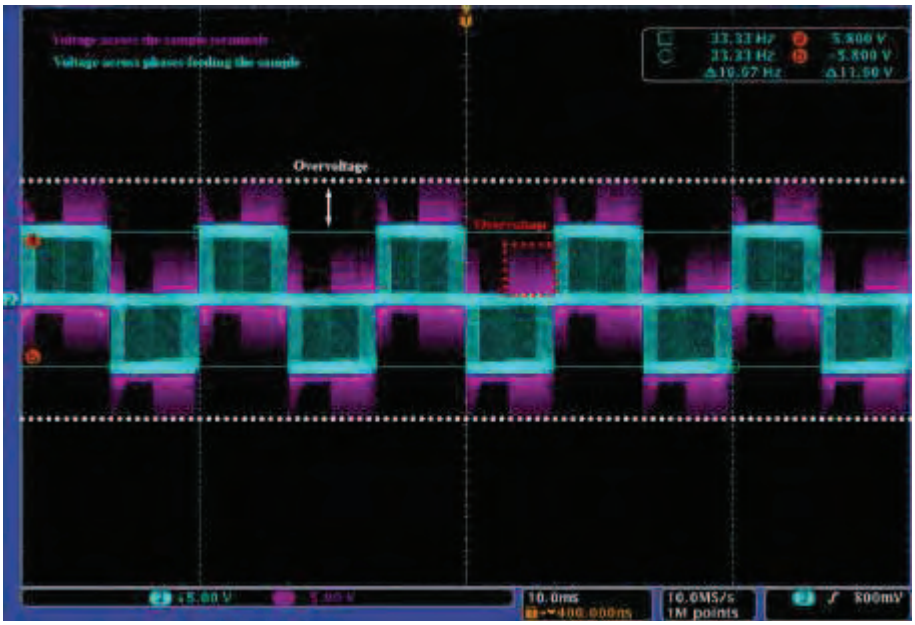

Figure 38: Overview of voltage and overvoltage

Figure 38 displays both voltage across the sample terminals (purple) and voltage across the phases feeding the sample at PWM output terminals (blue) on a large time scale (10ms per division). The aim of this figure is to assess the impact of the rheostat and cable length on the sample electrical stress. The main information here is that severe overvoltages (about 40-50% of regular phase-to-phase voltage – dotted white line) are occurring on a regular basis across the sample. Moreover, in a negative phase-to-phase voltage, overvoltage could be positive (dotted red square). On a side note, the nominal stator frequency (stator field rotating frequency) is easily observable (50Hz), that is to say a period of 20ms.

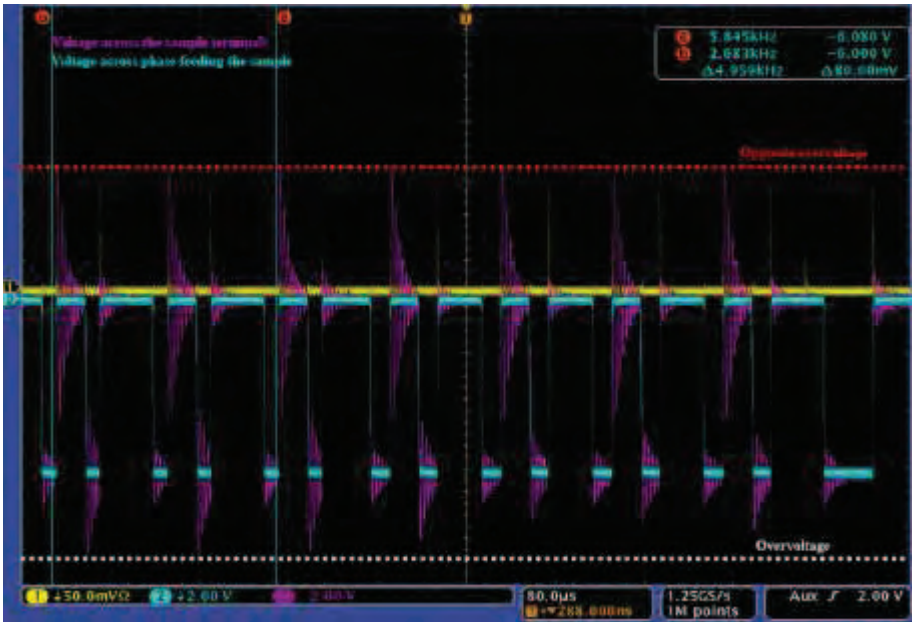

Figure 39 : PWM signals and overvoltage

In figure 39, the time scale is smaller (80µs per division) than in figure 38 so that more details on PWM waveforms signals can be observed, here in negative polarity. Lengths of PWM signals vary usually from 20µs to 60µs and time between surges vary from 10µs to more than 50µs. Overvoltages vary from 20% to 60% of the phase voltage both in the same polarity (white dotted line) and in the opposite polarity (red dotted line). The opposite polarity overvoltage is, on average, higher than the standard overvoltage.

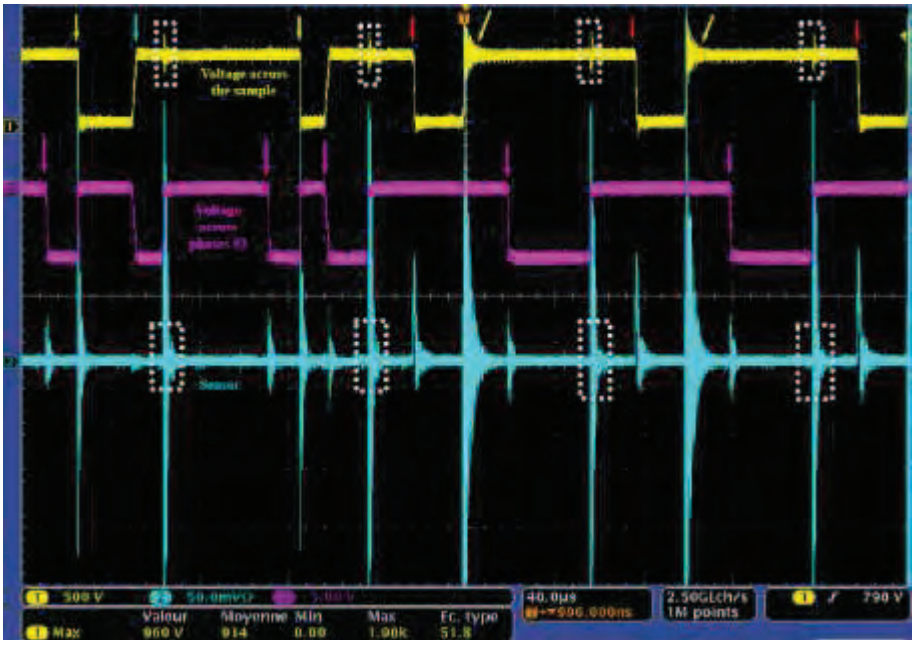

Figure 40 : PWM signals and sensor signal

In figure 40, the time scale is smaller (40µs per division) than in figure 9 so that more details can be observed about sensor's different reaction to switching. As explained in the experimental set-up, the sensor is placed in the vicinity of the sample but is not close to the three main phases. The sensor is only close to phases (1 and 2) feeding the sample through the rheostat.

The yellow arrows represent switchings with the lowest rise or fall time. Sensor's output for such rapid switchings is high frequency oscillating and large magnitude signals.
Sometimes, the switching appears to be slower (red arrows) and, accordingly, sensor's output is different from the faster switchings. The sensor's signal magnitude, in that case, seems to be lower and, more importantly, is made up of a less disturbed rise time hinting that the frequency spectrum is different. The blue arrow points toward a quite slow switching and the sensor is not really detecting it.

But the sensor is not only able to detect switchings in the two observed phases (1-2). Indeed, as the white dotted boxes suggest, the sensor could also observe high frequency oscillating and large magnitude signals when a switching in the remaining phase (3) occurs as shown by the "Voltage across phases #3" trace which represents voltage across phases 2-3. And, as the purple arrows point, even slower switchings could be detected, albeit with a smaller amplitude.

These small and high frequency oscillating signal are actually very close to what would be a partial discharge signals. So, in order not to confuse potential partial discharge signals with switchings occurring in the remaining phase, at least two phase-to-phase voltages should be observed at the same time to prevent any mistake. Another hint of false positive partial discharge signal is the occurrence of such a phenomena, which is not as erratic as partial discharge signals should be. Here, switching appears periodically.

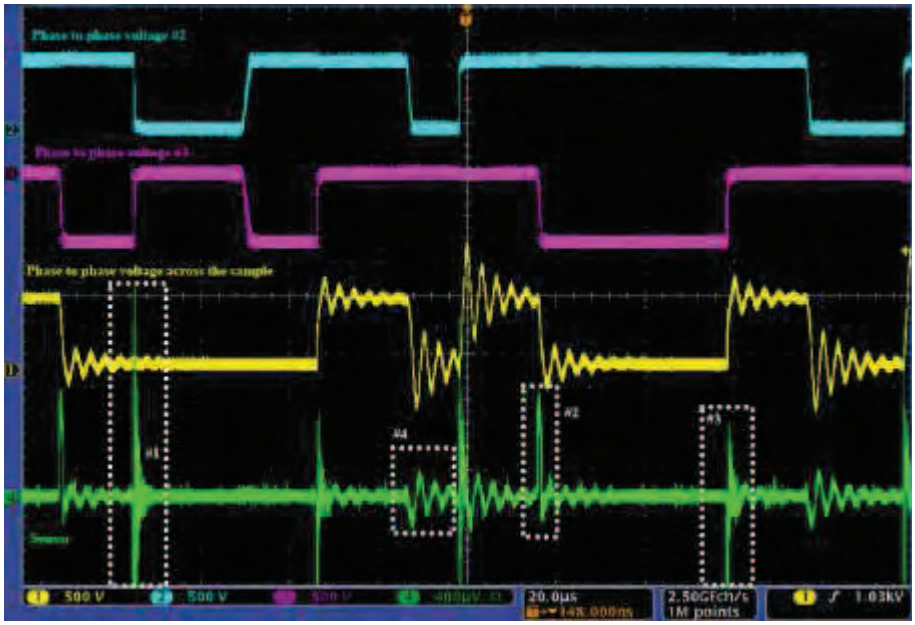

Figure 41 : PWM switchings and sensor's output

In figure 41, the time scale is, once again, smaller. Depending on the characteristics of the switching, the sensor's output is different. White dotted box #1 underlined a typical fast switching even if it doesn't belong to the two phases connected to the sample and observed in the yellow trace. Whereas box #2 highlight a much slower falling switching and the sensor's output is not oscillating at the same frequency. Box #3 is underlining a mixed type of switching, in-between case #1 and #2, with a fast rise time followed by a lower frequency oscillating component. So, sensor's output is of a smaller amplitude but still high frequency at the beginning, but the last part of the sensor's signal is much more close to case #2. And, finally, box #4 focus on a slow switching but featuring a very oscillating voltage and the sensor's output is, in that case, very oscillating as well.

Sensor's output is thus very sensitive to the different kinds of switchings.

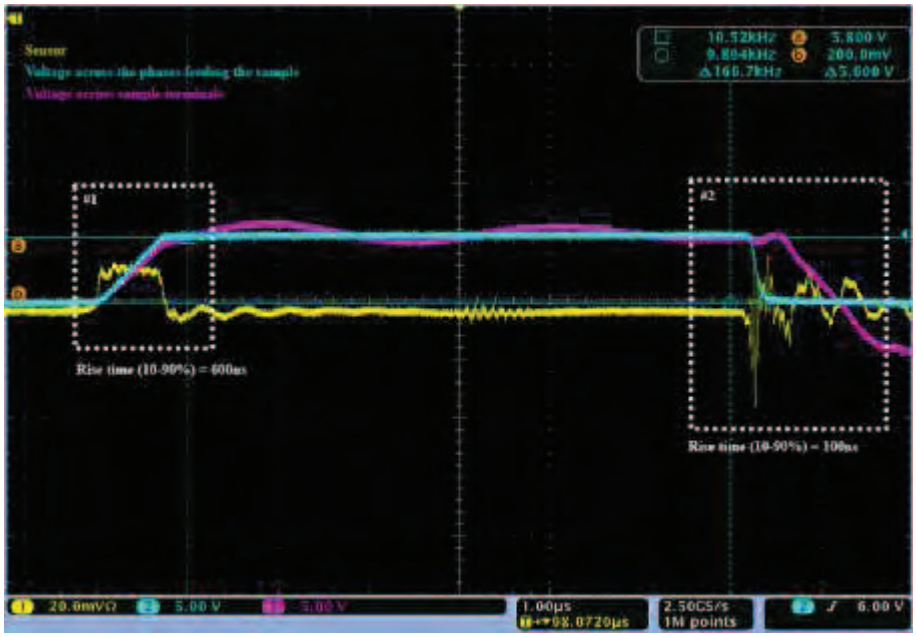

Figure 42 :Sensor's output and voltage variation

In figure 42, the time scale of 1µs is much more smaller than those in previous figures and focus on sensor's signals. Between boxes #1 and #2, a big difference could be observed between rise times and sensor's output. In box #1, the rise time is quite long (600ns) and the voltage increase is linear and steady. As the sensor's output is function of electric displacement variation, a linear increase in voltage is, logically, represented by the sensor as a step output voltage, whose magnitude is proportional to the slope of the increase. This example is a direct observation of the sensor's output function, which is thus indirectly function of the electrical field variation, so electric potential variation. But, the step voltage is not perfectly square and very small perturbations of higher frequency could be observed.

In box #2 the fall time is quicker, (100ns). Moreover, the fall time does not vary linearly as in the previous switching but is much more like a part of a decreasing sinusoidal curve. The sensor's output main component is thus a sinusoidal, damped signal. In addition to that, small perturbations could be observed as in box #1 case.

So the sensor's output signal is directly function of the length of the rise/fall time and can thus, give rough indications on PWM inverter switching characteristics.

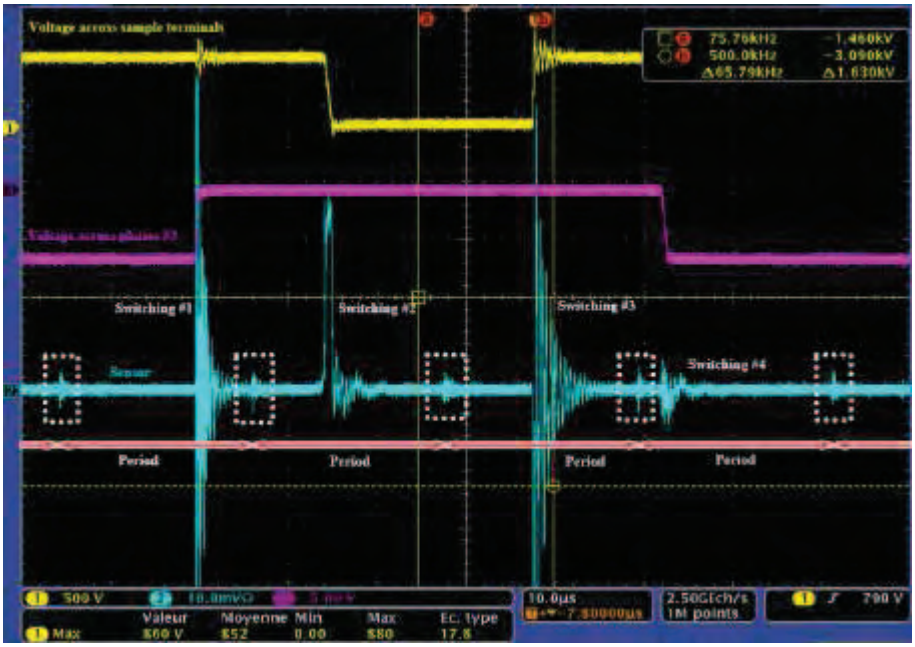

Figure 43: Sensor's output and power electronics noise

In figure 43, a time scale of 10µs per division allows a detailed observation of both sensor outputs, voltage characteristics regarding rise times and overvoltage and a sample of the different kinds of switching observed by the sensor.

Thus, switching #1 and 3 are both quick but are not occurring on the same phase. Actually, switching #1 is not occurring in a phase feeding the sample, where the sensor is placed. The main difference between sensor's signal for both switchings is how defined the sinusoidal part is since no significant magnitude difference is observed. The sine damped curve is not as clear in switching #1 as it is in switching #3. The reason maybe that the electric displacement field variation wave caused by the switching #1 is either coming from further away than the switching #3 feeding the sample, thus causing distortion in the radiative transmission process. Or, the electric displacement field variation wave is conveyed in power cable while transmitting information, thus also causing distortion of information in the transmission line. These are hypothesis since nothing can assess with certainty the fact that the two switchings were actually very similar. Maybe attenuation is into play but switching #1 was much more powerful than switching #3.

Switching #2 is typical of a slow rise/fall time and the sensor is featuring a step-like output voltage caused by the linear variation of the voltage. Switching #4 is likely to be similar to switching #2 but seems, if true, to have been modified by attenuation and distortion when transmitted.

Finally, an important observation has to be made regarding the signals in the white dotted boxes. These small, high frequencies signals, are periodic as highlighted by the red and whites arrows between each of them. The period is around 12µs, which correspond to a 83kHz frequency. Actually, these small and periodic signals are caused by power electronics in the PWM inverter drive and have been identified by moving around the sensor and following the amplitude variation towards the origin. These signals should not be confused with partial discharge signal. Once again a regular occurrence is a clear warning of false positive partial discharge signals.

4.5.4.2. Partial discharge detection

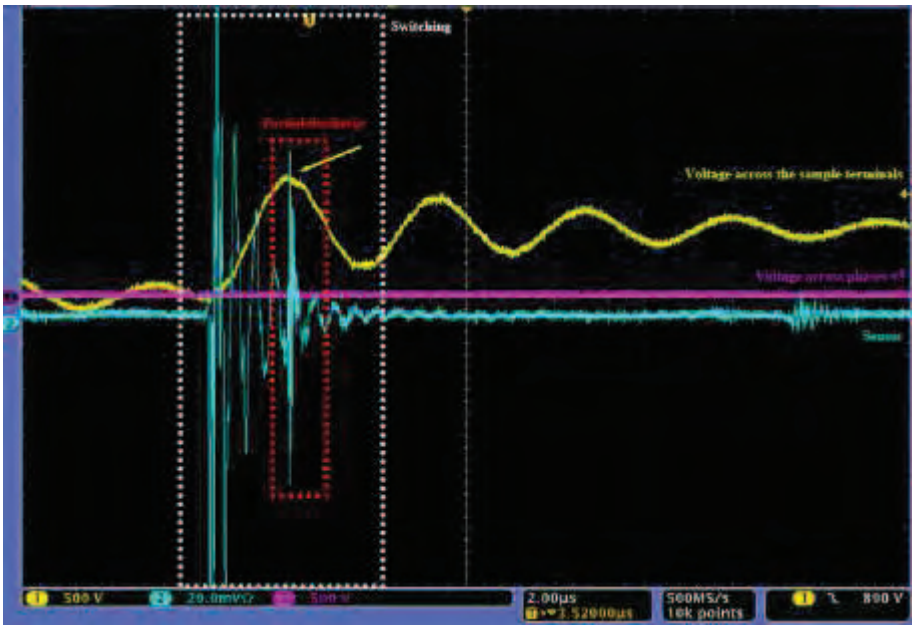

Figure 44 : Partial discharge #1

In figure 44, the first partial discharge could be observed. In the dotted white box, the switching is of large magnitude (out of range here) and very oscillating due to the sine shape of the voltage increase. But, this switching is not that quick with a rise time of a bit less than 2µs and the different oscillations could easily be identified. In addition to that, the effect of the rheostat and cable length is very clear. Indeed, the maximum voltage has been delayed and has a time off-set of around 2µs as shown by the yellow arrows. Thus, the rheostat is actually shifting the likely location of partial discharge away from the noise generated by the switching which is quite an advantage.

These last two observations allow for a clear identification of the partial discharge (in the red dotted box) exactly at the maximum voltage, which is 1 kV. The partial discharge signal as seen by the sensor is on top of the switching signals. Moreover, these two different kinds of signals seem to have a very different frequency spectrum and time constant. For the switching, the main frequency component is around 2-5MHz and the time constant (from 90% to 10%) for this system is around 4µs. Regarding the partial discharge, the main frequency component is so high that it could not be measured on this figure but one can safely assume the frequency range is composed of much higher frequency. The time constant in this case is around 300-400ns.

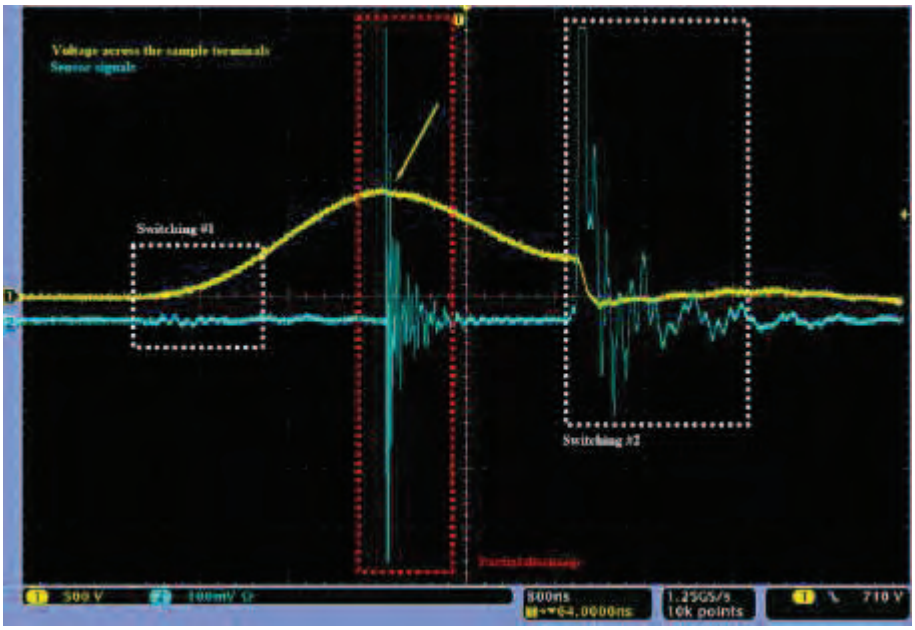

Figure 45 : Partial discharge #2

In figure 45, another partial discharge signal could be observed very easily. In the dotted white boxes, two different kinds of switching could be seen. Switching #1 image through the sensor is almost non-existent for a sine-type rise type of a bit less than 2µs which is the same as in figure 15 (attention: time scale are different in figure 15 and figure 16). Thus, no PWM noise from switching #1 is interfering with the partial discharge detection. Whereas switching #2 is much more quick and produce lots of oscillating phenomena and would make the detection more difficult.

The partial discharge in the red dotted box is exactly at the maximum voltage, which is a bit less than 1kV this time. The frequency spectrum of the partial discharge is still difficult to assess but the higher frequency components would start at 20-50MHz (period 50-20µs).

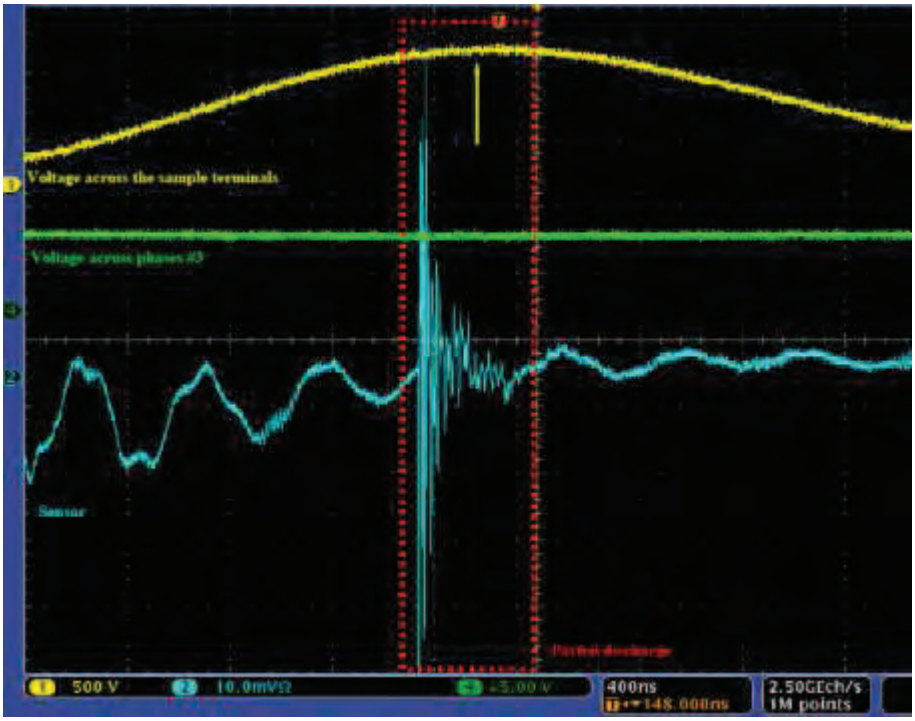

Figure 46: Partial discharge - zoom

Figure 46 is a zoom of a partial discharge (red dotted box) signal with a time scale of 400ns. The partial discharge occurs almost at maximum voltage (1kV) and this shorter time scale supports the fact that discharge signal feature higher frequency component. On a side note, late oscillations caused by the switching have a 2.5MHz frequency

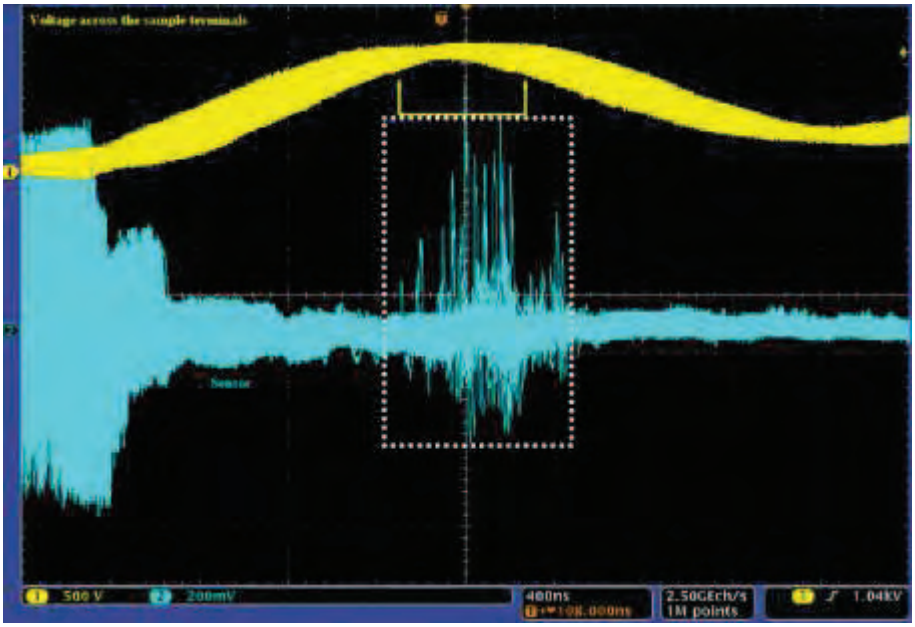

Figure 47 : Partial discharge – persistence

Figure 47 shows partial discharge signals acquired in persistence mode over several dozen of seconds. Since the trigger on the voltage across the sample is moving slightly, the yellow trace is a bit thick. Nonetheless, most of partial discharge signals are within the limits shown by the yellow arrows, delimiting maximum voltage area across the whole acquisition.

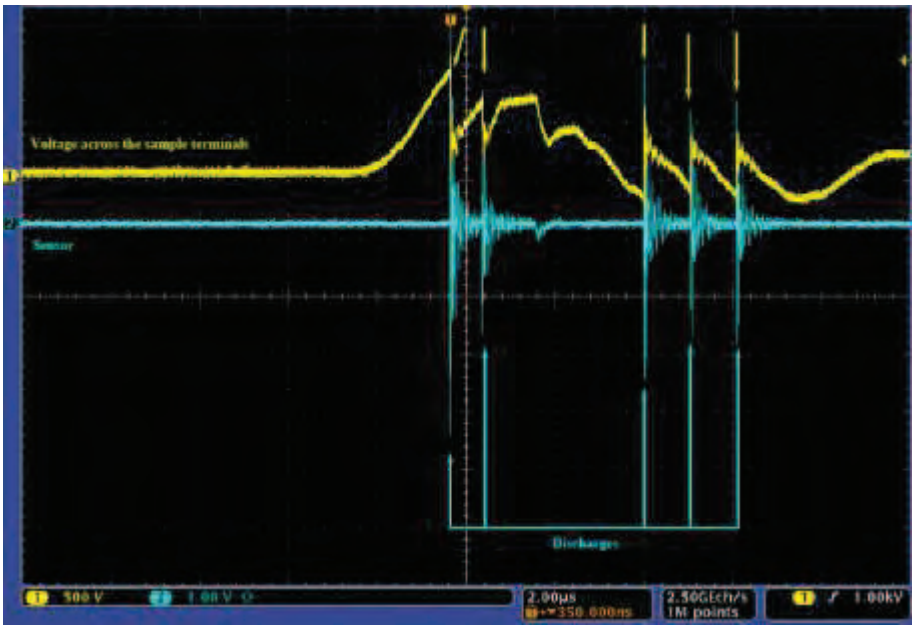

Figure 48: Partial discharge, statorette and breakdown

In Figure 48 above, the sample under test is a statorette fed (turn-to-turn insulation is tested in one coil) indirectly by the PWM inverter instead of the previous twisted pair. At that point, the sample seems to be very close to breakdown with a very high number of discharge events. As these discharges repeat at a very high rate, showing that discharge inception voltage is lower (first partial discharge inception voltage at 900V, then around 700V) than the previous twisted pair sample. Voltage across the sample is severely dropping at each occurrence, thus hinting that a large flow of current is going through the insulation system at each discharge event. Accordingly, the sensor response to such supposed large magnitude discharges are very large amplitude signals (several V compared to several dozen or hundreds of mV previously). Even if a universal calibration of sensor is definitely not on the agenda, some simple relative comparisons could be made between amplitude of perceived discharge signals in the same kind of sample and in the same experimental set-up.

4.5.4.3. Sensors comparison and non-intrusive method performance

In this part, performances of the coaxial cable sensor and current transformer sensors are compared to the D-Dot sensor, which is the reference.

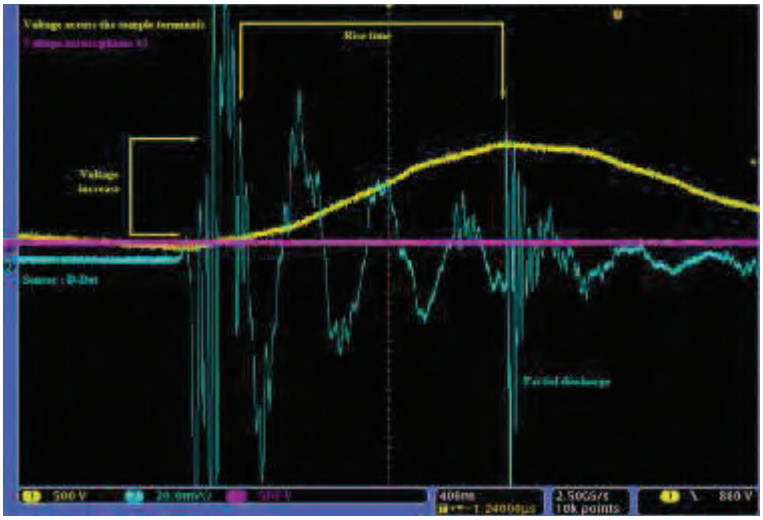

Figure 49 : Partial discharge detection – D-Dot sensor

Figure 49 shows a typical partial discharge detected by the D-Dot sensor. The sensor detects the partial discharge signal occurring at the maximum voltage easily. The switching is of very high amplitude (out of range) and exhibits a main low frequency component of around 2.5MHz

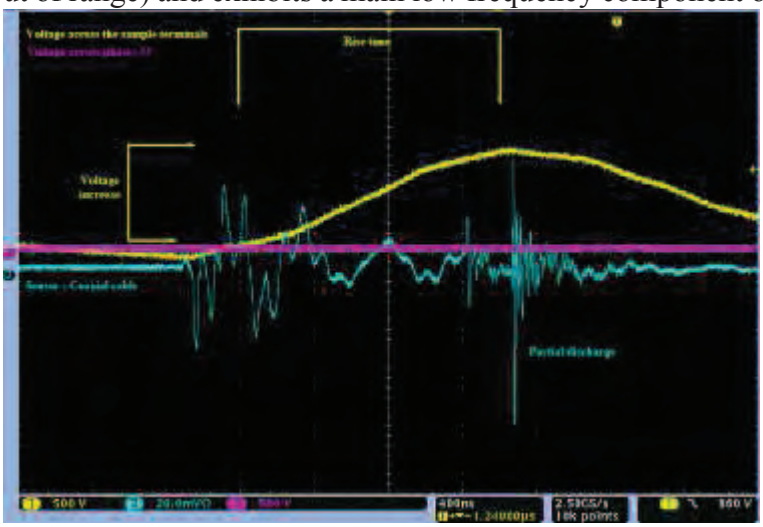

Figure 50: Partial discharge detection – Coaxial cable sensor

Figure 50 shows, with the same parameters (time and volt scale), another typical partial discharge detected by the coaxial cable sensor positioned at the exact same location. What is important is the fact that in both figures (20 and 21), partial discharges are detected. Since each partial discharge is different, cautious comparison should be made. Switchings are almost the same in both case and it seems that the coaxial cable sensor is almost operating like a high-pass filter, attenuating the noise generated by the PWM inverter. Obviously, an accurate signal-processing and sensor's calibration should give different results from the coaxial cable sensor to the D-Dot sensor. But in this part, only detection potential matters and the self-made sensor is, on this aspect, at least as much efficient as the D-Dot sensor.

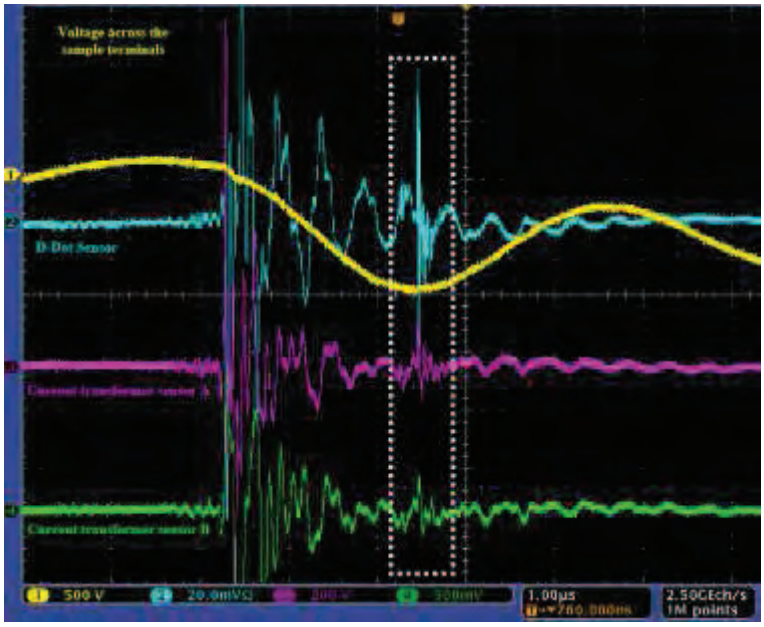

Figure 51: Partial discharge detection and current transformer sensor #1

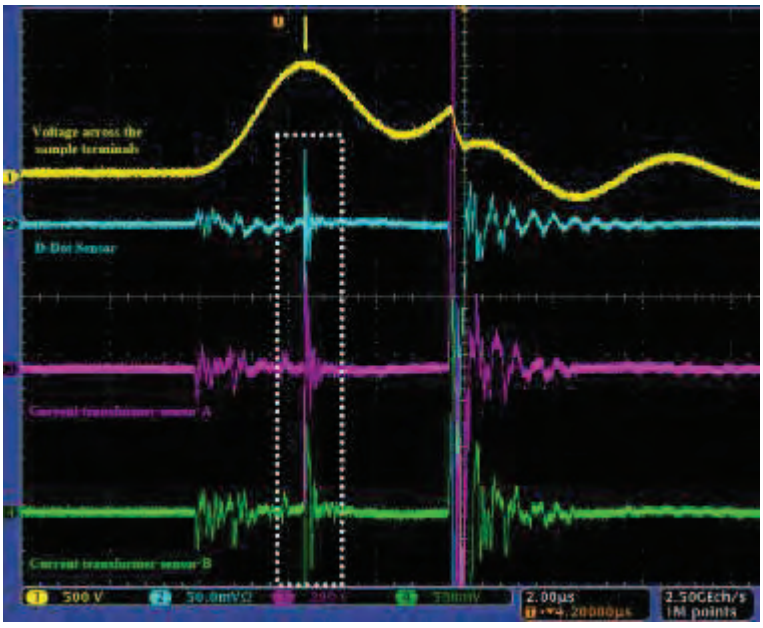

Figure 52: Partial discharge detection and current transformer sensor #2

Figures 51 and 52 both display a comparison between the D-Dot sensors and two current transformer sensor. All sensors are positioned as much as possible in the same area to prevent any significant delay or attenuation effect. In both cases, all sensors are connected to the oscilloscope at the same time, thus ensuring the same input signals for all sensors. All sensors easily detect partial discharges in the two above cases, whatever the type of switching. But, one should be cautious making further statement since in figure 51, D-Dot partial discharge magnitude is much higher than the current transformer sensors. Indeed, in figure 52, all partial discharge magnitudes are more or less the same for all sensors.

The D-Dot sensor is not the only electro-magnetical coupling device allowing partial discharge detection. For the following experiments, the coaxial cable sensor is used, unless stated otherwise, as the primary sensor. The performance of current transformer sensors in the following experiment has not been investigated in this work.

4.5.4.4. Differential filtering

Before going with a high-pass filtering in the next paragraph, an easy to use and carefully crafted filtering method to improve partial discharge detection within switching noise is presented.

Figure 53 displays the slightly modified experiment set-up. Instead of one sensor, two sensors are used at the same time but at different location. In order to have comparable results, two jack SMA sensors have been used for their standardized design. The first "discharge" sensor (SMA #1) is placed in the vicinity of the sample, pointing towards power cable, to detect potential partial discharge events. The second "source" sensor (SMA #2) is positioned right next the PWM inverter drive, as far as possible away from the sample under test in order not to detect as clearly as SMA #1 the partial discharge events.

This filtering solution proposes to use the property of power cable as an imperfect transmission line. Indeed, partial discharge signals as seen by the sensor are usually small magnitude and high frequency components signals whereas, PWM inverter drive signals as seen by the sensor have a larger amplitude and not so much high frequency components. But these partial discharge signals face attenuation and distortion as they propagate in the circuit. In short, transmission line acts as a low-pass filter and the longer the transmission line is, the lowest the cut-off frequency.

Thus, by subtracting SMA signal #2 from SMA signal #1, the resulting signal is the equivalent of a high-pass filter. In theory, PWM noise should be subtracted for both sensors and only partial signals should remain, although surely affected by the operation.

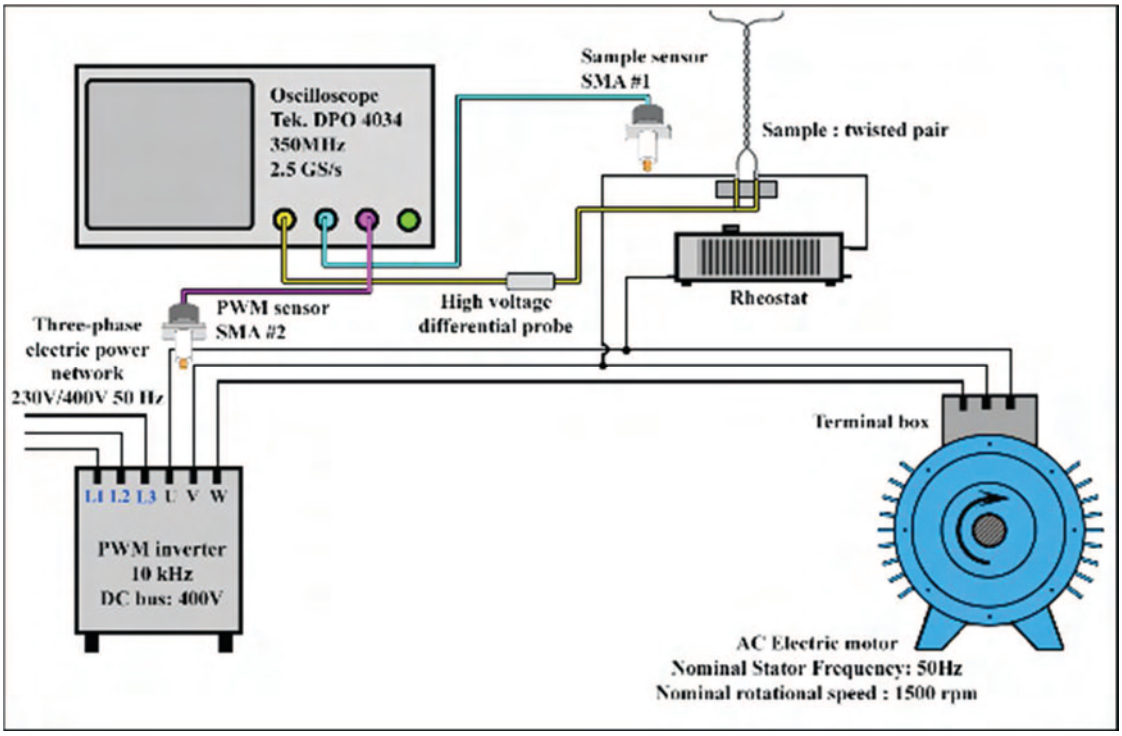

Figure 53: Differential filtering – experimental set-up

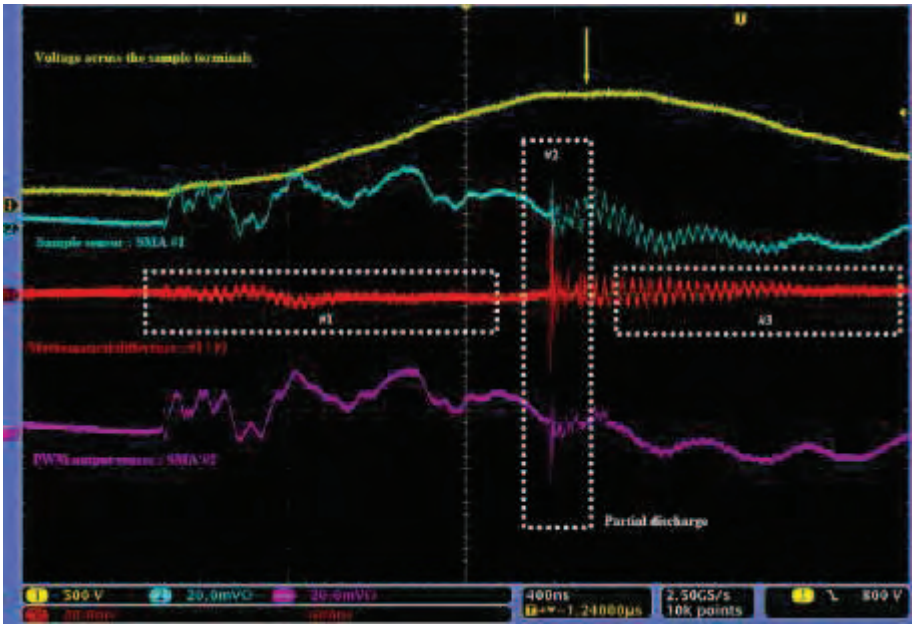

Figure 54 : Differential filtering – Signals subtraction

Figure 54 displays the result of the aforementioned subtraction between signals originating from SMA #1 and #2. The partial discharge is the small signal in the dotted white rectangle, juts before the maximum voltage symbolized by the yellow arrow. This partial discharge signal is obvious on either SMA #1 and SMA #2 for an expert eye used to look for such phenomena, in that case a filtering is not mandatory. In this example, the switching's image by the sensor is indeed neither very oscillating nor large compared to the partial discharge signal

But, in this case the subtracting operation is working well in zone #1 (dotted white rectangle) and almost all the low frequency components of the signal have disappeared. Whereas, a small magnitude and high frequency oscillating signal is still remaining. In the partial discharge zone #2, the resulting partial discharge seems to be larger than, individually, before the subtracting operation. A small delay or not the exact same output to transient and high frequency phenomena could explain such a result. Nonetheless, the partial discharge is clearly visible. Finally, in zone #3 after the partial discharge, the low frequency component has been erased with a small oscillating signal remaining. All in all, this method proves to be efficient on this kind of noise.

From a theoretical point of view, one should note that SMA #2 signal is freer of small noise oscillating signals that signals coming from SMA #1, thus illustrating the transmission line theory. When switching's image through the sensor has higher frequency components, the subtracting method is less impressive. But, this differential filtering solution could be associated with a Schmitt trigger in order to automate a discharge counting process based on the subtracting filtering method while taking into account potential false positive signals. Indeed, by subtracting signals, some partial discharge like signal could appear. A frequency analysis could be wrong as well because this subtracting operation could create artificial high frequency signals.

4.5.4.5. High-pass filtering

Another mean to increase the signal to noise ratio, and thus enhancing partial discharge detection close to the switching, is to use a high-pass filter directly connected to the sensor. To do so, a second order high-pass filter (RLC) has been built in order to reject some of the "low frequency" PWM generated noise during measurements.

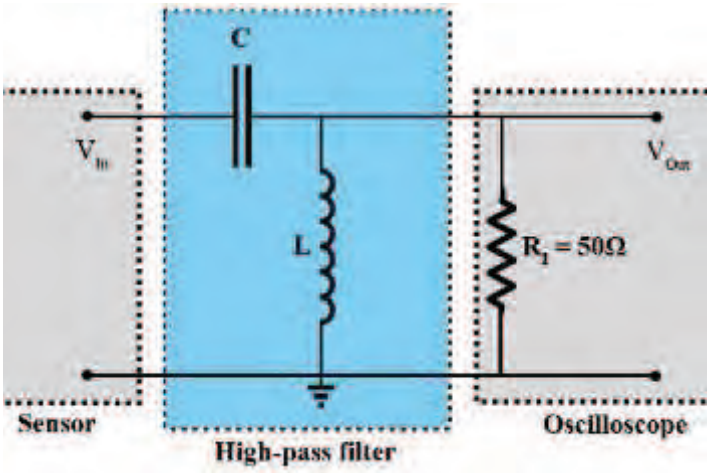

Figure 55 : High-pass filter diagram

The target cut-off frequency (f) is chosen at 5MHz after a rapid frequency analysis of switching's typical spectrum. The second target is a damping factor (z) of 1, so that no oscillations are created and that the system converges to zero as fast as possible. This cut-off frequency should just lower amplitude of PWM electro-magnetical noise and makes partial discharge detection easier. Here, only the input's impedance of the oscilloscope has been considered and fixed at 50Ω for the high pass filter calculation, matching it in the process with the coaxial cable sensor whose impedance is 50Ω. Thus, the inductance and capacitor values are chosen (final equations 5 and 6 below) to fit the aforementioned requirements as explained in the following synthetized keys equations.

$$\frac{V_{out}}{V_{input}} = \frac{RCLp^2}{R+Lp+RCLp^2} = \frac{LCp^2}{1+\frac{L}{R}p+LCp^2} \quad (1)$$

$$\omega_n = \frac{1}{\sqrt{LC}} = 2\pi f \quad (2)$$

$$\frac{L}{R} = \frac{2z}{\omega_n} \Leftrightarrow R = \frac{L\omega_n}{2z} \Leftrightarrow R = \frac{1}{2z}\sqrt{\frac{L}{C}} \Leftrightarrow R = \frac{1}{2zC\omega_n} \quad (3)$$

$$\frac{V_{out}}{V_{input}} = \frac{LCp^2}{1+\frac{2z}{\omega_n}p+\frac{p^2}{\omega_n^2}} \quad (4)$$

$$L = \frac{2zR}{\omega_n} \quad (5)$$

$$C = \frac{1}{2zR\omega_n} \quad (6)$$

$$Z = \frac{1 + \frac{L}{R}Cp + LCp^2}{Cp(1 + \frac{L}{R}p)} \quad (7)$$

Once the filter has been built it is then characterized to check phase and impedance changes over frequencies and analyse along the impedance equation (7). Measurements are performed with a HP4194 Gain-Phase analyser from 10kHz to 40MHz after short-circuit and open-circuit compensation have been carried out.

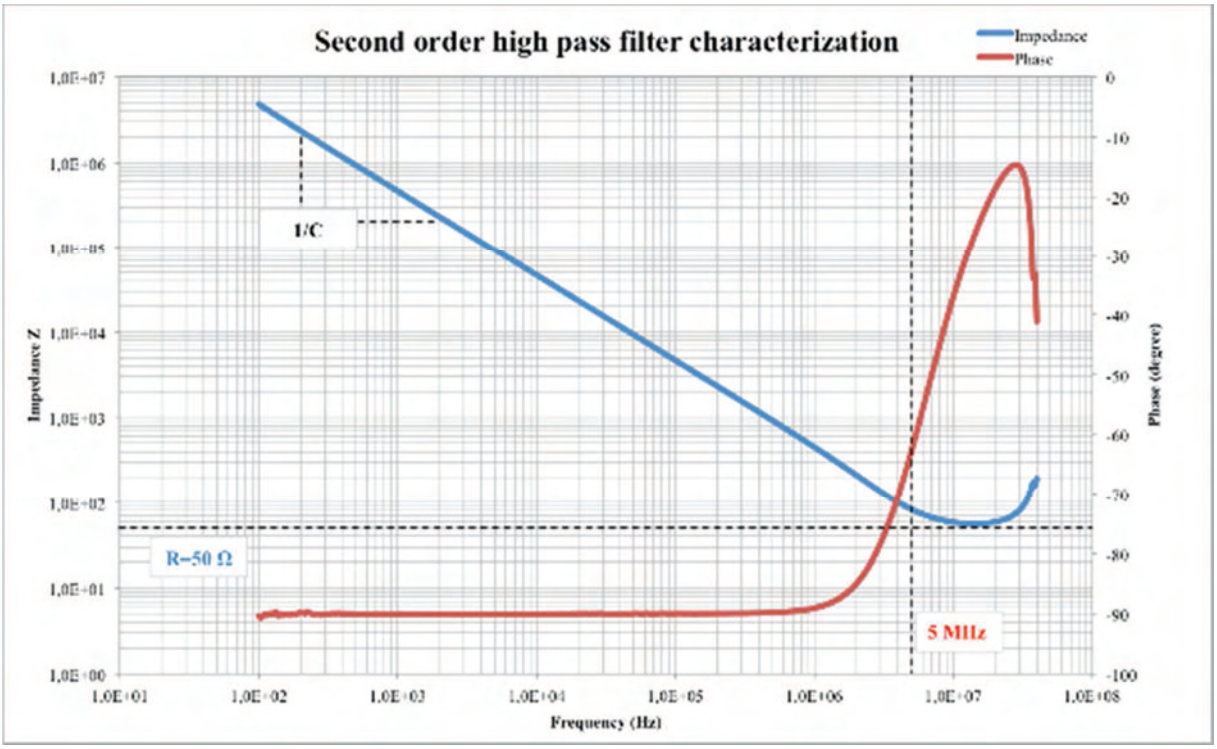

Figure 56 : High-pass filter - characterisation

The limit of Z as frequency approaches zero is the inverse of the capacitance. Indeed, at low frequency, the inductance is equivalent to a short circuit and the resistance is small compared to the inverse of the capacitance. Thus, the lower the frequency, the higher the impedance and the lower the gain. The limit of Z as frequency approaches infinite is simply the resistance R. At high frequency, the inductance is equivalent to an open circuit whereas the capacity is equivalent to a short circuit, thus leaving only the resistance.

Measurements plotted in Figure 56 confirm this analysis, when frequency approaches zero, the impedance is high whereas when the frequency approaches infinity, and the limit of the impedance is the resistance R. The slope should be equal to the inverse of the capacitance. The phase seems correct at low frequency with a minus ninety degree phase shift, then increase towards zero as frequency approaches the cut-off frequency. For both phase and impedance measurements, higher frequency points should be read with caution as they are close to the spectrum analyser limits.

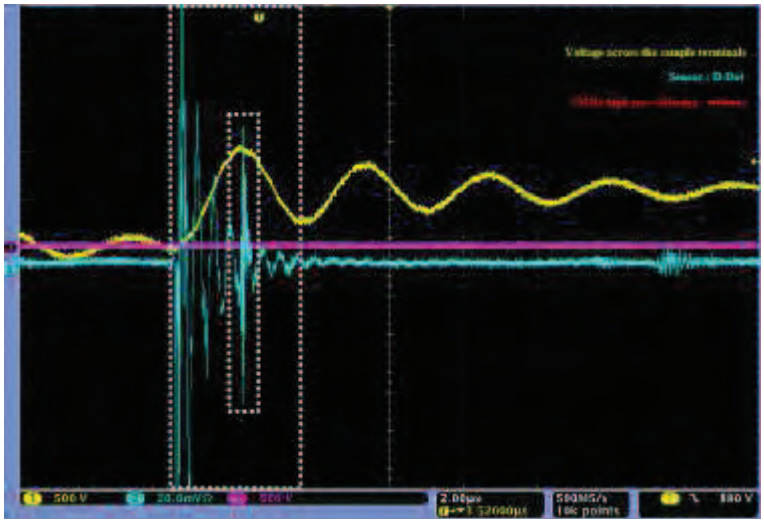

Figure 57 : D-Dot sensor without high-pass filtering

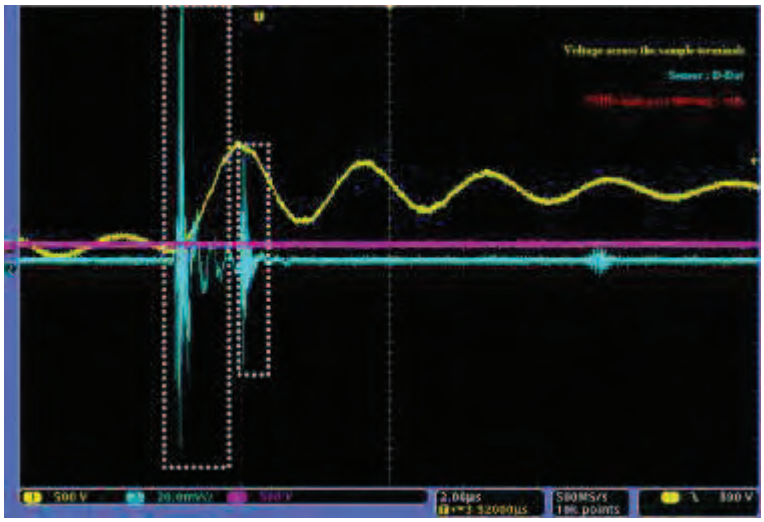

Figure 58: D-Dot sensor with high-pass filtering

Figure 57 displays the D-Dot sensor signal alone whereas figure 59 displays the D-Dot sensor with the high-pass filter, which has a cut-off frequency of 5MHz. In both figures, time scale and voltage scale are the same so that comparison is easier. Same kind of voltage increase parameters (rise time and maximum voltage) has been targeted for this experiment in order to compare both results on a as consistent as possible basis.

In the first case, the partial discharge is typically detected (white dotted rectangle) exactly at the maximum voltage while the switching's noise is still visible. In other words, the partial discharge signal is drowned among noise signals. For the switching's image through the sensor in itself, the magnitude is out of scope (more than 200 mV) and a clear 2.5-5 MHz oscillating component could be identified. In the second case, with the high-pass filter, the switching's image has a lower initial magnitude and, then, essentially less large oscillations and a shorter time constant which means the noise is lasting less than without filtering. The partial discharge signal does not seem to have been neither distorted nor attenuated greatly.
In conclusion, using a high-pass filter is a simple and efficient way of improving the signal-to-noise ratio. Although in these cases the maximum voltage is almost always delayed thanks to the rheostat and long cable, these first filtering results show that it can bring more visibility during the switching. Regarding the cut-off frequency, a 5 MHz limit seems to be not high enough to significantly attenuate switching's noise.

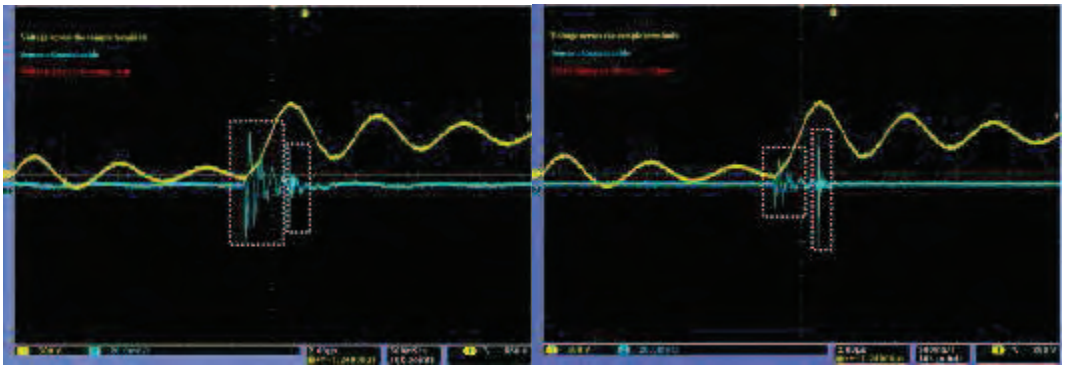

Figure 59: Coaxial sensor and high-pass filtering

As for the coaxial cable sensor, similar conclusions can be drawn from the use of the high-pass filter. The only difference is that this sensor seems to have less sensitivity to low frequency than the D-Dot sensor, thus the influence of the filtering is less significant.

4.5.4.6. Summary

In these first experiments, the following elements are identified as the main conclusions

- Non-intrusive sensors are able to detect partial discharge signals caused by a twisted pair in a PWM environment.
- Non-intrusive sensors' output is, indirectly, function of the variation of the electric field variation and is thus responding differently according to the type of switching events.
- Power electronics signals and switching events on other phases could be interpreted as partial discharge signals, check occurrence and other phase-to-phase voltage.
- Most of partial discharges seem to appear during or close to the switching events, obviously at the maximum voltage
- Partial discharge signals have higher frequency components than PWM noise signals.
- Thus, high-pass filtering is a mean to improve the signal-to-noise ratio during switchings and enhance detection abilities in this critical zone.
- Self-made coaxial cable sensor is as efficient as the D-Dot sensor for partial discharge signal detection.

4.6. Off-line partial discharge detection in an electric stator: one phase test

4.6.1. Purpose of the experiment

In this second experiment, the aim is to try to reach and detect partial discharge inception voltage in an electric stator fed by a PWM inverter off-line with a non-intrusive sensor. Building on the previous observations from the last experiments, the aim is to confirm that partial discharge detection is still possible in a more complex sample directly fed by a PWM inverter drive. Filtering techniques and detection methods have to be tested and adapted to the new sample and, more importantly, to the new PWM inverter.

4.6.2. Experimental set-up

As shown in Figure 61, the experimental set-up consists in a PWM inverter drive feeding an electric stator through the neutral point and one phase to put the maximum electrical stress on one phase at a time, thus increasing the chance of approaching partial discharge inception voltage. This PWM inverter has been entirely thought, designed and built at the Laplace Laboratory in two different copies, each one with its own specificities. Here, the focus is only on the first one, the second one will be used and presented in the third experiment. This PWM inverter is able to feed two phases at the same time with bipolar controllable voltage waveforms. As a result, the frequency of the PWM pattern could be modified at will, albeit with a maximum frequency of around 15kHz. By controlling directly the three key parameters of the inverter drive command, lots of signals waveforms can be chosen to feed a sample. These three command parameters, which are used to build the final voltage signals across phases are: period, high time and delay between the two command signals.

As shown in figure 60, when the two commands signals are similar, no voltage is applied across the two phases. When the two command signals are different, depending on which one is greater than the other, the output voltage is positive or negative.

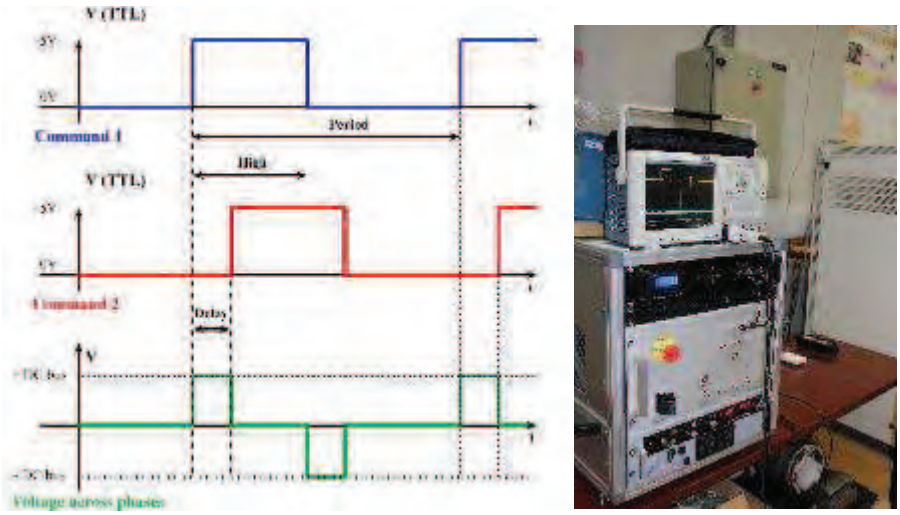

Figure 60: Lab-made PWM command

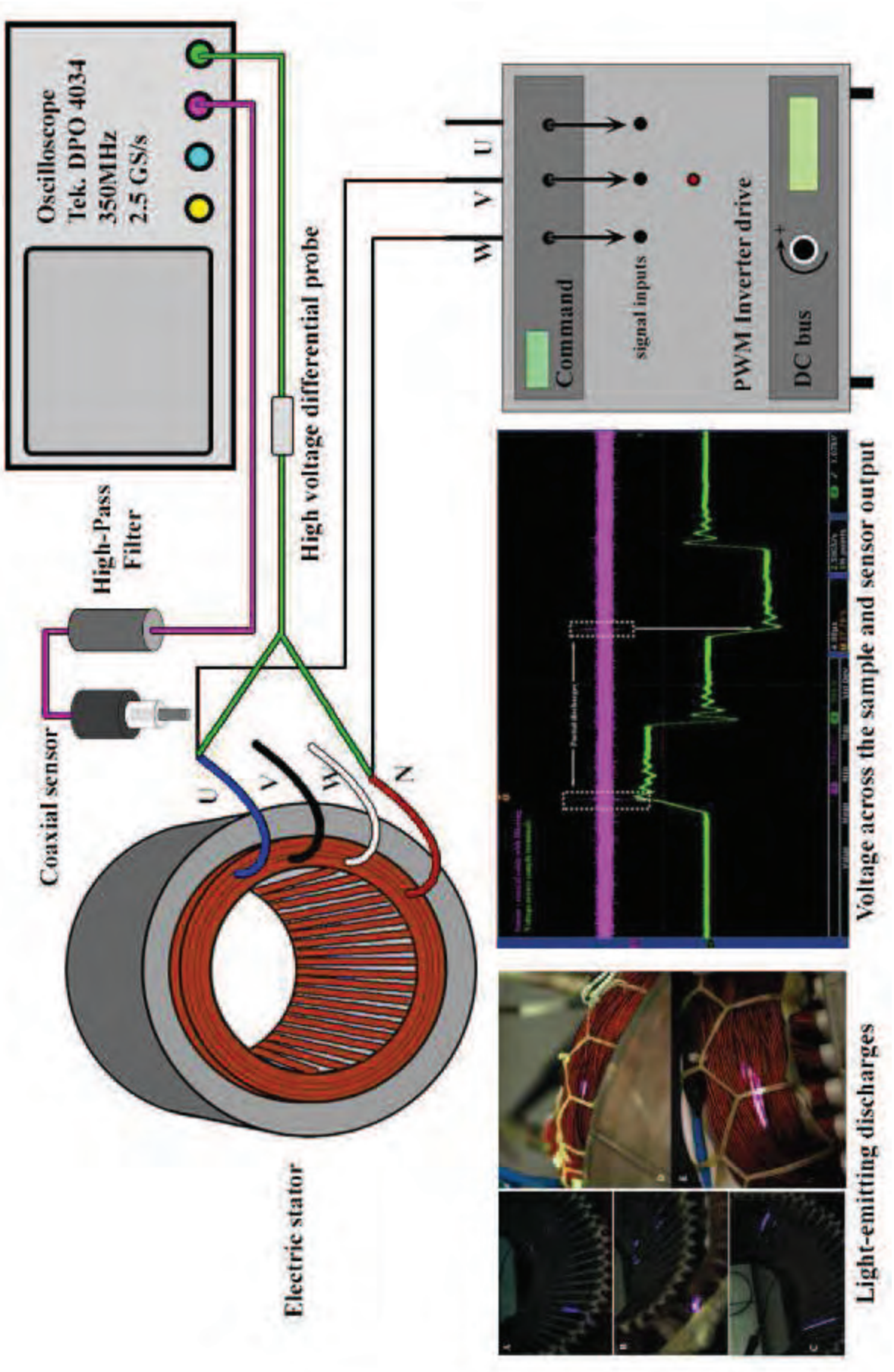

Figure 61 : Experimental set-up #2

With only these three input parameters, the duty cycle and the voltage waveform could fit all situations. Once validated, these command signals are transmitted to the inverter drive composed of Insulated Gate Bipolar Transistor (IGBT) with a maximum service voltage of 1.5kV. The direct current voltage source, emulating the DC bus, can deliver up to 5kW and has a maximum output voltage of 1.5kV.

Power and current are needed to feed the electric stator phases, either through the neutral point or through another phases. Such an electric circuit is the equivalent of connecting a voltage source to a short circuit composed of several coils, thus increasing the demand on current supply. To protect the PWM inverter, several security systems have been incorporated to define an average current limit per period, prevent overheating or true short-circuit when in case of an dielectric breakdown short-circuiting several turns.

As for the sample, the electric stator is put under test for the first time since it's a brand new machine. Preliminary tests have been performed by the cars manufacturer and give a PDIV of 1200-1300 V RMS. In addition, a surge voltage test qualified this electric stator around 2.2-2.4kV. These values are far above the DC bus of 400V used in electric vehicle application and it may be hard to reach PDIV in these samples considering the maximum output voltage of 1.5kV of the PWM inverter drive.

Regarding the partial discharge detection device, the coaxial cable sensor is located in the vicinity of the power cables connected to the electric stator terminals and pointing towards them as previous experiments have shown

The voltage across the sample is monitored through a high voltage differential probe directly connected at motors terminals.

4.6.3. Test procedure and PDIV measure.

Contrary to the previous experiment procedure, this PWM inverter can increase its output voltage up to 1.5 kV. Since only one phases is tested at a time, the three combinations will be put under electrical stress. The aim of this experiment is to reach PDIV, either by a sensor's partial discharge like signal or by other clear discharge activity signals, like light emitting discharge or intense ozone production if the sensors prove to be blind in such an environment. With this PWM inverter, PDIV is defined as the DC bus voltage and is not taking into account potential overvoltage caused by impedance mismatch.

4.6.4. Discussion of results

4.6.4.1. Voltage waveforms

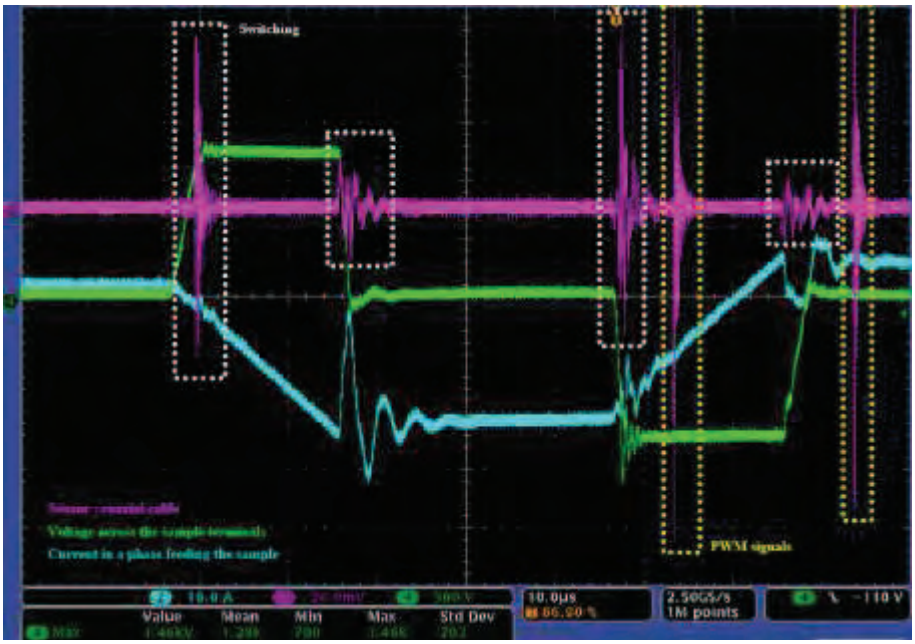

Figure 62: Electric stator : typical waveforms

Figure 62 displays typical voltage, current and sensor waveforms. The bipolar voltage waveform is composed of a positive pulse during 20µs, separated from the negative impulse of 20 µs as well, by a dead time of 40µs. Overvoltage due to impedance mismatch and the cable length may be observed quite easily. Typical value of such overvoltage is 200V or 20% of the DC bus voltage. The DC bus voltage here is 1.3kV and almost 1.5kV peak. Even at this voltage, nothing hints towards a partial discharge activity during the switchings or during the voltage plateau.
Regarding the sensor's output signals, those switching's image are not that different from the one from the first motor test bench. Indeed, the highest magnitude ones seem to have a damped oscillating frequency component whereas the others feature a slower sine curve and a longer time constant. For some reasons, rise times are very slow here, between 1 and 4µs.

Nonetheless, it should be noted that despite rather slow rise time, noise generated by switching are quite important. As a consequence, partial discharge detection during switchings events will prove to be difficult. As a matter of fact, using the high-pass 5MHz filter designed in the previous experiment didn't help in gaining visibility in that location. Since partial discharges phenomena caused by surge voltage seem to occur at the maximum voltage, being able to look through that noise will be key in detection the inception voltage.
The two signals in the yellow dotted rectangle are neither partial discharge nor pure switchings. Actually this kind of signals is always more or less visible whatever the voltage. In addition, these signals have a steady occurrence, almost periodic and are very stable over time.
Finally, at almost maximum output voltage, the high-pass filtering is not efficient enough to gain visibility during the switchings events and no partial discharges signals were detected elsewhere.

4.6.4.2. Light emitting discharges

Still, despite not seeing anything with the sensor and the 5 MHz high-pass filter, something actually brings the proof that some partial discharge activity was occurring at 1 kV voltage level. Thus, the PDIV was not defined using the non-intrusive sensors but rather by careful observations of light-emitting discharges within the stator slots and the end-windings. So, something is definitely happening in the electric stator.

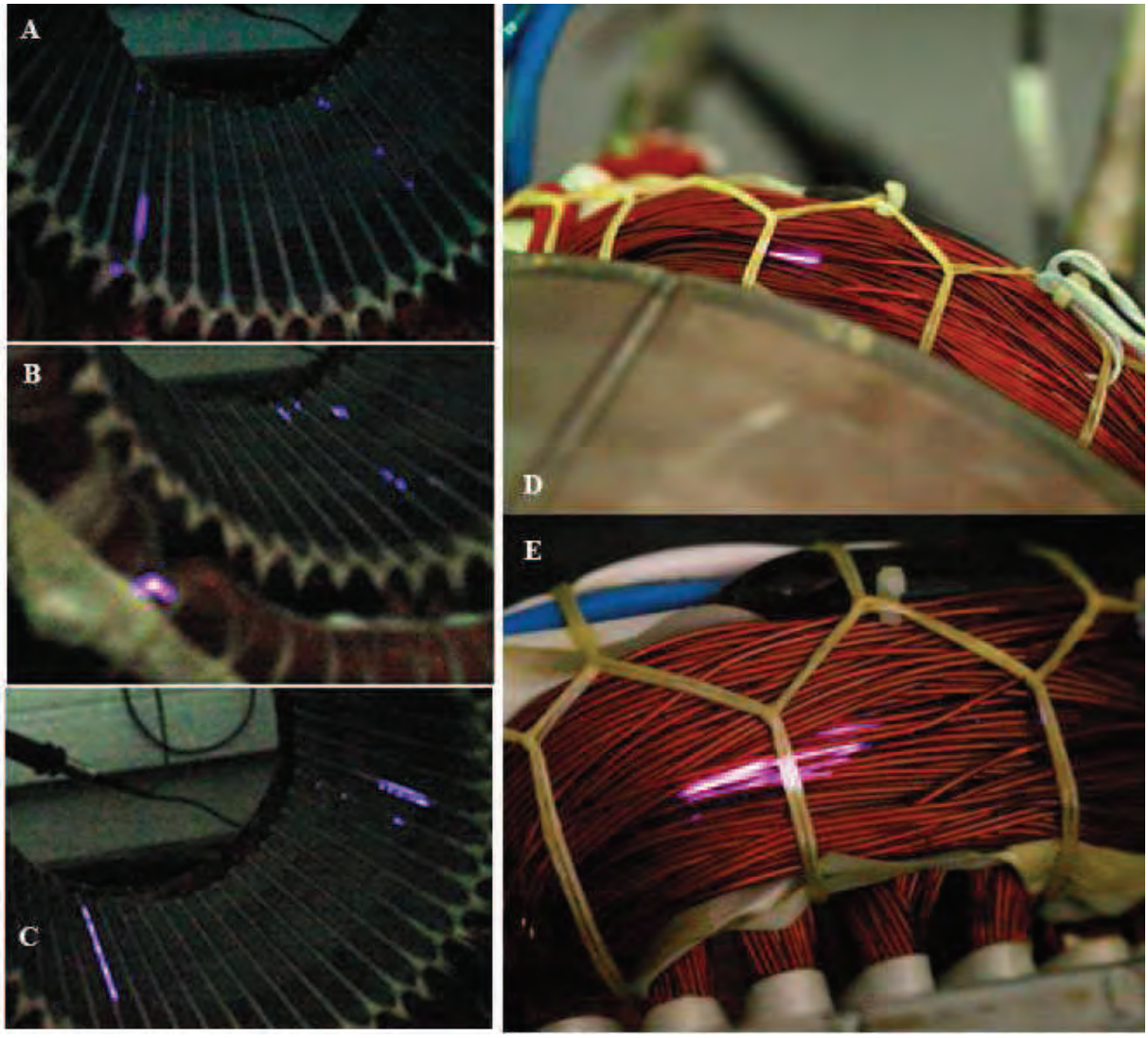

Figure 63 Light emitting partial discharges

All these pictures have been taken with a conventional digital reflex camera and a tripod to ensure stability while shooting. Indeed, even if all these light emitting discharge are noticeable with a careful naked eye, a long opening time (between thirty seconds and one minute) is needed to make quality pictures in a dark environment as it's daylight. No image intensifier have been used in this experiment and all pictures have been taken 200-300V above partial discharge inception voltage defined here as light appearance. As pictures were taken and voltage kept constant, light emitting discharges phenomena seem to consume energy and produce a lot of ozone. Indeed, the power supply is always going to switch off automatically at some point thanks to its current limitation protection.

- **Picture 63.a, 63.b and 63.c:** View inside the stator with the frame connected to ground while keeping voltage constant. Several partial discharge locations can be easily spotted on the three pictures, either dots are more extended discharge. Slots discharges are typical of phase-to-ground insulation default. In picture 63.b foreground, a discharge in rear end winding could be noticed while typical slots discharge also lays in the background. Note as well in picture 63.c how long the slot discharge is compared to the length of the stator. The discharge is almost as long as the slot!

- **Picture 63.d and 63.e:** Picture of the end windings above partial discharge inception voltage. Surface discharge in both picture are typical of turn-to-turn (of the same coil) insulation default or between turns of different phases default. Notice the difference of light spread between 63.d and 63.e. Picture 63.d is actually taken at 200V lower than picture 3.e where the surface discharge is much more extended.

But, despite all this light emitting surface discharges and a large ozone generation, detection of electrical signal through sensors is not possible. So an enhanced version of the high-pass filter has to come into play.

4.6.4.3. Filtering choice and partial discharge detection

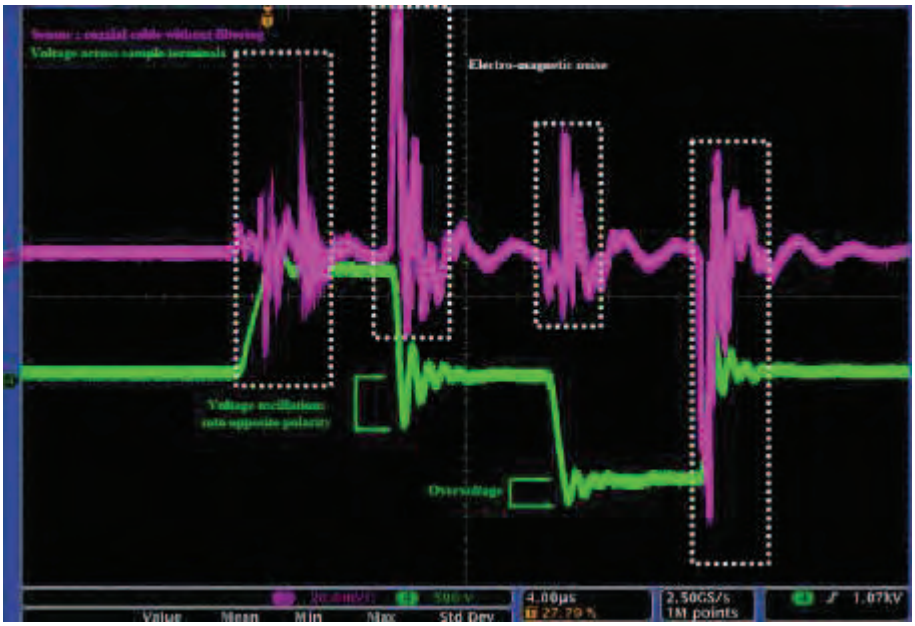

Figure 64 : Electric stator Typical waveform without filtering

Again, above in figure 64 is a typical voltage waveform applied between a phase and the neutral point while surface light emitting discharges are already buzzing in the electric stator while large amount of ozone are generated. The applied voltage is a bipolar signal with a period of 100 µs, including a positive impulse (20 µs), dead time with no voltage (20 µs), a negative impulse (20 µs) and finally dead time for the rest of the period. These signals, while simple, are nonetheless very close to those faced by electric motor in an on-line use.

Rise times vary from 500 ns to 2 µs in that case. Overvoltages (15-25% of the DC bus of 1kV in that case) are created right after the switching, thus favouring partial discharge activity in this short time window. But, at the same time, the very first moments following switching are also almost impossible to investigate because of the noise generated by the PWM inverter and seen by the sensor. Noise amplitude is very large (80-100mV), making it almost impossible to detect very small amplitude partial discharge. Worse still, by increasing voltage to the limit of PWM inverter drive (1.5kV), no partial discharge-like signals could be detected outside of the noise like in the twisted pair experiment. Still, light-emitting surface discharges are occurring more than ever in the electric stator but remained undetected by the sensor.

In order to gain visibility in the switching area and considering the inefficiency of the 5MHz high-pass filter in this case, another high-pass filter with a much higher cut-off frequency of 395MHz (Minicircuits – 15542 - BHP 400+ - 395-3200MHz) has been connected series to the sensor in order to try to remove noise generated by the PWM inverter. Hopefully, by selecting only the higher part of the partial discharge frequency spectrum detection will prove to be possible. On a side note, this cut-off frequency hits the numerical bandwidth limit of our oscilloscope (350MHz) so further attenuated signals are unlikely to be detected.

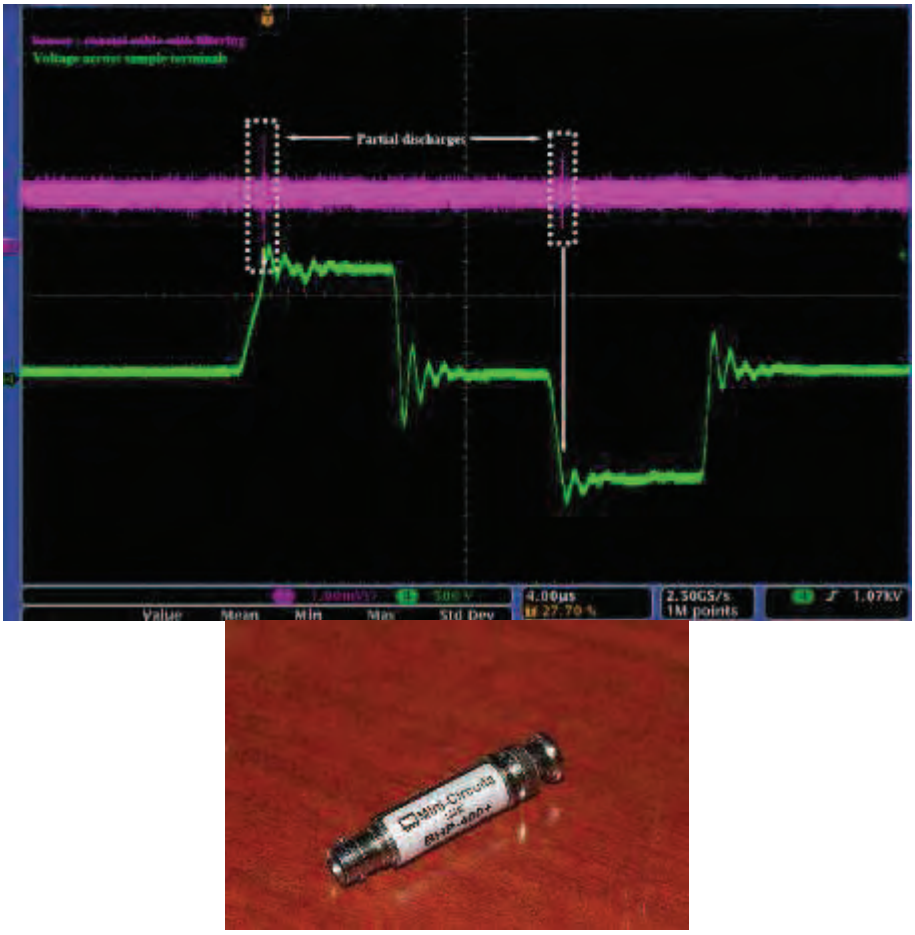

Figure 65 Electric stator: Typical waveform with filtering and partial discharge + high-pass filter

The above figure displays the sensor signal with the high-pass filter. The first point to notice is that all noise generated by the PWM inverter drive switching simply vanished. Only two small signals remain right on, or very close of, the maximum voltage.

These two signals are not always visible but seem to appear at a voltage around 1-1.1 kV. Thus, these signals are not always generated by the PWM inverter drive. When increasing voltage by small increments (100V) while, at the same time, monitoring light emitting partial discharge activity in known locations with the camera, it appears that the ignition of light emitting discharges perfectly matches with the apparition of these two very small signals around switching. With that in mind, it seems pretty safe to say that these two signals are the image through the sensor of the ignition of surface light emitting discharge. One interesting point is the fact that this stator prototype was previously qualified at around 2kV in a conventional surge test which is quite different with the partial discharge inception voltage found here.

But, what is even more interesting here is the fact that we observe only one discharge signal during one out of two rise/fall of voltage. Nowhere else in the plateau discharges were detected with our sensor. In other words, it seems that only discharge signals are detected when the voltage is increasing or decreasing from zero, but none in the voltage plateau, in-between or when coming back to zero. Still, light and ozone emission are large and only small signals (1mV) are detected. So, without the appropriate filtering, partial discharge inception voltage under PWM like signals could not be detected.

4.6.4.4. Summary

In this second experiment, the following elements are identified as the main conclusions

- When fed by a PWM-like inverter drive, light-emitting surface partial discharge are occurring both in stator slots and end-windings at 1 kV.
- The non-intrusive sensor can only detect these light-emitting signals by monitoring the rise time zone, no partial discharge signals have been detected elsewhere. Moreover, there is only one partial discharge signal for each rise time.
- High-pass filtering with an adequate cut-off frequency is mandatory to detect the partial discharge signal during the rise time.

4.7. Off-line partial discharge detection in an electric stator: three phases

4.7.1. Purpose of the experiment

In this third experiment, the aim is to go one step further regarding partial discharge detection in electric stator with more complex signals, closer to true PWM waveforms. In addition, by feeding the machine with three phases at the same time, tests are almost emulating off-line a true PWM inverter drive and should bring more information about partial discharge occurring in the electric stator.

4.7.2. Experimental set-up

As shown in Figure 66, the experimental set-up consists in a PWM inverter drive feeding an electric stator with three phases at the same time. Apart from the fact that three-phases could be used at the same time, this second PWM inverter main difference with the first one lies in the fact that more complex command signals could be created and loaded into the PWM inverter. This feature is especially useful to perform fatigue tests under representative signals.

For the sample, the electric stator is similar to the one tested in the previous experiment. This time, the rotor could be positioned inside the stator. As usual now, the coaxial cable sensor is located in the vicinity of the power cables connected to the electric stator terminals and pointing towards them as previous experiments showed. The high-pass filter with a cut-off frequency of 395MHz is directly connected to the sensor. The voltage across the sample is monitored through a high voltage differential probe directly connected directly at motors terminals.

4.7.3. Test procedure and PDIV measure.

Similarly to the previous experiment procedure, this PWM inverter can increase its output voltage up to 1.5 kV despites power converter are 1.7kV voltage rated. Three phases will be tested at the same time. The aim of this experiment is also to reach PDIV, as defined by the DC bus voltage when the partial discharges signals are first detected during the switching events since the filter enables now to perform the detection.

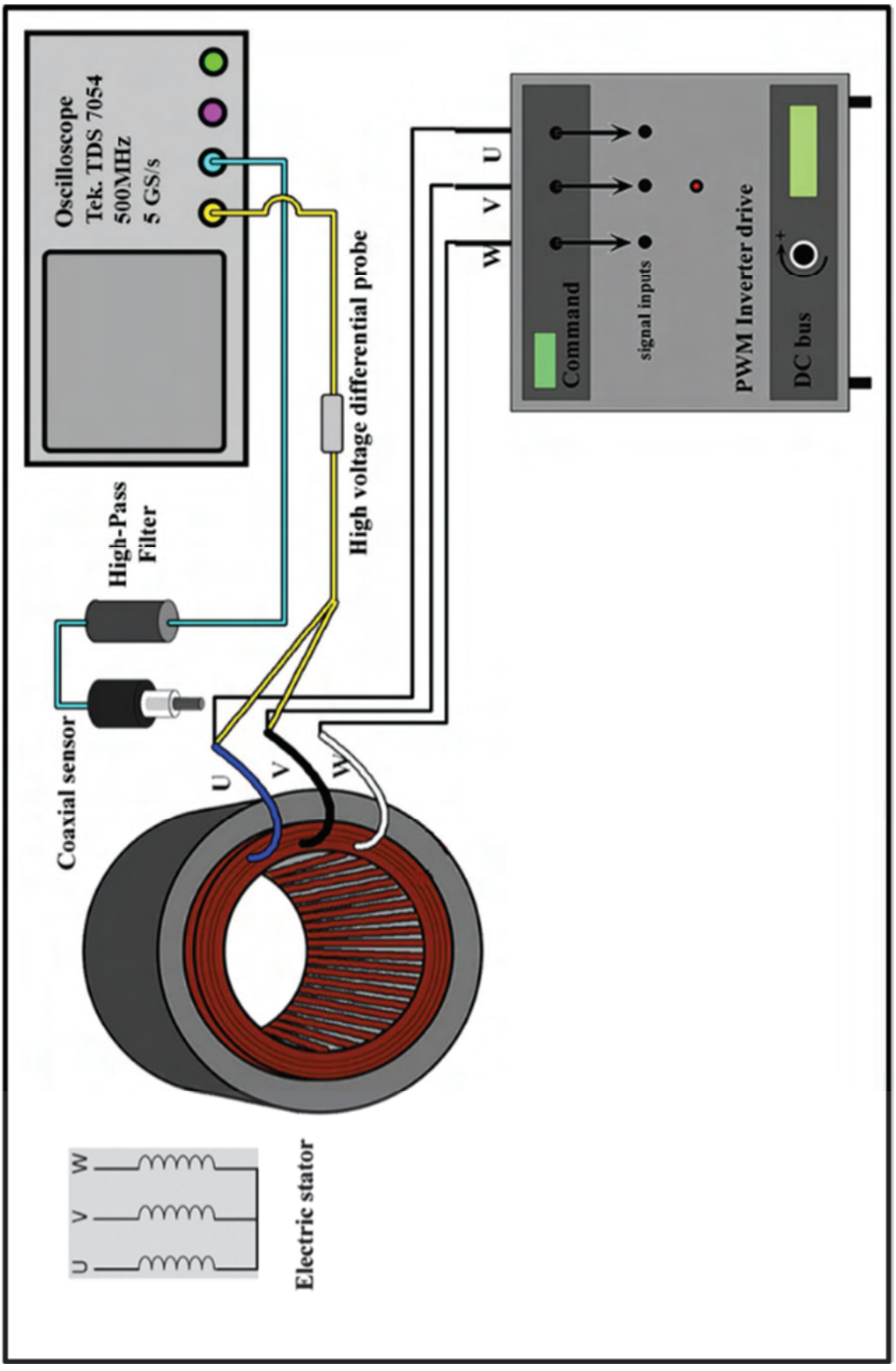

Figure 66: Experimental set-up #3

4.7.4. Discussion of results

4.7.4.1. Voltage waveforms, partial discharge detection and pattern analysis

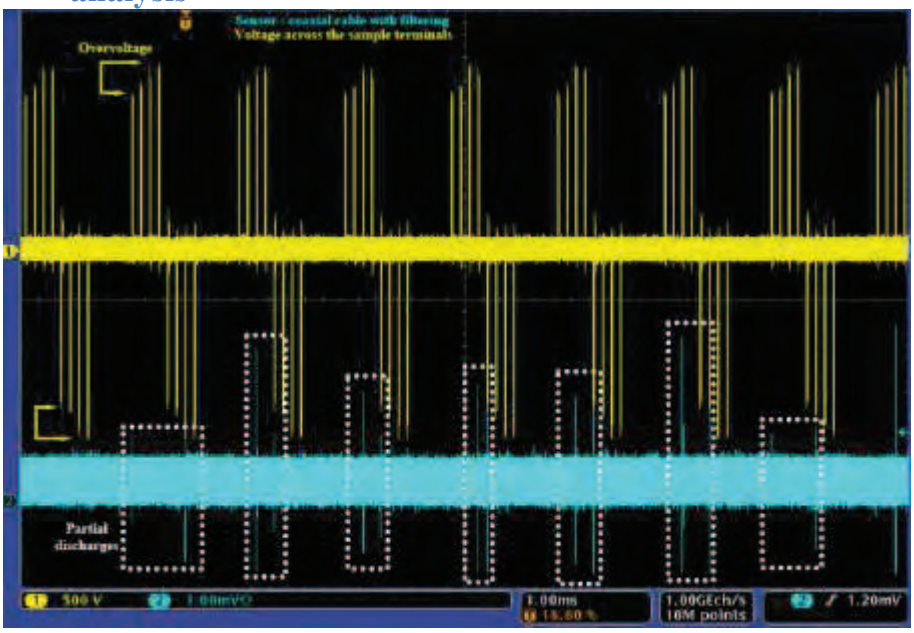

Figure 67 : Overview of voltage across the sample

In figure 67, both the voltage across the sample terminals and the coaxial cable sensor with its high-pass filter are plotted. The typical waveform applied here consists in a periodic bipolar voltage with consecutive impulses before changing polarity. In this example each sequence consists in four impulses in a row. Each impulse lasts 20µs while the full period of the voltage signal, four positive impulses and four negative impulses including all dead times, is 1.2 ms. Intermediate dead times separating each impulse is set to 100µs. The final dead time is 300µs. This kind of voltage waveform is used in fatigue tests in an oven at controlled temperature. These waveforms are supposed to model simple PWM signals and to assess, in more representative conditions, both PDIV and lifetime.

As suggested by the two yellow arrows, overvoltages are occurring on a regular basis due to the cable length between the electric stator and the PWM inverter. In figure 67, the DC bus voltage is set at 1.2kV and, always on the two last impulses of each polarity sequence, overvoltage approaches 300V which is a 25% overvoltage. This overvoltage regularity is important to note and to recall when observing partial discharge. The causes of this regular overvoltage pattern may lie in the power electronics of the inverter drive but it's just an assumption.

All in all, at 1.2kV, PDIV is reached and, actually, largely exceeded. More accurate PDIV measurements give around 1kV for the inception threshold. At this exceeded PDIV level, it seems that most of discharges are occurring in pair for each complete period. More precisely, it seems that partial discharges in the positive polarity sequence are mainly located on the last two impulses, where the voltage is higher. On the contrary, in the negative polarity sequence, partial discharges seem to be mainly located in the two first pulses. This may be due to the fact

that positive overvoltages are occurring in the negative polarity sequence. Or because the dead time between positive to negative polarity sequence is much smaller than the dead time between negative to positive polarity sequence.

Of course, far left and far right white dotted rectangles are proving us wrong, showing that, once again, cautiousness is important when analysing partial discharges picture without any solid statistical data to back it up. Thus, no clear patterns regarding the preferred location of discharge could be drawn in this case.

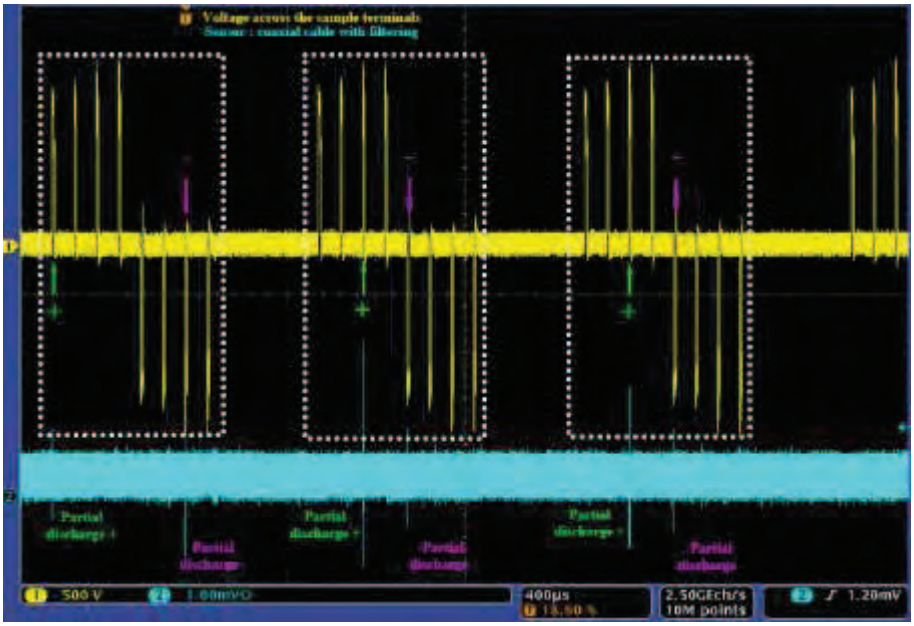

Figure 68 : Positive and negative polarity partial discharge

Figure 68 is on a shorter time scale and is thus displaying three full voltage periods more accurately. Building on the previous observations, one pattern could be distinguished from the partial discharge activity.

Figure 68 is typical of an established partial discharge activity 100-200V above the PDIV (voltage here is 1.2kV DC bus). In this case, each period only feature two partial discharge signals, occurring in pairs as shown by the white dotted rectangles. By looking more carefully, one could observe that there is only one partial discharge in each polarity sequence within a period. As hinted by the green arrows representing partial discharge in the positive polarity sequence, only one is found at each time. The same goes for partial discharge in the negative polarity sequence, highlighted by purple arrows.

What is even more interesting here is the fact that the polarity switch seems to be an important parameter for partial discharges inception. For example, in the middle and right dotted white rectangles, partial discharges are occurring at the first impulse of the negative sequence. There is no more detected partial discharge activity for the last three impulses despite a higher peak voltage. In order to trig another partial discharge, a significant polarity switch has to be made. The exact same thing is happening for the far left partial discharge on the first impulse of the positive sequence, a 300V increase in voltage is not triggering anything. This phenomenon is hinting towards a conditioning effect between each discharge.

If the latter is true, one important conclusion could be drawn at that point regarding partial discharge activity. Since it appears that only two partial discharges occur in each period, the number of partial discharge event is related to the nominal stator frequency and indirectly, depending of the rotor design, to the nominal rotational speed of the motor. Or more simply, related to the modulating sinusoidal signal with two partial discharges events occurring for each modulating period in an established partial discharge activity state. So, the higher the nominal stator frequency, the higher the number of partial discharge per unit of time.

4.7.4.2. Partial discharge type: classification propositions

Feeding an electric stator with three phases at the same time with the possibility to connect the stator frame to the ground open several testing opportunities. Three partial discharge typical locations compared to the rise time appears as electric stators were tested.

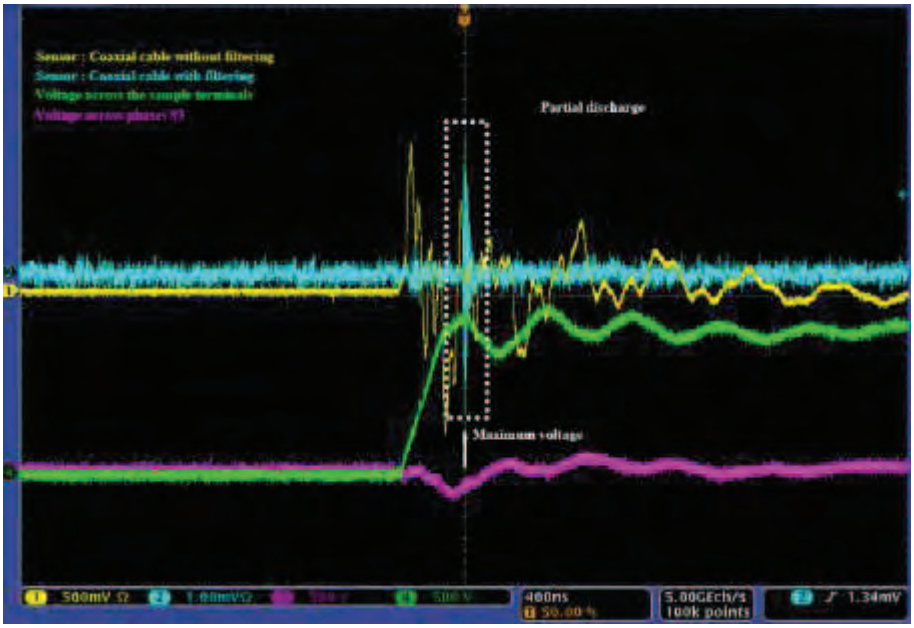

Figure 69: Maximum voltage partial discharge

In figure 69, the partial discharge signal appears exactly at the maximal voltage, overvoltage taken into account. This location is likely to represent partial discharge activity in turn-to-turn insulation of the same phase where the surge voltage is creating voltage difference between the very first turns of the coil and the others, which are, at that time, seeing no voltage. The shorter the rise time, the higher the number of turns are likely to face potential difference thus increasing the probability of partial discharge inception in turn-to-turn insulation. The location of this discharge signal is typical as well of test performed on twisted pair and neutral-phase tests on electric stator where only two phases are feeding the sample. The “maximum voltage partial discharge” is thus the more typical kind of partial discharge.

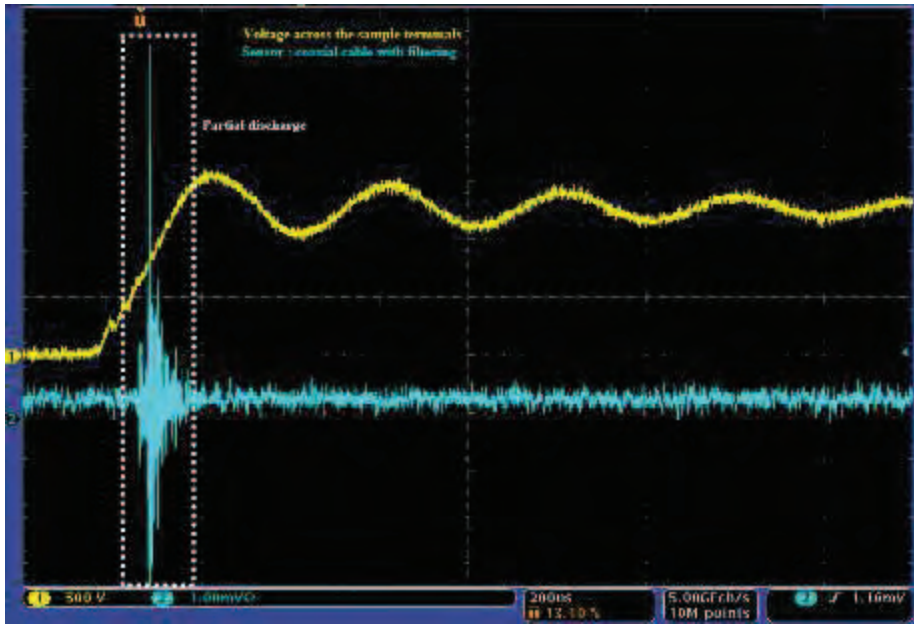

Figure 70: Premature partial discharge

In the example shown in figure 70, the partial discharge signal appears very early compared to the maximum voltage across the sample, which will be 100ns later. At the time of the discharge, the first turns of the coil are hardly facing a 500V voltage difference with the other turns of the same coil. Whereas, phase-to-phase voltage is well above 1kV and this early discharge location is, of course, not triggered at 500V. This "location" is thus likely to represent phase-to-phase discharge with the remaining phase, the one which is not observed here. In other words, if the voltage across phases 2-3 is under -1kV but is not yet triggering turn-to-turn discharges, a voltage increase of +500V in phase 1 actually add further potential difference, thus stressing greatly phases 1-2 or phases 1-3 insulation system. As the electric stator is random wound, it may be possible that these early discharge locations are phase-to-phase defaults between turns of different phases that may be close to each other.

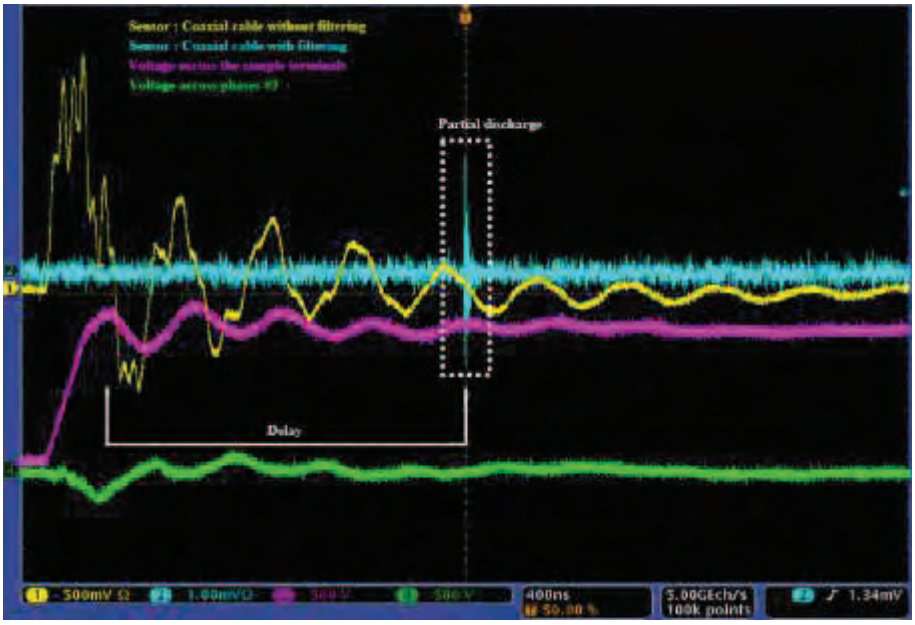

Figure 71: Late partial discharge

As shown in figure 71, these kinds of discharges are late compared to the maximum voltage and occur several µs after the switching. Actually, this late discharge location seems to be typical of phase-to-ground insulation problem. Indeed, when feeding an electric stator with three phases at a time, this discharge location seems to appear/disappear only when the stator frame is connected/disconnected to the ground.

4.7.4.3. Summary

In this third experiment, the following elements are identified as the main conclusions

- Expanding from previous results, only one discharge is observed for each polarity sequence. A significant polarity switch is needed to trig again a partial discharge.
- Different kinds of partial discharge could be identified based on their location compared to the maximum voltage.
- Lifetime of stator a hundred volt above PDIV proves to be very short, a dozen of hours, thus proving the extreme nocivity of partial discharges

4.8. On-line partial discharge detection in an electric motor: engine test bench

4.8.1. Purpose of the experiment

This experiment is the final and decisive step. An industrial engine test bench, usually used to carry out all kind of thermal, mechanical, dynamic or electrical measurements, has been made available for this experiment. The aim of this experiment is to demonstrate that efficiently detecting partial discharge signal on-line in a running electric motor fed by its PWM inverter drive is possible by using simple non-intrusive sensor placed outside of the motor and a high-pass filter.

4.8.2. Experimental set-up

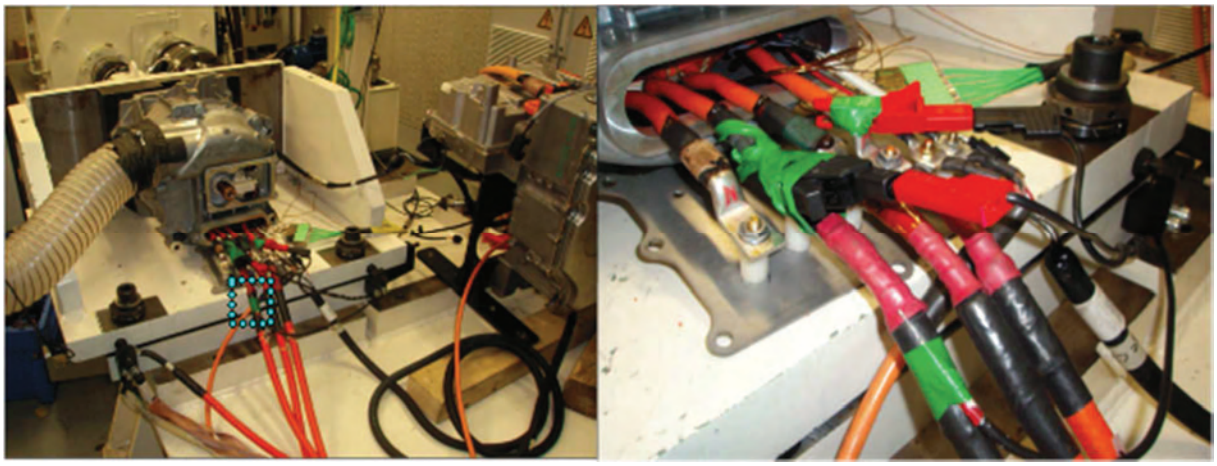

Figure 72: Pictures of experimental set-up #5

Figure 72 shows two pictures of the engine test bench used in this experiment to perform on-line partial discharge detection. In the left picture, the light blue dotted rectangle highlights the location of the coaxial cable, just outside of the electric motor terminals. The electric motor is protected by a high number of shielding plates, as he would be in an electric vehicle, and cooled by a ventilation system.

From a practical point of view, the sensor has been fixed with adhesive tape to one phase before motor terminals (phase U). On the right side picture, the sensor could be seen in the foreground, on the first phase with some green adhesive tape wrap around. In the small picture, the high voltage differential probe terminals equipped with big crocodile clips (red and black) are positioned to measure the voltage between two phases directly at the electric motor inputs. These clips on motor terminals have to be immobilized by using adhesive tape to prevent any electrical problem, would the clips move. The oscilloscope used here is the same as in the previous experiment

Since this experiment is in an industrial engine test bench, while its on, nobody is allowed to stay in the engine test bench room and all control equipments and panels are thus located outside. So, to connect the oscilloscope, which is about 10m away from the electric motor, extension cables have to be added to both the sensor (coaxial cable) and the high-voltage probe. In the latter case, a twisted pair of high voltage cable has be made to prevent inductive distortions as much as possible, and is connected to the crocodile clip almost from the high

voltage control panels. In the right side, image the beginning of the twisted extensions cables could be observed.

As shown in figure 73, the experimental set-up consists in an industrial engine test bench. The DC bus voltage could reach up to 400V, which is the standard value for electric vehicle DC bus generated by the battery. This electric power device is thus emulating the battery. The PWM inverter drive is also of the same type of the one used in the electric vehicle and is controlled by the person (the pilot) responsible of driving the engine test bench. So, the rotational speed of the motor could be changed at will, as for resistive torque and almost all mission profile could be performed. For example, a controlled and linear motor acceleration followed by a steady state and then a rapid braking can be simulated. The engine test bench pilot also controls ventilation flows and monitor lots of signals, like temperature in different points of the engine.

A measurement box is in-between the motor terminals and PWM inverter and is connected to the control panel of the engine test bench. These measures could be displayed on the oscilloscope as well. But, despite its measure completeness, this measuring device seems to provide distorted and highly perturbated voltage waveforms. All measures seem to be distorted by switching on other phases and display higher than expected overvoltages and weird voltage value. Indeed, by comparing the same measure between the high-voltage differential probe and the one provided by the measurement box, lower overvoltages are actually found at motor terminals. Thus, these phase-to-phase voltage, rotor voltage and phase to neutral voltage magnitudes should be taken very cautiously. All in all, what is important here is the location of all switching events and these measures, though perturbed, still provide that. More importantly, the high-voltage probe is unaffected by such problems and could be relied on.

It should be noted that, in this experiment, the cable length between the three motor terminals and the inverter is around 5 meters so that overvoltage could be created and could impact the twisted pair sample. The nominal stator frequency could not be directly controlled, the switching frequency is 10kHz. The nominal rotational speed of the rotor is set at 2000 revolutions per minute with a braking torque applied on the rotor of 60 N.m. The electric motor and the PWM inverter are producing a typical background electro-magnetic noise to test the different sensors detection abilities in a harsh, yet representative, environment.

But, considering all the aforementioned elements, this experimental set-up is actually worse than the one used in electric vehicle. First, there is no measurements box right in the middle of power cable. And, secondly, the PWM inverter drive is right on top of the electric ‘s motor terminal box. So that very short power cables are used and are thus less likely to cause severe overvoltage. As presented in the following experiments, quite large (up to 50%) overvoltages are created in this experimental set-up.

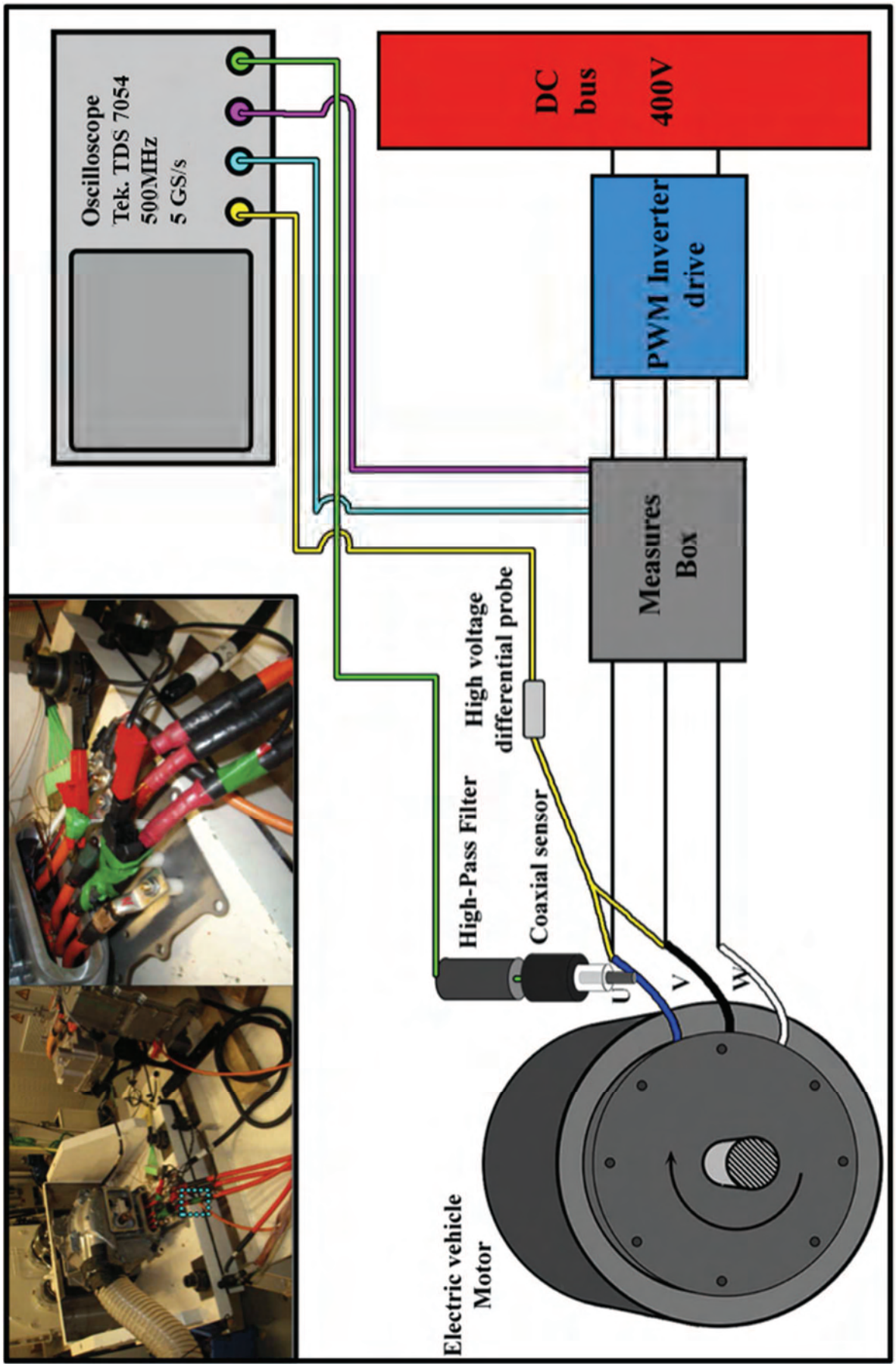

Figure 73: Experimental set-up #4

4.8.3. Test procedure

The coaxial cable sensor is detecting perturbations in the starting phase of the machine, as in the first experiment. Thus all measurements are only carried out when the electric motor is at steady state to avoid early false positive signals. Since phase's output voltage can not be controlled over a DC bus voltage of 400V maximum, partial discharge detection method in the electric motor only relies on trying to find them at that fixed voltage. Adding difficulty compared to previous experiment, there is only one sample available and the maximum output voltage may not be large enough to trig partial discharge in the electric motor, and it can not be removed or replaced by a more favourable sample.

Our two previous experiments hinted that a realistic PDIV value is around 1 kV for brand new electric stator prototypes. With a maximum DC bus of 400V, and even considering the long power cable, reaching this value will be next to impossible. But, maybe on-line electrical stresses at 400V could be even more harsh and demanding on the insulation system than our off-line electric stresses at 1 kV. Concerning this electric machine, its exact electrical stress history is not known so maybe PDIV is lower than in electric stators. Moreover, since shielding plates protect the electric motor, it's impossible to look for light-emitting partial discharge at the same time or even take a remote control picture.

All in all, our detection set-up only consists in a coaxial cable sensor, a high-pass filter and all detection experiences gathered in the previous experiments. One more thing has been added though, an ozone sensitive paper to monitor what may be as well a partial discharge consequence. This chemical sensor has been placed as close as possible to the stator end-winding

4.8.4. Discussion of results

4.8.4.1. Voltage waveforms and on-line partial discharges detection

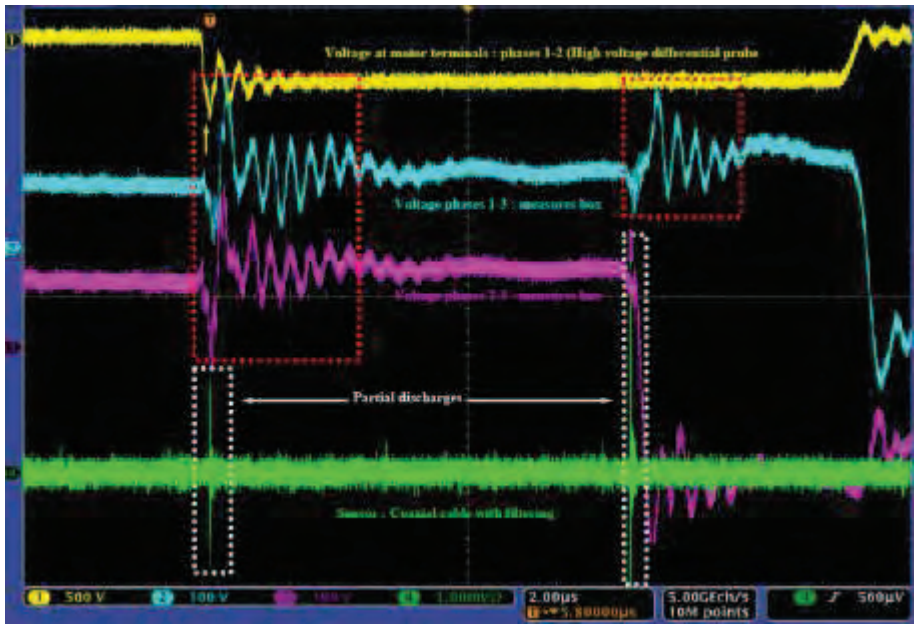

Figure 74: Online partial discharge

Figure 74 shows the first two partial discharges detected on-line by a non-intrusive sensor in an electric motor fed by its PWM inverter. All the phase-to-phase voltages are displayed at the same time to have information on all switching events and prevent any confusion. The DC bus is set at 400V and, at motors terminals, overvoltages up to 50% are detected in the yellow trace, thus reaching sometimes more than 600V peak.
The sensor's signal proves that the high-pass filter is still efficiently suppressing all noise caused by the PWM inverter switching events as in previous experiment. The green trace is free of any perturbations and allows visibility, thus detection, of high frequency phenomena during the switching events. Finally, only the two partial discharges remained detected and are highlighted in the white dotted rectangles. These discharges are occurring at the same time as switchings events, as in the two previous experiments again, as underlined by the yellow and purple arrows. Similarly, no discharges have been detected in between switching events or during the voltage plateau. Globally, occurrence of these phenomena is quite scarce with only twenty events, at most, per second.
Considering all these elements and all the information accumulated in the previous experiments, it's pretty safe to say that these two small signals are actually partial discharges as been observed a countless number of time in off-line test: same partial discharge location an unregularly occurrence.

On a side note, phase-to-phase voltage provided by the measurement box (channels 2 and 3) seems to be highly perturbed by switchings events (red dotted rectangles) of 200V peak-to-peak. Worse, the reference line symbol (on the far left of the figure) of these phase-to-phase voltages suggests a continous level of voltage as if waveforms have been shifted up or down. Indeed, even if the phase-to-phase voltage is around 400V, the purple signal (according to the reference line) should be +100V and – 300V. Exactly the same problems lie in the blue trace. So, switching events locations are correct but voltage measured magnitude should be taken cautiously.

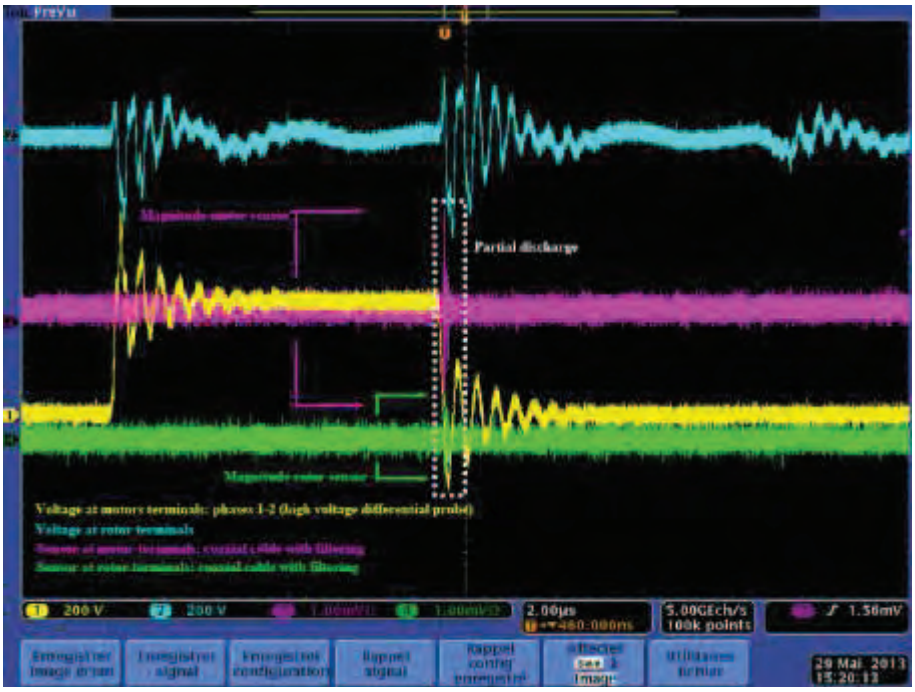

Figure 75: On-line partial discharge

Figure 75 displays at the same time the voltage across the rotor in light blue, the voltage at motor terminals in yellow, a sensor's signal close to motor terminal in purple and sensor's signal close to rotor power cable in green. Both sensor signals are filtered with the high-pass filter whose cut-off frequency is 395MHz. In each case, the high-pass filtering is making sensor signal noise free.
Both sensors are detecting at the same time a partial discharge signals (white dotted rectangle) whose occurrence matches a switching event in one of the observed phase. The voltage across motor terminal is 400V with overvoltage up to 250V, thus giving a peak voltage of 650V between phases. As in the previous figure, this 650V peak is enough to trig partial discharge activity.

This PDIV value is actually quite low compared to the one previously assessed off-line on electric stator. Two different main conclusions could be drawn from this partial discharge detection. First, the electric motor under test has already faced an important number of especially demanding characterisation, fatigue and endurance tests, or even mechanical and thermal stresses. As a consequence, its insulation system may be already weakened and its PDIV is thus close to the DC bus voltage, considering overvoltages created by cable as an aggravating factor. If that's not the case (insulation performance is not overly weakened) then insulation system design and materials may be considered again to improve the overall insulating performance. Hopefully, in the electric vehicle, overvoltage should be much more lower because of the position of the inverter drive on top of the machine.
Secondly, the two off-line tests previously performed to assess insulation performance are maybe not yet representative enough of the real electrical stresses as seen by an electric motor in service. Worse still, the partial discharge detection was carried out while in favourable conditions (steady state at a 2000rpm rotational speed in engine test bench) whereas true electric vehicle mission profiles in service are almost unpredictable (braking, brutal acceleration, harsh climatic conditions, etc…) so that even more unfavourable case may be faced, thus putting the insulation system in even more difficult situation.

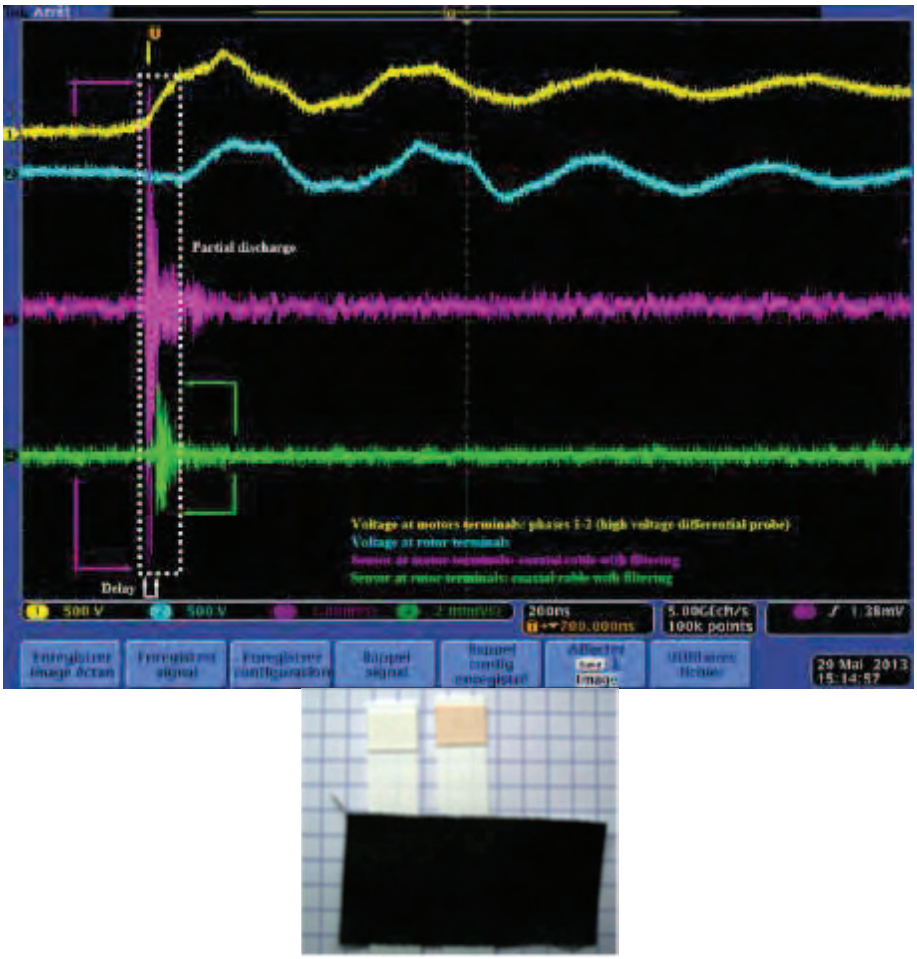

Figure 76: Zoom on partial discharge and positive ozone paper.

With the same signals configuration as in figure 75, figure 76 has a smaller time scale at 200ns and allows observing in details partial discharge signals. As previously, the high-pass filtering is perfectly removing the electro-magnetic noise generated by switchings events.

It should ne noted that several filters have been tested in the engine test bench. High-pass filters with a cut-off frequency of 27.5MHz, 40MHz and 90MHz have been connected to the sensor and were not able to negate the electro-magnetic noise. Thus, this PWM inverter drive is generating frequency components of at least 100MHz. Clearly, there is not one size fits all filtering solutions to detect partial discharge, the cut-off frequency value highly depend on frequency spectrum generated by the switchings events. So, to perform an efficient on-line partial discharge detection, different high-pass filters are needed to select the best one on a sample-by-sample basis. In addition, a large enough oscilloscope numerical bandwidth is needed as well.

Both sensors are detecting partial discharge. Even if the magnitude are a bit different (voltage scale between the two sensors are not the same), the more interesting thing is that a small delay of several dozen of ns could be observed between the two sensors' partial discharge signal. If the partial discharge electro-magnetic wave is conducted as well in the circuit, one should assume that, circuit-length wise, the rotor terminal sensor is further away than the motor terminal sensor from the initial partial discharge location. The ozone test proves to be positive with a light brown color, the left (white) one being the reference for comparison purpose.

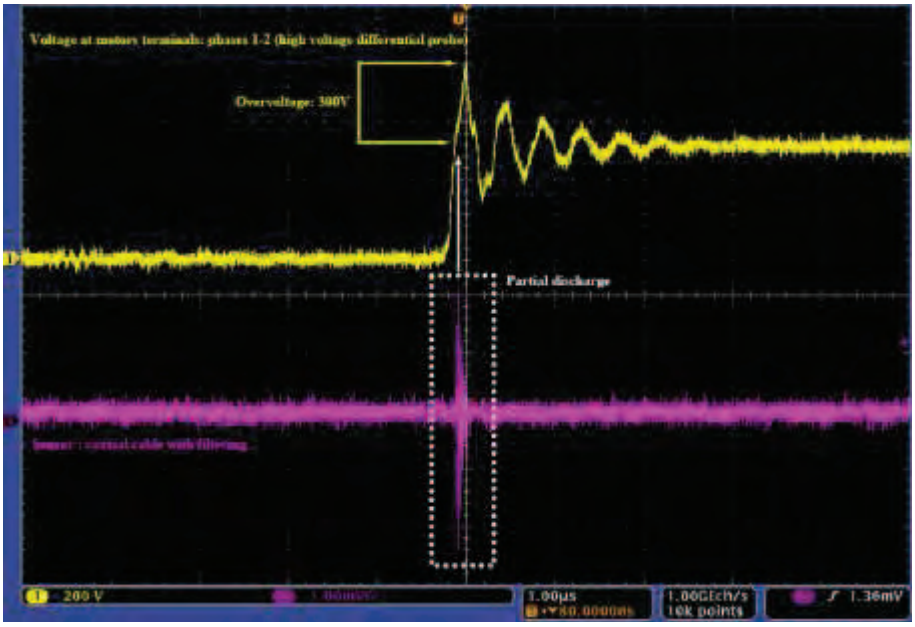

Figure 77 : On-line partial discharge – Zoom

Figure 77 displays a typical partial discharge signal, detected on-line with the coaxial cable sensor and the high-pass filter.

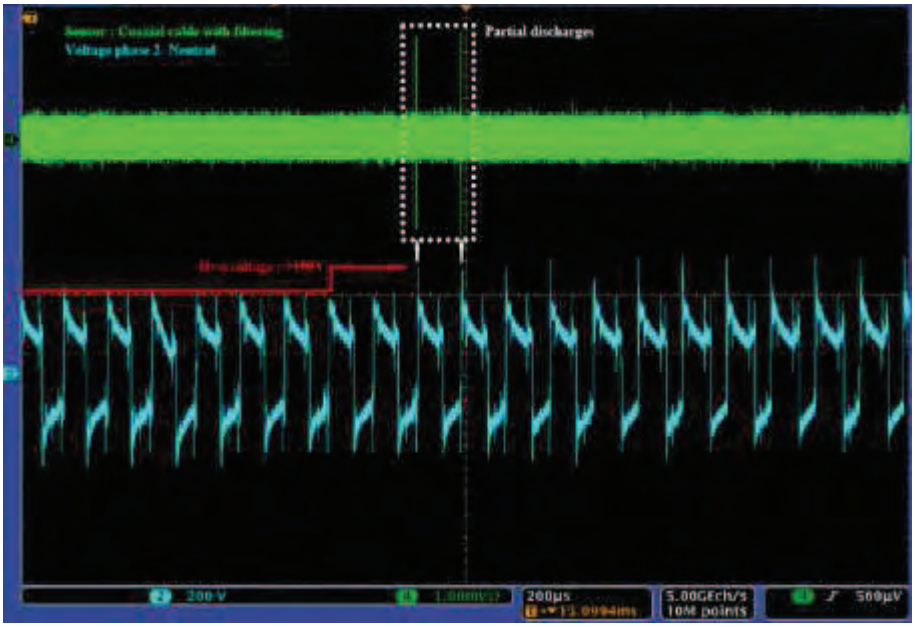

Figure 78: Consecutive partial discharge after an increase in voltage

In figure 78, the phase-to-neutral voltage is displayed along the coaxial cable sensor's output signal after going through the high-pass filter. Plotting phase-to-neutral voltage is not conventional in partial discharge detection but has an advantage in knowing exactly which phase's switching was the discharge trigger. But, it does not mean that the partial discharge is occurring in the turn-to-turn insulation of the considered phase nor with which phases a phase-to-phase partial discharge is occurring.

In the above example, the phase-to-neutral voltage is moving regularly between -300V and +300V. But, for unknown reasons, a +100V overvoltage appears as underlined by the red arrows. Consequently and immediately, two partial discharges are triggered as shown by the white dotted rectangle.

4.9. Conclusions and next chapter perspectives

In the last experiment, **the main achievement is the ability to accurately detect partial discharge on-line in an electric motor fed by its PWM inverter drive using simple and non-intrusive sensors and an adequate high-pass filtering to suppress PWM noise during switching events.** The technological problem has thus been unlocked by the last experiment after sharpening the partial discharge detection tools and method and in previous three experiments. Besides this achievement, two clear paths could be investigated to build on that results and bring more efficiency in the detection method and more understanding on the physics of light-emitting discharge.

Indeed, interesting phenomena has been observed regarding partial discharge activity in electric stator fed by PWM inverter signals. Large light-emitting surface discharges, preferred location of only one partial discharge signal as seen by the sensor during the switching and the influence of polarity switch in the partial discharge pattern over several signal periods are all intriguing clues which triggered a more extensive and targeted analysis of the physics of the discharge under such conditions. First results of this physical analysis are presented in the next chapter.

As for the signal processing, and once the sensor could detect partial discharges, this tool is very useful to gather data and statistical information when carrying out fatigue test on electric stator, frequency analysis or partial discharge location pattern investigation. But initially, signal processing was used in the first experiment to analyse randomly acquired data and determine if some partial discharge events were occurring in the sample. The next chapter is presenting the chosen method to automate classification of data function of partial discharge activity.

5. Complementary experiments: surface discharge and numerical processing

5.1. Physics of light emitting surface discharges

As it has been shown in chapter 4, light emitting surface discharges have been observed in an electric stator fed by a PWM inverter drive, both in slots and in the end windings. Interestingly, these discharges can only be detected with our non-intrusive sensor with a high-pass filtering. In other words, without any visual observation or high-pass filtering, light-emitting surface discharges would have remained unnoticed. A clear correspondence between the apparition of light and the detection of the single pulse signal has been established.

Moreover, during these measurements with a PWM inverter drive, assessed partial discharge inception voltage is quite lower than expected compared to previous off-line and sinusoidal qualifications. Moreover, large quantities of ozone could be detected while in the vicinity of the sample under discharge activity. Last but not least, some electric stators stressed with a voltage a few hundred volt above partial discharge inception voltage fail prematurely hinting towards a very harmful effect on insulation system.

The possibility of detecting partial discharge inception voltage presented as in the last two experiments is thus even more important and useful when designing and testing electric motor insulation performance.

The fact that standard qualification test (AC, step in off-line) fail to detect these light emitting discharges, PDIV are very different, may hint towards the fact the physics of discharge has changed and that the type of power supply could not trigger such discharges, thus making these tests irrelevant to predict on-line insulation performance.

Regarding the physics of the discharge, a few things could be pointed out in order to explain such discharges behaviours. First, these surfaces discharges could spread along large distances (several cm) and seem to be quite intense and could even be seen with the naked eye in a dark environment. Pictures in the previous chapter speak for themselves. At PDIV, surface discharge takes place between enamel wires.

Secondly, only one discharge pulse could be observed during the rise of the voltage whereas several pulse-like discharges may have been expected at first as in a standard AC test. This is not the case here as far as our observations on different PWM set-up and electric motor sample go. This single feature may be one of the main reasons why detecting partial discharge on-line in motors fed by PWM inverter proves to be difficult.

Finally, a significant switch of polarity is needed to trigger another pulse-like discharge event on the following rise time. In itself a null voltage across different wires is not enough to trigger another pulse-like discharge event. Thus in the case of a series of step voltage of the same polarity, only one discharge will be observed with our set-up.

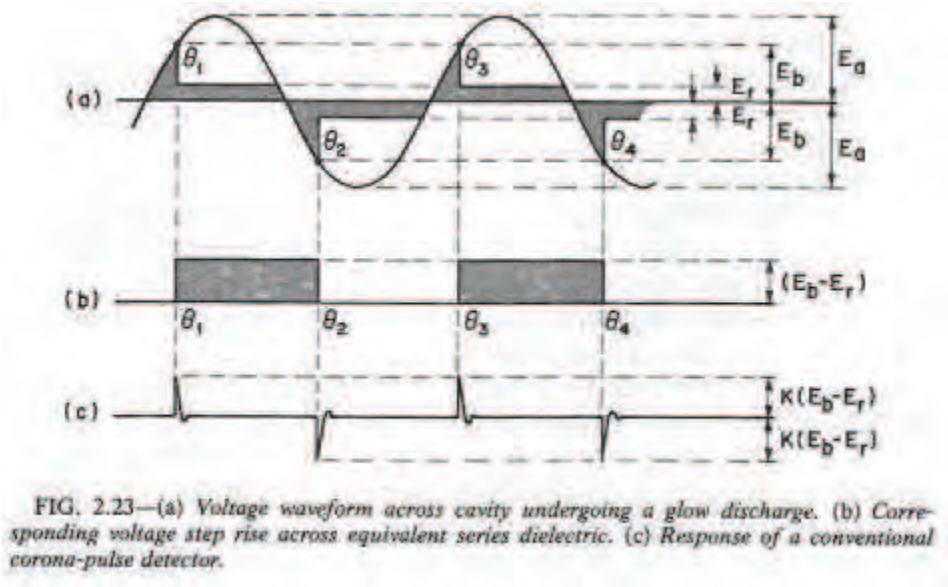

FIG. 2.23—(a) *Voltage waveform across cavity undergoing a glow discharge.* (b) *Corresponding voltage step rise across equivalent series dielectric.* (c) *Response of a conventional corona-pulse detector.*

Figure 79 : Glow discharge as in [BART]

According to Bartnikas [BART71], among different discharges mechanisms, glow discharge features only one discharge pulse that could be seen by a conventional partial discharge detector. Typical spark discharge behaviour under AC has been presented in chapter 2. In fig.79, the typical process of a glow discharge is explained in AC. [DAN93]

The first thing to notice is the fact that the number of pulse discharges is limited at two per cycle, or in other word one in each polarity since the voltage in the defect does not rise largely again as in pulse cases. This is consistent with our observation of only one discharge event in each polarity in PWM signals. As a recall, if the sample had been subjected to true pulse discharge mechanism, much more pulse signals would have been detected in AC.

In the glow discharge case, the full discharge mechanism is composed of a first pulse-like signal, which could be seen by the sensor in AC (with filtering in PWM case) and followed by a longer diffuse discharge until a change of polarity occurs. Thus, the full glow discharge starts at PDIV with a pulse, then the discharge is still lasting until polarity is reversed. The latter consideration is what has been observed in the last experiment. And finally, what is important here as well is the fact the energy dissipated in the discharge is not only function of the pulse discharge and should be considered on the whole discharge, which may be consistent with the large ozone emission and intense light. Thus potential harmful effect of glow type discharge should not be underestimated.

All in all, hints may point towards the fact that the PWM inverter drive is causing glow type or pseudo-glow discharge to occur in air at atmospheric pressure in the electric motor.

5.1.1. Purpose of the experiment

Building on the previous consideration, the main hypothesis to be tested to shed some light on the physics at work here is the following.

> *When fed by a PWM inverter, the discharge signal is not only composed of a single pulse signal but with a lasting, light-emitting, glow discharge.*

To do so, a time-resolved analysis of light distribution evolution has to be carried out to check if indeed, some discharge activity is still occurring after the pulse discharge seen by the sensor. But, if true, that does not directly mean that the discharge mechanism is glow and, if possible, a spectroscopy could be done on light emitted to gather as much information as possible on the mechanism. The work presented in the following experiments consists in series of tests on a twisted pair with different PWM parameters. The impact of the voltage shape or frequency is investigated and monitored on the twisted pair thanks to an intensified CCD camera.

5.1.2. Experimental set-up

As shown in figure 80, the experimental set-up consists in a PWM inverter drive feeding a twisted pair of enamel wire which is representative of the worst electrical stress that could be applied on the turn insulation of the same winding. From a practical point of view, a short twisted pair (2-3 loops) has been made to allow the camera to accurately focus where discharges are known to occur on a regular basis, the space between adjacent wires. The sample is fed by the PWM inverter with a 100 µs long period signal composed of a positive impulse (20 µs), dead time with no voltage (30 µs), a negative impulse (20 µs) and finally dead time for the rest of the period (30 µs here). PDIV for this kind samples are around 800-850 V. Depending on the parameter to be tested (frequency or duty cycle), the shape of the signal will be modified accordingly.

The intensified CCD camera is synchronized with the power supply control, with an adjustable delay, in order to start accurately the evaluation of light distribution as a function of the time and so of the voltage applied to the sample. To monitor when the camera is actually recording, its gating output signal is displayed on the oscilloscope to be sure it matches with the start of the PWM period.

The non-intrusive sensor and its 395MHz high-pass filter are in the vicinity of the power cable feeding the twisted pair. Almost the whole set-up (camera, sample, sensor and filtering, high voltage differential probe) is within a dark box to prevent any external light to disturb the measure. The room where the experiment is carried out is additionally dark while measuring to further prevent any disturbance.

5.1.3. Data and signals acquisition

In the experiment with the twisted pair and the intensified camera, a 2 GHz bandwidth digital oscilloscope is used (Tektronik MSO 5201, 2 GHz, 10 GS/s). All signals coming from high-voltage differential probe or sensors are displayed simultaneously.

5.1.4. Intensified CCD Camera

In order to assess the temporal evolution of the light distribution caused by the discharges, an intensified CCD Camera (PI-MAX-3, Princeton Instrument) is synchronized with the PWM power supply. An adjustable delay allows to monitor the temporal evolution of the light intensity distribution. In the following experiments, one image includes 10 000 CCD accumulations of 1µs exposure time at the same time after the starting point of the acquisition, thus persistence effect are ruled out. Thus it is possible to follow the development of the PD with the PC software. At each image (time), light intensity of PD area is averaged and plotted. The same operation is performed in part of the image without PD. Thus, the noise intensity is obtained and subtracted to the intensity of the PD area. Afterwards, for each curve, intensity is normalized with its maximum.

5.1.5. Test procedure

To perform our analysis, voltage is increased up to 1 kV that is to say around 100V higher than PDIV to gather more light.

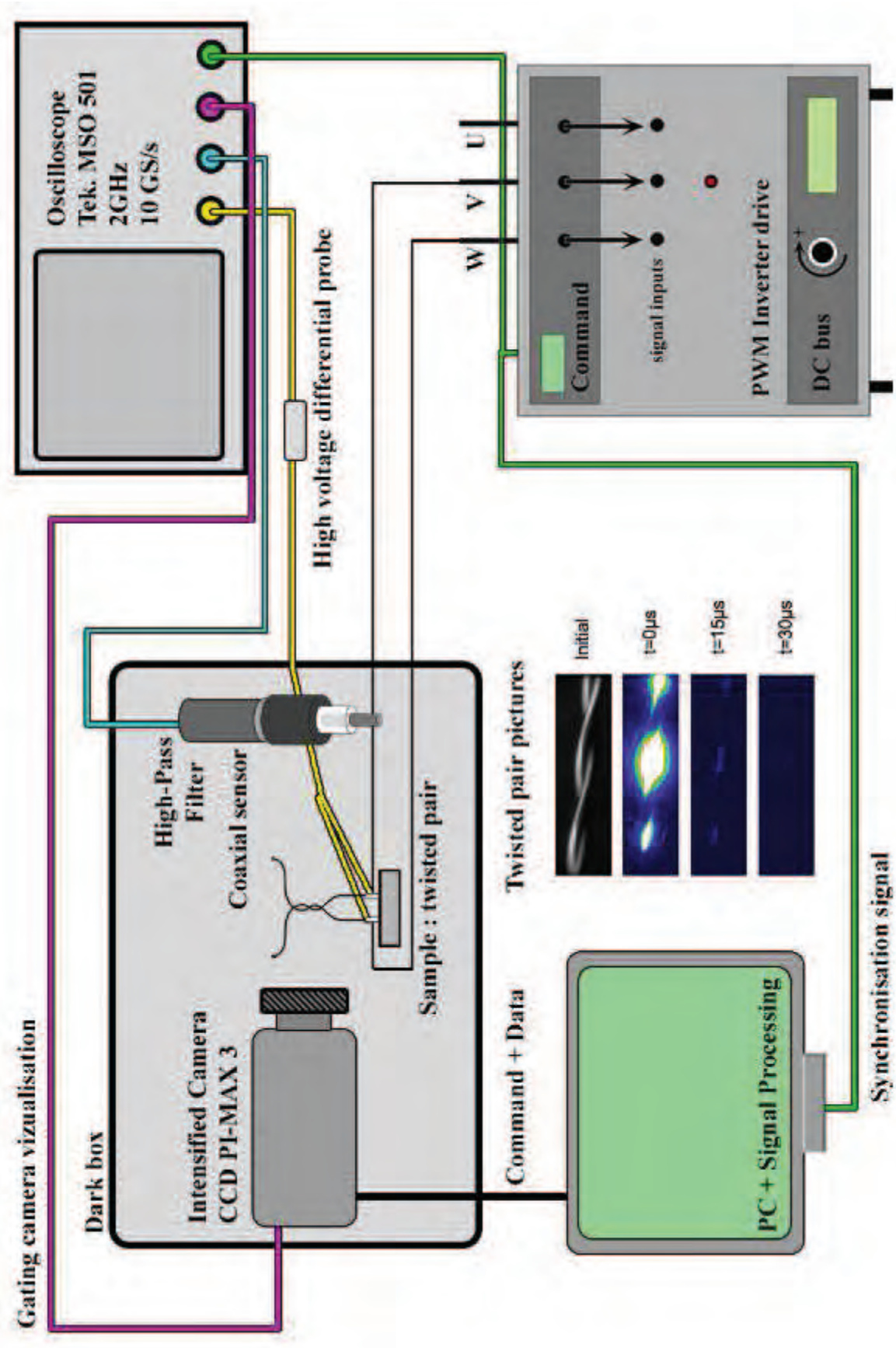

Figure 80 : Experimental set-up

5.1.6. Discussion of results

5.1.6.1. Light distribution evolution over time

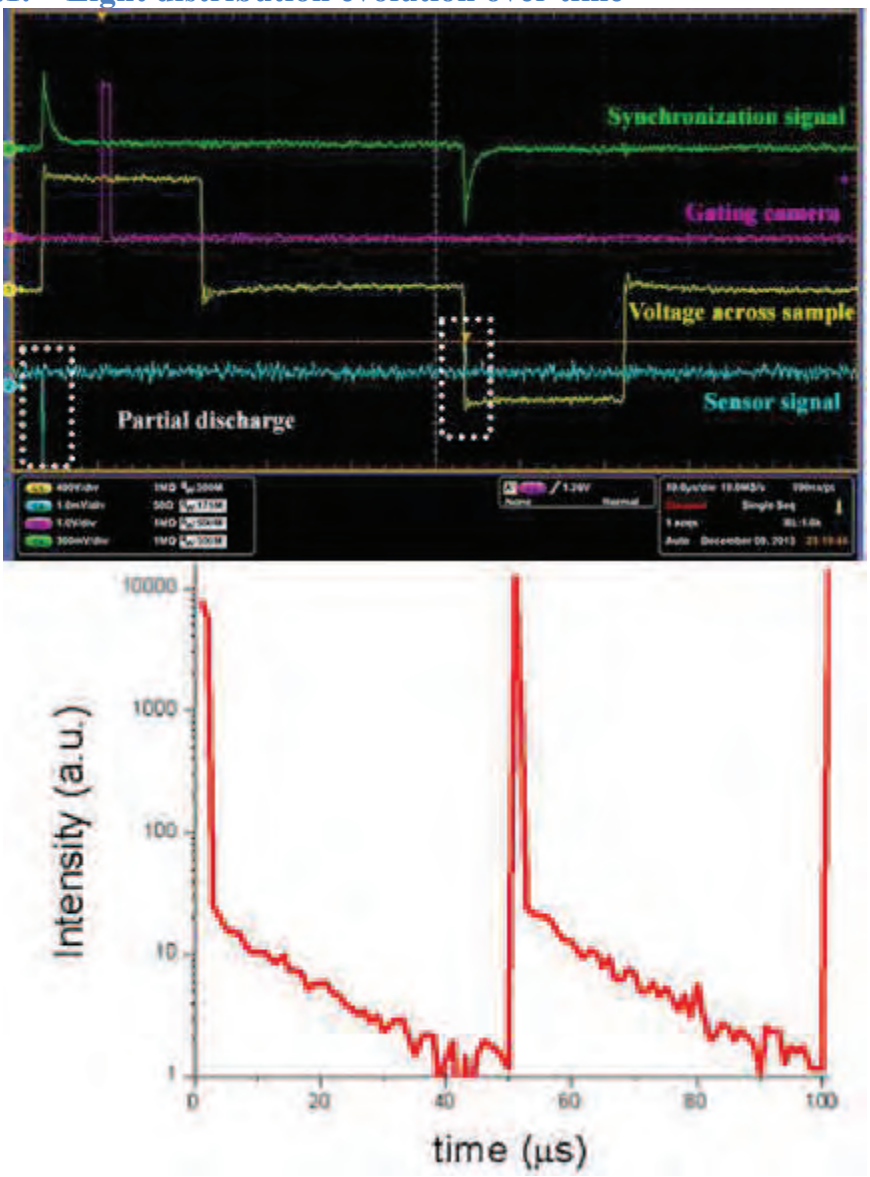

Figure 81 : Light distribution evolution #1

In figure 81, both signals displayed at the oscilloscope and light-distribution change over time are plotted. In the upper figure, the voltage across the sample is plotted in yellow and shows the typical voltage waveform applied to the sample. In blue is the filtered sensor signal, two pulse signals could be seen when the voltage increases (white dotted rectangles). In purple is the gating camera signal and in green is the synchronization signal sent to the camera from the PWM inverter drive.

From analysing light intensity change plotted in Fig.81 (log scale), very bright light peaks are created while voltage increases at the very start of the period and at 50µs. At the same time, the sensor is detecting a single partial discharge for each event. Then, the intensified camera is still detecting light emitting phenomena of a lower magnitude while the sensor is not detecting any PD-like signals. These secondary light emitting phenomena are decreasing slowly in about 30 µs without being disturbed when voltage across the sample is back to zero. Thus, after the pulse discharge, other light-emitting phenomena are still occurring, confirming the fact that the whole light emission lasts longer than what is detected with the sensor.

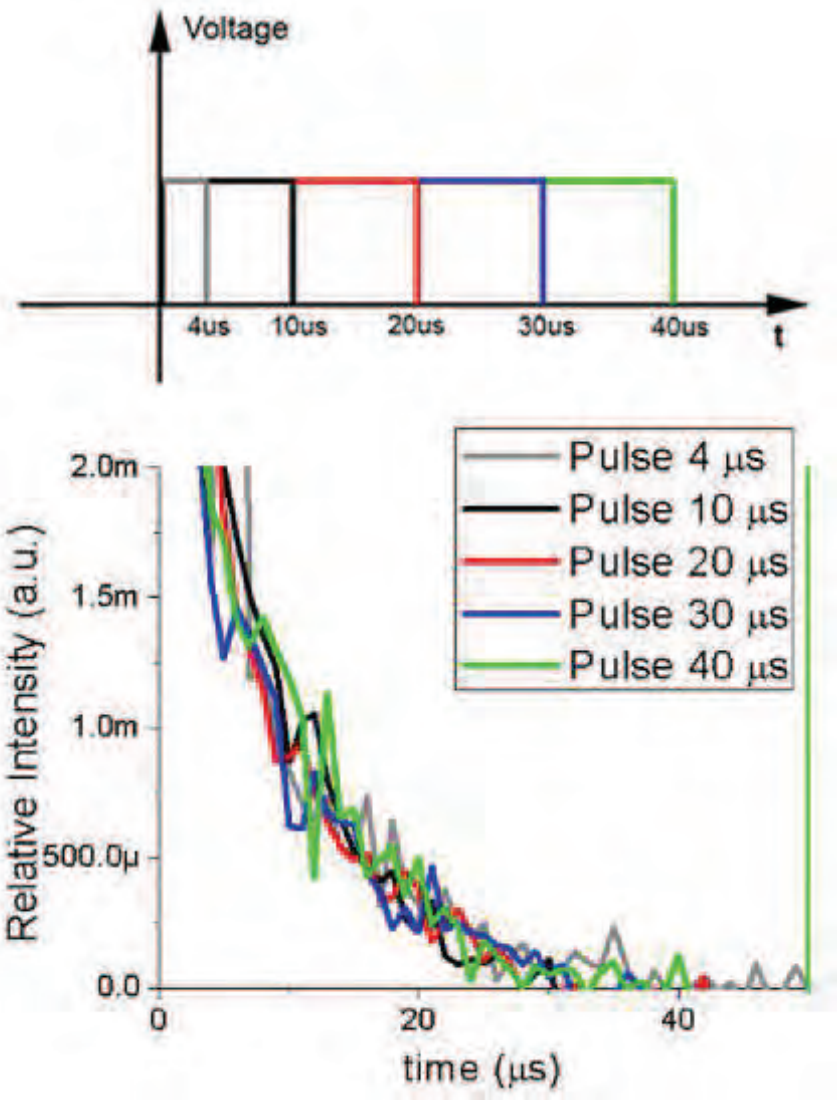

Figure 82 : Ligh distribution over time #2

In figure 82, the upper diagram explains how the PWM period signal is modified and how each colour represents a different signal. The PWM period is fixed to 100 µs. The duty cycle is modified to increase the length of time at maximum and minimum voltage. In other words, for the the same frequency (10 kHz), the effect of the duration at maximum voltage (ranging from 5 µs to 40 µs) is investigated following the previous experiment observation. So for example, the red trace is the same signal as in the previous experiment while the green signal means a positive voltage of 40µs is followed by a dead time of 10 µs, then a negative voltage of 40µs and finally a dead time of 10 µs.

From analysing data of light distribution changes over time, it appears that light evolution is not function of the pulse duration. Indeed, no significant difference could be observed for the different values investigated from 5 µs to 40 µs. So it means that the discharge has to be trigged at a defined PDIV but then, the behaviour of the discharge is not influenced by the duration of the pulse.

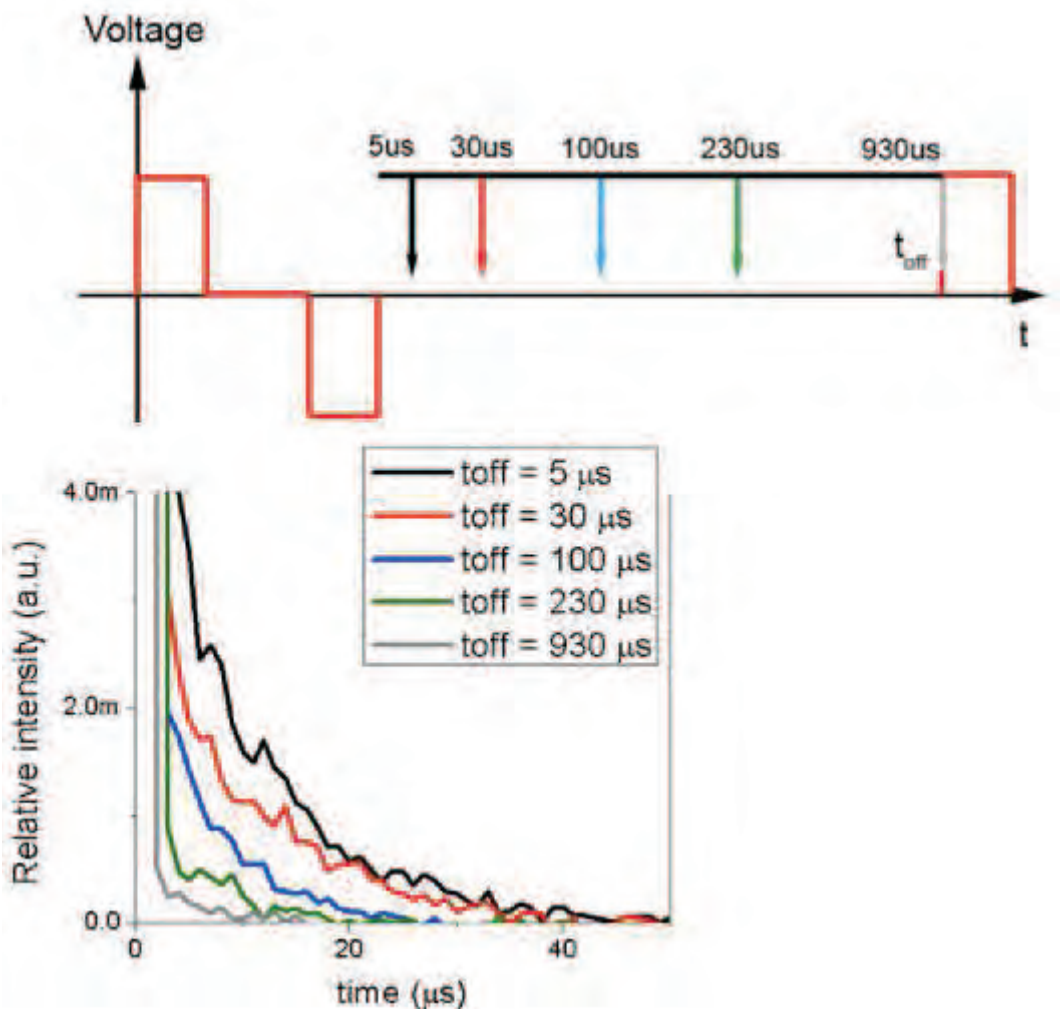

Figure 83 : Light distribution evolution #3

In figure 83, the upper diagram explains how the PWM signal is modified and how each colour represents a different signal. The aim of this experiment is to investigate the effect of the PWM period on the intensity of the diffuse light emitting phenomena, which are decreasing and do not seem to be drastically affected by the voltage after the pulse signal. Here, only PWM period is modified, so the voltage signal is thus always composed of a positive impulse (20 µs), a dead time with no voltage (30 µs), and a negative impulse (20 µs). Finally, the dead time for the rest of the period is modified to change PWM period (ranging from 5 µs to 930 µs). The red trace is the base signal as in the first experiment while the grey signal has a final dead time of 930 µs.

From the different traces plotted above, a clear difference regarding light distribution changes as a function of time, with period as a parameter, could be noticed. Indeed, the longer the period (time between impulse), the faster the decay of light. Similarly, the shorter the period is, the slower the decay. Since no significant relationship between the duration of the voltage pulse has been established in the previous experiment, this last result highlights only the influence of the frequency of impulse on the decay of the diffuse light emitting phenomena.

5.1.7. Spectroscopy

With the twisted pair sample, although different kind of spectroscopic measurements and materials have been tried, no spectroscopic data have been gathered. The main reason is the insufficient amount of light emitted by the sample, even at high frequency, several hundreds of volt above PDIV and with the maximum number of accumulation.

5.1.8. Discussion and conclusions

The technique for analyzing light emitting phenomena using an intensified CCD camera proves to be successful in showing that light emitting phenomena are still occurring in air after the main discharge occurred during switching. More importantly, the electrical detection system (sensor and its filter) is not able to detect any electrical signal related to these secondary light-emitting phenomena, which are thus pulseless from our PD detection point of view. Recalling results for PD detection in a PWM environment, it means that without any filtering or close light or ozone observation, nothing hints towards PD activity although it may be harmful for the insulation system since the energy dissipated is not function of the main pulse signal.

Secondary light-emitting phenomena intensity is function of PWM frequency but not function of pulse duration, thus hinting towards memory effects caused by the most intense and first discharge. Among mechanisms that may be at work, either recombination in gas of metastable remaining from the previous discharge at high frequency or post-discharge surface emitting phenomena may be responsible. All in all, more experiments are needed to truly know what kind of physics is at work for both type of discharges and a conclusion can not be made yet on the hypothesis of glow discharge

To further expand on these results from a reliability point of view, relative harmful effects between the first, main, discharge and secondary light emitting phenomena, has to be investigated. Indeed, even if the pulse part of the discharge seems to be much more intense, the more diffuse and faint part of the discharge lasts much longer. Knowing the physics of these diffuse discharges may help to understand how the insulation material is affected.

5.2. Signal processing and partial discharge identification

5.2.1. Introduction

Detecting partial discharge is not as simple as it looks like. Lots of information should be taken into account (PD shape, PD position, dismiss false positive, recurrence of events, detection set-up problems, etc…) to make confident calls. So, to assess properly insulation system performance, a human expert is often needed, especially in tricky case like on-line testing.

This signal processing method is meant to be the very first step of an effort towards designing a numerical signal processing method that could provide a more automated PD detection and a simple and adaptable tool to go through a lot of data and assess statistical information. This method was designed to be used without any filtering to see if a numerical signal processing could help to identify PD?

Such a signal processing method could be used for example to monitor and record partial discharges activity in an electric machine during service or endurance test, thus freeing the human expert. The signal processing could thus be done later, to count discharge event or make an analysis over time.

5.2.2. Purpose of the experiment

The aim of this series of testing of different signal processing methods is to determine whether PD may (or may not) be detected in a noisy electromagnetic environment, especially disturbed by PWM inverter switching. As this is the very first step of an automated or semi-manual signal-processing tool, the less severe environment (experiment 1) for PD identification has been chosen to acquire data.

So, the purpose of these measurements is to be able to determine if a PD signal, contained within a large and noisy signal, could be detected. To do so, two different methods have been used, both based on frequency domains properties. The first one is automated and the second is semi-manual.

To gauge the performance of these two methods, a human expert has first classified all studied signal into two categories, providing a target result of PD assessment. So, one group is made up of signals containing PD, while the other group is made up of all remaining signals that should be PD free. Of course, the human expert is not unfailing, so misclassification of some signal is possible leading to false positive or false negative. But, on a large scale, the target is that the results from signal processing method should match with those determined by the human expert

5.2.3. Experimental set-up

The experiment set-up is exactly the same as the experimental set-up described in Chap 4.5. The only difference lies in the fact that the coaxial cable has been used without any filtering device so that every possible signal, coming either from PD or from the environment, is recorded; this is, of course, intended.

5.2.3.1. Data acquisition

All data (time, voltage, sensor signal) are acquired and recorded using a Tektronix DPO4034 Digital Oscilloscope with a numerical bandwidth of 350 MHz, 4 analogic channels and a 2.5 GS/s sampling rate without any filtering applied.

5.2.3.2. Test procedure, recordings and processing

Since the sensor can detect some perturbations in the starting phase of the machine, all measurements are only carried out when the motor is at steady state. Data are randomly acquired and recorded while the electric motor is running and when PDIV has been reached. One hundred recordings have been made and will be analysed with the two proposed method. Each file size is 1 million points and is a text file. All files are read, processed and results are plotted using Matlab.

5.2.4. Signal processing

5.2.4.1. Signal extraction

Each file is made up of three kinds of data: time, voltage across the sample and sensor signal. The choice has been made to split each file into smaller parts with the main advantage to focus on one voltage increase or decrease at a time. Indeed, the very first experiment presented here (Chap 4.5) hints towards the fact the PD signal is usually close to the maximum voltage during rise time.

To split the raw file, an automated splitting method has been designed and is based on switching identification to create intervals used to create smaller files. In other words, each small file is the interval between two switchings. More precisely, a time-margin has been introduced ahead to be sure that the whole switching signal is part of the same file and not splitted between two different files. The figure below is a schematic illustration of the extraction process.

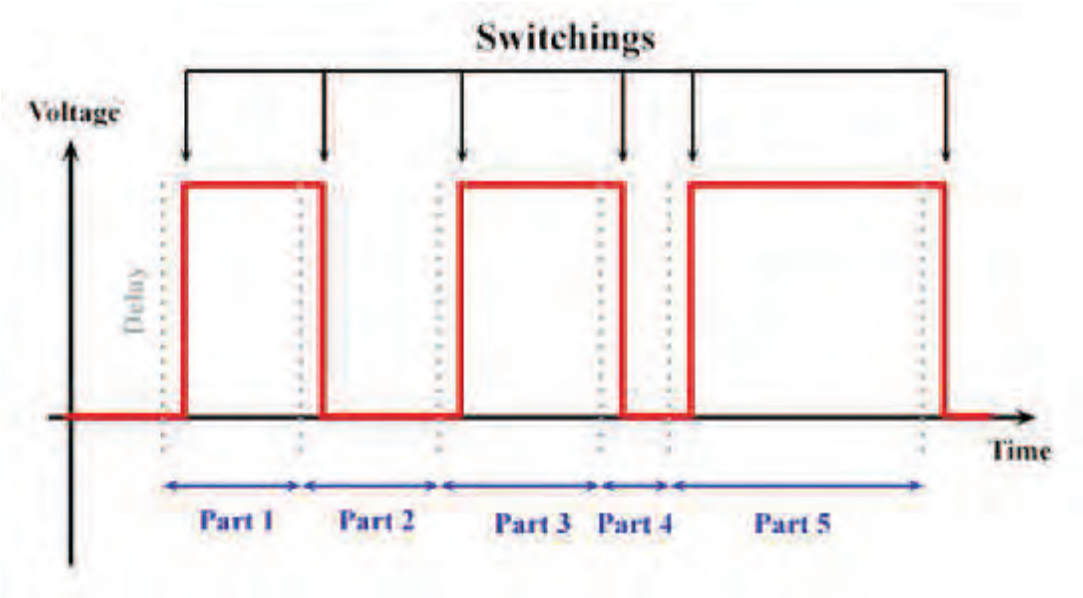

Figure 84 : Splitting raw file

As shown in Figure 84, the first step is to identify switching events (black arrows), then a time margin of several µs has to be considered ahead for the aforementioned reasons (grey dotted lines). Intervals between each switching, time margin corrected, is defined as part. One should notice that the very first interval with no voltage is not taken into account. The last part extracted from the raw file lasts until the end. All in all, around five hundreds parts have been extracted from one hundred raw files.

5.2.4.2. Signal classification

All these five hundreds parts have now to be classified into two exclusive groups: with or without partial discharge. To do so, a human expert has assessed each part, one by one, by plotting the sensor signal and then, has decided if a partial discharge was detected or not. As warned previously, false positive part (labelled as containing at least one partial discharge) or false negative part (labelled as partial discharge free) could exist. Below is a typical part signal with a partial discharge, plotted for classification before carrying out the signal processing.

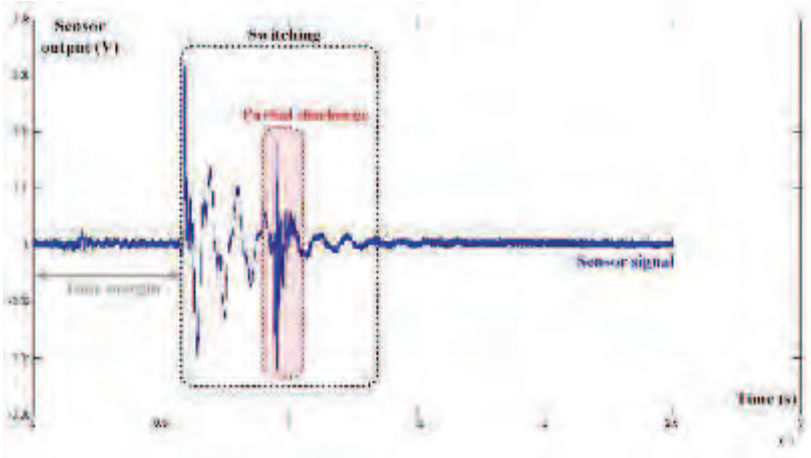

Figure 85 : Partial discharge and switching

As shown in Figure 85, the sensor signal (blue trace) is featuring two very distinct signals. First, the switching signal is of a larger magnitude, albeit not that larger, and with a clear frequency component (black dotted rectangle). But, within the switching seen by the sensor, a more rapid signal could be noticed. This signal is supposed to be a partial discharge (red dotted rectangle). The human expert has to go through all the five hundreds parts to decide to which class it belongs. Unfortunately, not all parts are this easy to classify, thus resulting in false positive or false negative. On a side note, the time margin before the switching could be noticed (grey arrow)

5.2.4.3. Target

At that time, each part has been classified in one category. To assess the performance of each signal processing method, the criteria is that the results match as close as possible to the classification made by the human expert. To do so, a graphical representation of each method's result has been plotted with each part symbolized as red or blue dot. The former representing part without partial discharge, the latter gathering parts with a partial discharge signal. The better the signal processing, the easier the delimitation will appear between the two categories of dots.

5.2.4.4. Frequencies based pre-processing

Before going on the results of both methods, a common set of mathematical operation is applied on all parts.

First, a Fast Fourier Transform (FFT) is computed on each part signal. From this point, the Energy Spectral Density (ESD) is derived, equal to the squared absolute value of its FFT. Following is the normalization of the ESD. Then, the frequency-domain of the ESD for each part is split into adjacent subsets, each one computing the sum of ESD over the considered subset, in order to derive the normalized energy over adjacent 20-MHz-wide frequency bands. This yields 24 variables, denoted v1 to v24, where v1 is the normalized energy over the [0-20MHz[band, v2 is the energy over the [20-40MHz[band, and so on.

Then, for each recording two components, labelled c1 and c2, are derived from the above 24 variables. Then, the corresponding scatter plot, the set of points in the (c1, c2) plane consisting of one point per recording, is displayed to assess how each method is performing.

The c1 and c2 components are defined as a linear combination of v1 to v24. The aim of each method is to select the appropriate coefficient of these linear combinations so that each category (with or without partial discharge) appears as clearly as possible on the scatter plot. So, more or less complex boundaries or zones should appear to discriminate each category.The difference between the two methods is how the coefficients are selected.

Below is a diagram showing how all mathematical operations are performed

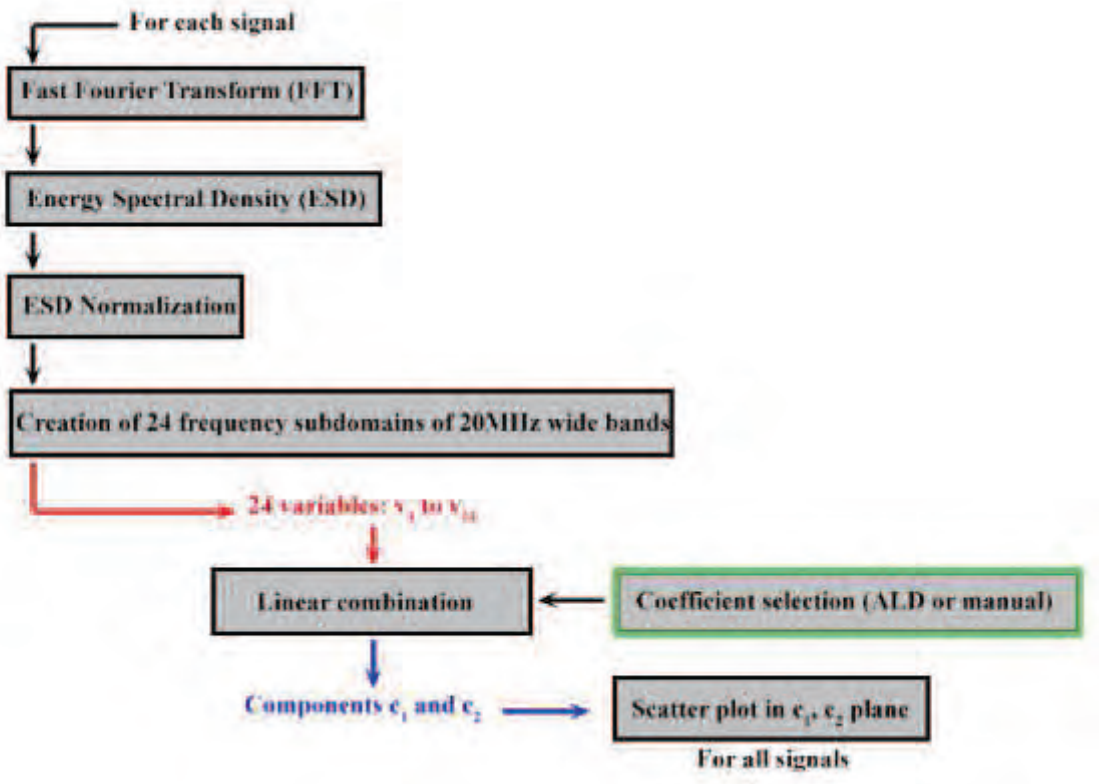

Figure 86: Sequence of operation

5.2.4.5. Manual method

Principle

A simple method was first created by "manually" analysing the values of v1 to v24 for all recordings, and noting that the considered two classes of recordings have different behaviors in the frequency bands [0, 20MHz[and [200MHz, 260MHz[. Therefore, c1 and c2 as the signal energies over these bands were defined as

$$c1 = v1$$
$$c2 = v11 + v12 + v13$$

Results

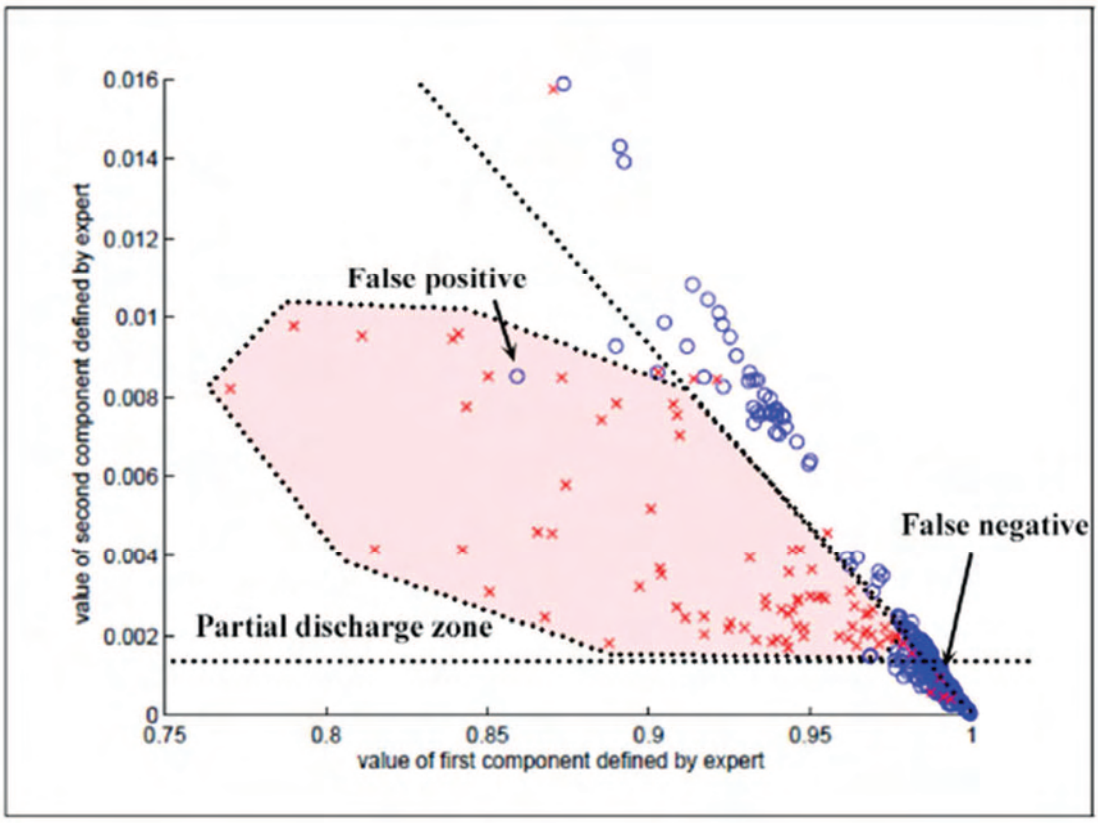

Figure 87: Scatter plot of recordings in (c1, c2) plane, with components determined manually defined by human expert

As shown in Figure 87, a partial discharge zone could be identified with a polygone containing of most partial discharge (red cross), or more simply by two linear boundaries delimiting a zone. Some false positive or false negative dots could be suspected in each category, but globally this method's performance is very good with only a few misplaced dots when try to delimit the partial discharge zone boundaries.

5.2.4.6. Automated method: Linear Discriminant Analysis

Principle

The second approach creates the two components c1 and c2 by linearly combining v1 to v24 by means of other coefficients. These coefficients are not predefined by human experts like in the previous method, but automatically derived from the data themselves: they are set to the optimum values corresponding to a classical statistical tool, i.e. Linear Discriminant Analysis (LDA) [SAP1]

Results

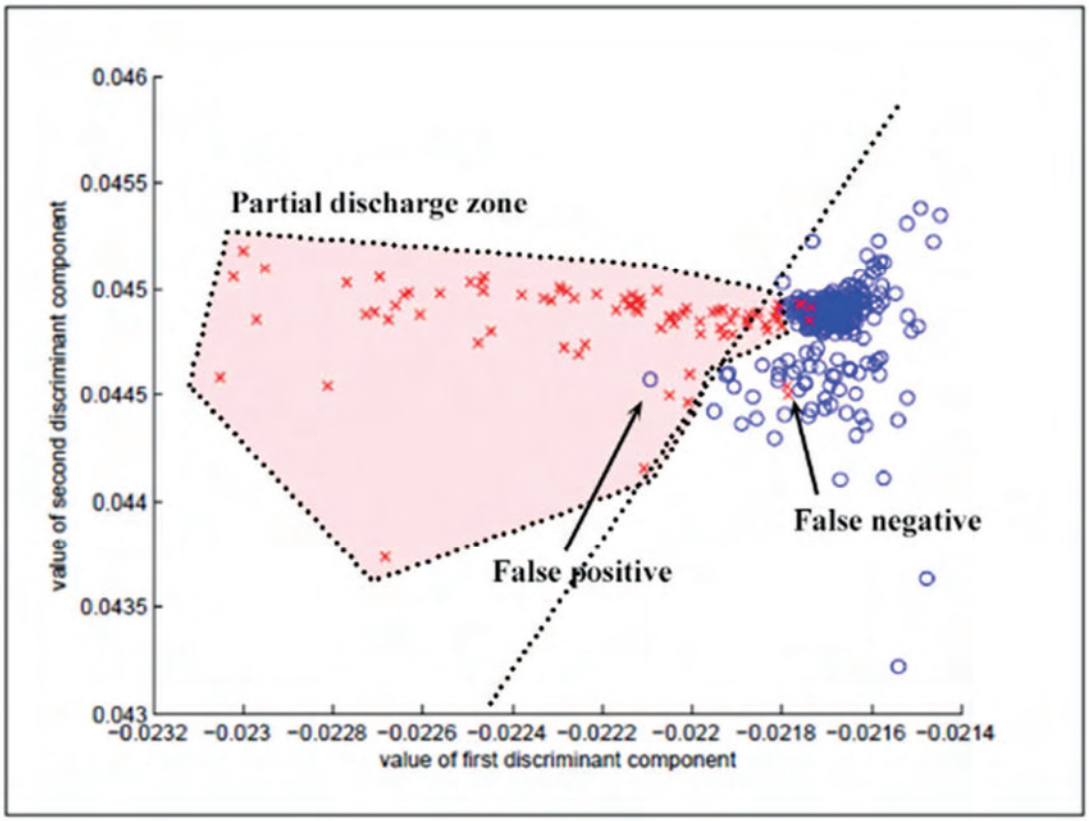

Figure 88: Scatter plot of recordings in (c1, c2) plane, with components determined by LDA.

As shown in Figure 88, the automated coefficient selection method based on LDA yields to good results as well. Indeed most of the partial discharges dots (red cross) could be isolated from the dots without partial discharges (blue dots) with a single boundary. Although, a polygon type zone would obviously yield to even better results with only one suspected false positive.

5.2.5. Conclusions

Applying two numerical signal-processing methods on data acquired is key to perform manual or fully automated PD detection and analysis. Both methods, based on energy spectral density split into bands, with either a human expert decision to assess a partial discharge zone, or the method using linear discriminant analysis to automatically derive optimum, yield to very good performance.

6. Conclusions and outlooks

The aim of this work was to develop an on-line (and off-line) partial discharge detection method using non-intrusive sensor on electric motor and stator fed by PWM inverter drive to assess easily, and with reliability, the insulation system.

In short, on-line detection of partial discharge on a real electric vehicle powertrain has been a success and is the major achievement and perfectly checks the initial objective. In addition, the experience gained during this work, both off-line and on-line, has been used practically in the company to enhance the design choice of insulating system in pure qualification tests or fatigue monitoring which is also very satisfying.

To get these results, this work has been carried out focusing on five key functions, which have all played a significant part in this achievement

1. The use of a non-intrusive, electromagnetic sensor, proves to be a good solution for on-line monitoring on engine test bench since it's completely independent of the powertrain, light and easy to position at will in the vicinity of motor terminal. Starting with a D-Dot sensor, it soon appears that much cheaper and simple sensors such as jack SMA connector, or even half coaxial cable, were good enough to perform detection without compromising efficiency. These simple sensors have been used extensively for most complex off-line and on-line testing and yield to good performance.

2. High-pass filtering proves to be key to gain visibility in the switching area where the most electromagnetic noise is generated by the PWM inverter. Since this is the most likely location of partial discharge event because of non-uniform distribution of voltage in the windings and overvoltage at motor terminal, a solution has to be found to perform detection. After using a differential method using two sensors, a self-made high-pass filter has been made before choosing a more radical cut-off frequency to remove frequency component of PWM inverter. Since, partial discharge detection off-line and on-line proves to be possible when fed by PWM inverter.

3. Availability of lab-made high power (around 60kW) random wound electric motor prototypes has been a fantastic opportunity to perform partial discharge detection on representative samples, instead of only twisted pair or motorettes samples, and to grow in complexity and representativity. The icing on the cake has been the availability of an industrial engine test bench in order to assess the performance in a real on-line situation.

4. The high voltage controllable PWM power supply is maybe the most significant element of this work. Indeed by allowing to fed EV stator up to 1.5kV one phase at a time or in a three-phases test set-up, numerous detection tests could have been performed at high voltage, allowing to reach PDIV on large electrical machine. In addition, the possibility to control precisely the shape of the bipolar pulse waveform allows, first, to make off-line testing as representative as possible to prepare on-line testing and, second, to perform representative fatigue test

5. Last but not least, high-speed acquisition means are mandatory to acquire the higher frequency components of partial discharge than stand out from the background noise. Having serious acquisition material is complementary to very high-pass filtering.

A very interesting by-product of this work has been the observation of light-emitting discharges on electric stator fed by PWM-like signal and the following investigation that has been started using an intensified CCD Camera. The main conclusion of these first tests has been the fact that the discharge is not limited to a quick pulse shape as voltage increase but actually lasts several µs with a diffuse and decreasing discharge activity.
Still, no final conclusion could have been drawn to explain the origin of this phenomenon that could be driven by metastable recombination or surface emitting phenomena. Obviously, more work could be carried out following this observation to really understand the physics of these discharges and assess how much nocive is that, diffuse and post-pulse, phenomenon for the insulation system.

Another prospect is signal processing and a very first step has been accomplished by using a linear discriminant analysis (LDA) based energy spectral density in different bands of frequency. On partial discharge created in a twisted pair, this method yields to good result in what is a favourable case. More tests in harsh electro-magnetic environment should be carried out to assess the reliability of such a method. Another outlook is to develop a numerical high-pass filtering instead of an analogical one to help the partial discharge identification method. Such a post-treatment and classification could be interesting for analysing a large number of data gather from fatigue test or even on-line monitoring under some specific mission profiles.

7. References

[AUS44] Austen, A. E. W. and Hackett, W., Journal, Institution of Electrical Engineers, Vol.91, Part I, 1944, pp. 298-322.

[BARTNIKAS] Bartnikas R. and McMahon E. J., "Engineering dielectrics – Volume 1 – Corona measurements and interpretation", American Society for Testing and Materials - STP669, published in 1979

[BART71] Bartnikas R., "Some observations on the character of corona discharges in short gap space" IEEE TRANSACTIONS ON ELECTRICAL INSULATION. VOL. EI-6, NO. 2, JUNE 1971, pp.63-75

[BEE99] Beeckman R.J., "Inverter drive issues and magnet wire responses", Proceedings of Electrical Insulation Conference and Electrical Manufacturing and Coil Winding Conference, IEEE, 1999, pp. 139-141.

[BEW51] Bewley L.E., "Travelling Waves on Transmission Systems. New-York: Wiley, 1951,2nd ed.

[BID 01] Bidan P., Lebey T., Montseny G., Neacsu C., Saint-Michel J., "Transient voltage distribution in inverter fed motor windings: Experimental study and modeling", IEEE Transactions on Power Electronics, Vol 16, No 1, janvier 2001.

[BIL14] Billard T., Lebey T. and Fresnet.F., "Partial Discharge in Electric Motor Fed by a PWM Inverter: Off-line and On-line Detection", IEEE Transactions on Dielectrics and Electrical Insulation, Vol.21, pp. 1235-1342, 2014.

[BOGGS90] Boggs Steven. A., "Partial discharge – Part III: Cavity induced PD in solid dielectrics" IEEE Electrical Insulation Magazine, Vo1.6, No.6 Nov./Dec.1990, pp.11-20.

[BON92] Bonnett A. H. and Soukup G. C., "Cause and analysis of stator and rotor failures in three phase squirrel-cage induction motors," IEEE Trans. Ind. Applicat., vol. 28, pp. 921–937, July/Aug. 1992.

[BON96] Bonnett A.H., "Analysis of the impact of pulse-width modulated inverter voltage waveforms on AC induction motors", *IEEE Transactions on Industry Applications,* Vol. 32, No. 2, March-April 1996, pp. 386-392.

[BON 97] Bonnett A.H., "A Comparison Between Insulation Systems Available for PWM-Inverter-Fed Motors", IEEE Transactions on Industry Applications, Vol. 33, No. 5, September-October 1997, pp. 1331-1341.

[BOW85] Bowes S.R., Mech M.I., Midoun A., "Suboptimal switching strategies for microprocessor-controlled PWM inverter drives", IEE proceedings, Vol. 132, No. 3, pp. 133-148, May 1985

[BRA89] Braun, J.M. and J.H. Groeger., "Determination of Gases and Gas Pressure in GIS Spacer Voids". 1989 Annual Report of the Conference on Electrical Insulation and Dielectric Phenomena, IEEE Publication 89CH2773-0,p. 105.

[CAV10-1] Cavallini A., Lindell E., Montanari G. C., Tozzi M., "Inception of Partial Discharges under Repetitive Square Voltages: Effect of Voltage Waveform and Repetition Rate on PDIV and

RPDIV", 2010 Annual Report Conference on Electrical Insulation and Dielectric Phenomena, 17-20 Oct. 2010, pp.1-4

[CAV10] Cavallini A., Lindell E., Montanari G. C., Tozzi M., "Off-line PD Testing of Converter-fed Wire-wound Motors: When IEC TS 60034-18-41 May Fail?", IEEE Transactions on Dielectrics and Electrical Insulation Vol. 17, No. 5; October 2010, pp.1385-1395

[CAV11] Cavallini A., Montanari G. C., Fabiani D. and Tozzi M., "The influence of PWM voltage waveforms on induction motor insulation systems: perspectives for the end user", IEEE International Symposium on Diagnostics for Electric Machines, Power Electronics & Drives (SDEMPED), Bologna, 5-8 Sept. 2011, pp. 288-293.

[COR 82] Cornick K.J., Thompson T.R., "Steep-fronted switching voltage transients and their distribution in motor windings", IEE Proceedings, Vol. 129, Pt. B, No. 2, March 1982, ("Part 1: System measurements of steep-fronted switching voltage transients", pp 45-55; "Part 2: Distribution of steep-fronted switching voltage transients in motor windings", pp 56-63).

[DAN93] Danikas M. G., "The Definitions Used for Partial Discharge Phenomena," IEEE Trans. Dielectr. Electr. Insul., Vol. 28, No. 6, pp. 1075-1081, 1993.

[FABIANI] Fabiani D., "Accelerated Degradation of AC-Motor winding insulation due to voltage waveforms generated by adjustable speed drives." Ph.D Thesis, University of Bologna, 2003.

[FAB04] Fabiani D., Montanari G. C., Cavallini A. and. Mazzanti G, "Relation between Space charge accumulation and partial discharge activity in enamel wires under PWM-like waveform", IEEE Transactions on Dielectrics and Electrical Insulation, Vol.11, No. 3, Junne 2004, pp. 393-405.

[FAB08] Fabiani D., Cavallini A. and Montanari G. C., "A UHF Technique for Advanced PD Measurements on Inverter-Fed Motors", IEEE Trans. Power Electronics, Vol. 23, No. 5, pp. 2546-2556, September 2008.

[FEN03] Fenger M., Stone G., "Investigation of the effect of humidity on partial discharge activity in stator windings", Proceedings of the 7th International Conference on Properties and Applications of Dielectrics Materials, June 1-5, Nagoya 2003, pp. 1080-1083.

[FEN03-1] Fenger M., Campbell S.R., Pedersen J., "Motor winding problems caused by inverter drives" IEEE industry application magazine, Industry Applications Magazine, Vol. 9, Issue 4, July-August 2003, pp. 22-31.

[FEN05] Fenger M., Stone G., "Investigations into the Effect of Humidity on Stator Winding Partial Discharges", IEEE Transactions on Dielectrics and Electrical Insulation, Vol. 12, No. 2; April 2005, pp341-346

[GUAS10] Guastavino F., Cotella G., Dardano A., Massa G. F., Ratto A., Squarcia S., Torello E., "Influence of the rise time and of the temperature on the PD inception voltage of enameled wires", Annual Report Conference on Electrical Insulation and Dielectric Phenomena, 17-20 Oct. 2010, pp.1-4

[IEC-41] Rotating Electrical Machines – Part 18-41: Qualification and Type Tests for Type I Electrical Insulation Systems Used in Rotating Electrical Machines Fed from Voltage Converters, IEC 60034-18-41 - TS Ed. 1.0, 2007.

[IEEE00] IEEE, "IEEE Guide to the Measurement of Partial Discharges in Rotating Machinery", 26 avril 2000.

[JOUAN96] Von Jouanne A., Enjeti P., Gray W., “Application issues for PWM adjustable speed AC motor drives", IEEE Industry Application Magazine, Vol. 2, No. 5, Sept-Oct. 1996, pp. 10-18.

[KAU96] Kaufhold M., Borner G., Eberhardt M., “J. SPEC “Failure mechanism of the interturn insulation of low voltage electric machines fed by pulse-controlled inverters”, DEIS feature article, Vol.12, No.5, September-October 1996, pp.9-16

[KER96] Kerkman R., Leggate D., Skibinski G., "Interaction of drive modulation and cable parameters on AC motor transients", IEEE Transactions on Industry Applications, Vol. 33, No. 3, May-June 1997, pp. 722-731.

[KREUGER] Kreuger F., “Partial Discharges detection in High Voltage equipment”, Buttenvorths, London, 1989

[LEB98] Lebey T., “A theoretical approach of partial discharges under square voltage waveforms”, IEEE International Synopsium on Electrical Insulation, June 1998, pp. 257-260.

[LEB98-1] Lebey T., Castelan P., Montanari G. C., and Ghinello I., “Influence of PWM type voltage waveforms on reliability of machine insulation systems,” in Proceedings. 8th International Conference on Harmonics and Quality of Power, 1998, pp. 994–998.

[LUF 99] Luff S., Garvey S.D., Norris W.T., “Predicting high frequency characteristics of the windings of large electrical machines: A transmission line analysis approach", Ninth International IEE Conference on Electrical Machines and Drives, 1999, pp. 218-222.

[MAS51] Mason, J. H., “The Deterioration and Breakdown of Dielectrics Resulting From Internal Discharges”, Proc. IEE,98Pt.1,Jan. 1951,pp 44-59.

[MBA96] MBaye A., Grigorescu F., Lebey T., Ai B., “Existence of partial discharges in low-voltage machine induction machines supplied by PWM drives”, IEEE transactions on Dielectrics and Electrical Insulation, Vol. 3, n. 4, August 1996

[MBA97] Mbaye A., Bellomo J. P., Lebey T., Oraison J. M., and Peltier F., “Elec- trical stresses applied to stator insulation in low voltage induction motors fed by PWM drives,” Proc. Inst. Elect. Eng. B, pp. 191–198, May 1997.

[MC53] Meek, J. M. and Craggs, J. D., “Electrical Breakdown of Gase”s, Clarendon Press, Oxford, 1953, pp. 251-290.

[MCMA68] McMahon, E.J.,“Corona Resistance of Materials”. IEEE Trans. Elec. Insulation, Vol.EI-3, No.1, pp. 3-10, Feb. 1968.

[NEACSU] Neacsu C., “Contribution à l'étude des défaillances statoriques des machines asynchrones” Ph;D Thesis, Univerty Paul Sabatier (Toulouse 3), 2002.

[OLI95] Oliver J.A., Stone G.C., “Implications for the Application of adjustable speed drive electronics to motor stator winding insulation”, IEEE Electrical insulation magazine, DEIS feature article, Vol.11, Issue 4, July-August 1995, pp.32-36.

[PERSS92] Persson E., “Transients Effects in Application of PWM Inverters to Induction Motors”, IEEE Transactions on Industry Applications, vol.28, no.5, Sep./Oct.1992, pp. 1095-1101

[RUD40] Rudenberg R., “Performance of traveling waves in coils and windings", AIEE Magazine , 1940, Vol.59 , p 1031

[SAP1] Saporta G., “Probabilités, analyse des données et statistique”, Technip, Paris, 1990.

[SAUND96] Saunders L.A., Skibinski G.L., Evon S.T., Kempkes D.L., “Riding the reflected wave-IGBT drive technology demands new motor and cable considerations", Industry Applications Society 43rd Annual Petroleum and Chemical Industry Conference, IEEE, 1996, pp. 75-84.

[SCHO64] Schonung A. and Stemmler H., “Static frequency changers with subharmonic control in conjunction with reversible variable speed AC drives,” Brown Boueri Rec., pp. 555-577, 1964

[SCHON69] Schonhuber, M. J., Transactions on Power Apparatus and Systems, Institute of Electrical and Electronics Engineers, Vol. PAS-88, Feb. 1969, pp. 100-107.

[STONE00] Stone, G.C., Campbell, S.R., Lloyd, B.A., Tetreault, S., “Which Inverter-Fed Drives Need Upgraded Stator Windings”, IAS/PCA, Salt Lake City, May 7-12/2000

[STONE07] Stranges M. K.W., Stone G. C., Bogh D. L., “New specs for ASD motors: exploring the IEC 60034-18-41 and IEC 60034-18-42 technical specifications for inverter duty motor insulation” IEEE Industry Applications Magazine, Vol.13 , Issue 1, Jan-Feb 2007, pp. 37-42.

[TOZ11] Tozzi M., Cavallini A., Montanari G. C., “Monitoring Off- line and On-line PD under Impulsive Voltage on Induction Motors, Part II: Criticality”, IEEE Electr. Insul. Mag July./August. 2011. Vol.27, No.4, pp.26-33

[TOZ10] Tozzi M., Cavallini A., Montanari G. C., “Monitoring Off- line and On-line PD under Impulsive Voltage on Induction Motors, Part II: Testing”, IEEE Electr. Insul. Mag., Sept./Oct. 2010.

[TOZ09] Tozzi M., Montanari G.C., Fabiani D., Cavallini A.and Gao G., “Off-line and On-line PD Measurements on Induction Motors fed by Power Electronic Impulses”, IEEE Electr. Insul. Conf. (EIC), Montreal, Quebec, pp. 420-424, 2009.

[VHIPP66] von Hippel, A., “Dielectrics and Waves”, MIT Press, Cambridge, Mass., 1966, pp. 234-252.

[WEED22] Weed J., “Prevention of transient voltages in windings", AIEE Journal, Vol. 41, 1922, p. 14

[WHITE53] Whitehead, S., “Dielectric Breakdown of Solids, Oxford University Press, Oxford, 1953,pp. 163-233.

[WRI83] Wright M. T., Yang S. J., and McLeay K., “General theory of fast fronted interturn voltage distribution in electrical machine windings,” Proc. Inst. Elect. Eng. B, vol. 130, no. 4, pp. 245–256, July 1983.

[YIN97] W. Yin, “Failure Mechanism of Winding insulation in Inverter Fed motors”, IEEE Elect. Insulation Magazine, Vol.13, n.6, pp18-23, November 1997.
[EPRI92] “Adjustable Speed Drives Applications Guide,” TR-1011140 EPRI Final Report, December 1992.
--

Web links

[ARC1]http://myrenaultzoe.com/Docs/2012_wien_vortrag_uv.pdf
[REN1]http://www.renault.com/fr/innovation/gamme-mecanique/pages/moteur-electrique-5a.aspx
[REN2]http://www.renault.com/fr/innovation/vehicule-electrique/pages/electro-techno.aspx
[REN3]http://www.renault.com/fr/innovation/vehicule-electrique/pages/le-moteur-electrique.aspx
[REN4]http://www.renault.com/fr/lists/archivesdocuments/moteur electrique_synchrone à rotor bobine.pdf
[CONT1]http://www.continentalcorporation.com/www/pressportal_com_en/themes/press_releases/3_automotive_group/powertrain/press_releases/pr_20110913_elektromotor_en.html

Author:	Thibaut BILLARD
Title:	Off-line and On-line Partial Discharges Detection in Low Voltage Motors of Electric Vehicle fed by a PWM Inverter using Non-Intrusive Sensor
Advisors:	Thierry LEBEY, head of research at CNRS Pierre BIDAN, Professor at the university of Toulouse III
Ph.D Defense:	Ph.D defended on the 3rd October 2014 at University of Toulouse III
Area of research:	Electrical Engineering
Laboratory:	Laplace Laboratory, CNRS/UPS/INP UMR 5213
Address:	118, route de Narbonne 31062 Toulouse cedex 9, France
Keywords:	Partial Discharges, Off-line, On-line, PWM inverter drive, Non-intrusive sensor, Electric Vehicle, Electric Motor

Abstract (short):

When driving an electric vehicle, speed needs to be controlled by the driver. To do so, a power electronics device, called PWM inverter drive, controls the electric motor rotational speed, following driver instructions. But, this inverter drive is creating severe electrical stress on the electrical insulation system of the electric motor and partial discharges could thus occur. These discharges are extremely harmful, damaging irreversibly the electrical insulation and could lead to premature failure of the machine. Worse still, detection of these phenomena during operation is very difficult and standard qualification tests could not guarantee a sufficient quality.

The aim of this Ph.D thesis is to develop a non-intrusive partial discharge detection method that could be used off-line and on-line in order to assess electrical insulation quality when facing realistic electric vehicle operating conditions.

Auteur:	Thibaut BILLARD
Titre:	Détection off-line et on-line de décharges partielles dans un moteur basse tension de véhicule électrique à l'aide de capteur non-intrusif
Directeurs:	Thierry LEBEY, directeur de recherche CNRS Pierre BIDAN, professeur à l'université Toulouse III
Soutenance:	Le 3 octobre 2014 à l'université Toulouse III
Domaine:	Génie Electrique
Laboratoire:	Laboratoire Laplace, CNRS/UPS/INP UMR 5213
Adresse:	118, route de Narbonne 31062 Toulouse cedex 9, France
Mots clés:	Décharges partielles, Off-line, On-line, Onduleur de tension MLI, Capteur non-intrusif, Véhicule électrique, Moteur électrique

Résumé (court):

Pour faire varier la vitesse d'une voiture électrique, le moteur est piloté par un dispositif d'électronique de puissance appelé onduleur de tension. Cet onduleur de tension, par son principe de fonctionnement et la contrainte électrique qu'il génère, nocif pour l'isolation électrique du moteur et des phénomènes appelés décharges partielles peuvent apparaître. Ces décharges partielles dégradent l'isolation électrique et provoquent un défaut prématuré de la machine. Cependant, il est très difficile de détecter ces phénomènes en fonctionnement et les tests de validation actuels ne permettent pas de garantir une fiabilité suffisante.

L'objectif de cette thèse est donc de développer une méthode de détection de décharges partielles non-intrusives pouvant être utilisée sur le moteur en fonctionnement afin d'être au plus proche des contraintes subies par la machine dans son environnement opérationnel